AFRL-IF-RS-TR-1998-218
Final Technical Report
December 1998

CONCEALED WEAPONS DETECTION TECHNOLOGIES

JAYCOR

Sponsored by
Defense Advanced Research Projects Agency
DARPA Order No. C141

APPROVED FOR PUBLIC RELEASE; DISTRIBUTION UNLIMITED.

The views and conclusions contained in this document are those of the authors and should not be interpreted as necessarily representing the official policies, either expressed or implied, of the Defense Advanced Research Projects Agency or the U.S. Government.

AIR FORCE RESEARCH LABORATORY
INFORMATION DIRECTORATE
ROME RESEARCH SITE
ROME, NEW YORK

DTIC QUALITY INSPECTED 2

19990203 061

This report has been reviewed by the Air Force Research Laboratory, Information Directorate, Public Affairs Office (IFOIPA) and is releasable to the National Technical Information Service (NTIS). At NTIS it will be releasable to the general public, including foreign nations.

AFRL-IF-RS-TR-1998-218 has been reviewed and is approved for publication.

APPROVED:

DAVID D. FERRIS, JR.
Project Engineer

FOR THE DIRECTOR:

JOSEPH CAMERA, Deputy Chief
Information & Intelligence Exploitation Division
Information Directorate

If your address has changed or if you wish to be removed from the Air Force Research Laboratory Rome Research Site mailing list, or if the addressee is no longer employed by your organization, please notify AFRL/IFEA, 32 Brooks Road, Rome, NY 13441-4114. This will assist us in maintaining a current mailing list.

Do not return copies of this report unless contractual obligations or notices on a specific document require that it be returned.

CONCEALED WEAPONS DETECTION TECHNIQUES

Franklin Felber

Contractor: JAYCOR
Contract Number: F30602-95-C-0274
Effective Date of Contract: 14 September 1995
Contract Expiration Date: 31 December 1996
Short Title of Work: Concealed Weapons Detection Technologies

Period of Work Covered: Sep 95 - Dec 96

Principal Investigator: Franklin Felber
Phone: (619) 535-3124
AFRL Project Engineer: David D. Ferris
Phone: (315) 330-4408

Approved for public release; distribution unlimited.

This research was supported by the Defense Advanced Research Projects Agency of the Department of Defense and was monitored by David D. Ferris, AFRL/IFEA, 32 Brooks Road, Rome, NY 13441-4114.

REPORT DOCUMENTATION PAGE	Form Approved OMB No. 0704-0188

Public reporting burden for this collection of information is estimated to average 1 hour per response, including the time for reviewing instructions, searching existing data sources, gathering and maintaining the data needed, and completing and reviewing the collection of information. Send comments regarding this burden estimate or any other aspect of this collection of information, including suggestions for reducing this burden, to Washington Headquarters Services, Directorate for Information Operations and Reports, 1215 Jefferson Davis Highway, Suite 1204, Arlington, VA 22202-4302, and to the Office of Management and Budget, Paperwork Reduction Project (0704-0188), Washington, DC 20503.

1. AGENCY USE ONLY *(Leave blank)*	2. REPORT DATE	3. REPORT TYPE AND DATES COVERED
	December 1998	Final Sep 95 - Dec 96

4. TITLE AND SUBTITLE

CONCEALED WEAPONS DETECTION TECHNOLOGIES

5. FUNDING NUMBERS

C - F30602-95-C-0274
PE - 62702F
PR - C141
TA - 01
WU - P1

6. AUTHOR(S)

Franklin Felber

7. PERFORMING ORGANIZATION NAME(S) AND ADDRESS(ES)

JAYCOR
9775 Towne Centre Drive
San Diego CA 92121

8. PERFORMING ORGANIZATION REPORT NUMBER

N/A

9. SPONSORING/MONITORING AGENCY NAME(S) AND ADDRESS(ES)

Advanced Research Projects Agency
3701 North Fairfax Drive
Arlington VA 22203-1714

Air Force Research Laboratory/IFEA
32 Brooks Road
Rome NY 13441-4114

10. SPONSORING/MONITORING AGENCY REPORT NUMBER

AFRL-IF-RS-TR-1998-218

11. SUPPLEMENTARY NOTES

Air Force Research Laboratory Project Engineer: David D. Ferris, Jr./IFEA/(315) 330-4408

12a. DISTRIBUTION AVAILABILITY STATEMENT

Approved for public release; distribution unlimited.

12b. DISTRIBUTION CODE

13. ABSTRACT *(Maximum 200 words)*

This effort considers the integration of an ultrasound sensor with an active radar sensor. The purpose of the active-radar sensor is to provide long-range detection of concealed weapons. The radar will then hand over the detection data to the ultrasound sensor which will produce an image of the suspected weapon. The fusion of radar and ultrasound produces a long range/high probability of detection/low false alarm rate system. The system was tested on both metallic and non-metallic weapons concealed under a variety of clothing. This testing showed that the system was effective but was highly dependent on clothing thickness and material and aspect angle.

14. SUBJECT TERMS

Acoustic Imaging, Weapons Detection

15. NUMBER OF PAGES

166

16. PRICE CODE

17. SECURITY CLASSIFICATION OF REPORT	18. SECURITY CLASSIFICATION OF THIS PAGE	19. SECURITY CLASSIFICATION OF ABSTRACT	20. LIMITATION OF ABSTRACT
UNCLASSIFIED	UNCLASSIFIED	UNCLASSIFIED	UL

TABLE OF CONTENTS

JAYCOR/Aerojet CWDT Program Overview 2

Ultrasound Sensor Design and Operation 39

Ultrasound Image Processing 48

Radar CWD Test Results 73

Conceptual Design 100

Dedicated CWD Radar 121

Appendix A: Fusion of radar and ultrasound sensors for concealed weapons detection A-1

Appendix B: Ultrasound Sensor for Remote Imaging of Concealed Weapons B-1

OVERVIEW

JAYCOR/Aerojet
CWDT Program Overview

OVERVIEW OUTLINE

This document is the final report for the Concealed Weapons Detection Technologies (CWDT) Program. The outline of this final report follows the outline of the overview. We report on progress during the Phase 1 Program. We describe the components and operation of the breadboard ultrasound sensor that we have developed and built. We show the results of concealed weapons detection (CWD) with the JAYCOR mine-detection radar. And we conclude with the conceptual design of a brassboard ultrasound and radar CWD sensor for Phase 2.

OVERVIEW OUTLINE

- Phase 1 Progress
- Ultrasound Breadboard Components/Operation
- Radar CWD Results
- Phase 2 Conceptual Design

PHASE 1 CWDT PROGRAM

The CWDT Phase 1 Program was sponsored by the Air Force Materiel Command and the Defense Advanced Research Projects Agency under Contract No. F30602-95-C-0274. The period of performance was from 14 September 1995 to 31 December 1996. The objective of the Phase 1 CWDT Program was to develop and demonstrate a breadboard CWD sensor that can detect and identify metallic and nonmetallic weapons at distances from 1 to 10 m. The technologies to be used were to be reliable, safe for both the users and the public, acceptable to the public, and preferably unobtrusive.

PHASE 1 CWDT PROGRAM

- Concealed Weapons Detection Technology (CWDT) Phase 1 Program managed by Rome Laboratories at JAYCOR, Sept. 1995 to Sept. 1996
- Objective: Develop and demonstrate breadboard CWD sensor that will:
  - Detect and identify metallic and nonmetallic weapons
  - At distances of 1 to 10 m
  - Reliably
  - Safely
  - Acceptably
  - Unobtrusively

MULTI-SENSOR APPROACH TO CONCEALED WEAPONS DETECTION

Our approach to meeting the CWDT objectives involves integrating an ultrasound sensor with an active-radar sensor. The purpose of the active-radar sensor is to provide long-range detection of metallic and nonmetallic weapons. The radar is expected to hand over the detection data to the ultrasound sensor, which will then produce images of the metallic and nonmetallic concealed weapons for positive identification. With this approach, the radar is responsible for producing a high probability of detection, particularly in crowded scenarios, while the ultrasound sensor, by imaging the weapons, produces a low false-alarm rate. The radar to be used is essentially the frequency-agile mine-detection radar that was developed by JAYCOR for the U.S. Army. This radar can find buried metallic and plastic mines at distances up to about 50 ft. We have shown that it is sensitive to concealed weapons at ranges well over 10 m. The ultrasound sensor has a shorter range, but has the ability not only to detect concealed weapons, but to image them as well. In a current program for the Army, JAYCOR, with Lockheed-Martin as the principal subcontractor, is producing a compact version of this mine-detection radar that will fit in a 2-cu. ft. volume. The ultrasound sensor has the potential to be scaled to even smaller sizes.

MULTI-SENSOR APPROACH TO CONCEALED WEAPONS DETECTION

- Ultrasound
  - Images metallic and nonmetallic weapons for positive ID
  - Reliable, safe, acceptable, unobtrusive
  - Scales to lightweight, handheld devices
- Radar
  - Provides long-range (10-m) detection of metallic and nonmetallic weapons
  - Based on JAYCOR's successful frequency-agile mine detection radar
  - Leveraged off Army program

JAYCOR/AEROJET ACCOMPLISHMENTS ON CWDT PROGRAM

Under the Phase 1 CWDT Program, JAYCOR published the first remote ultrasound images in air.[1] We have produced ultrasound images of metallic and nonmetallic weapons concealed on human bodies under sweaters and sweatshirts. We have invented and developed a novel, efficient, high-power ultrasound source that is tunable from about 10 kHz to close to 1 MHz. The efficiency of the source is of the order of 10% over most of this waveband. With our team member, GenCorp Aerojet, we have invented and developed novel, mm-sized, sensitive ultrasound detectors that can be easily fabricated in arrays costing $50 in quantities of at least 500, once prototyped. We have also gathered data demonstrating that an active radar can detect concealed weapons at ranges of 10 m. This data is shown for the first time in this final report.

[1] F.S. Felber, H.T. Davis III, C. Mallon, and N.C. Wild, "Fusion of Radar and Ultrasound Sensors for Concealed Weapons Detection," in *Signal Processing, Sensor Fusion, and Target Recognition V*, Ivan Kadar, Vibeke Libby, Editors, Proc. SPIE 2755, 514-521 (1996).

JAYCOR/AEROJET ACCOMPLISHMENTS ON CWDT PROGRAM

- First-published remote ultrasound images in air
- Ultrasound images of metallic and nonmetallic weapons concealed on human body under sweater, sweatshirt
- Novel, efficient, tunable, high-power ultrasound source
- Novel, mm-sized, sensitive ultrasound detectors in arrays
- Radar demonstration of concealed weapon detection at 10 m

CONCEALED WEAPONS RETURN MUCH LOUDER ECHOES THAN HUMANS

This chart vividly demonstrates the underlying principle of ultrasound CWD. Any hard objects, whether metal, plastic, glass, or ceramic, reflect ultrasound much better than clothing and human bodies. Fortunately, virtually all concealed weapons are hard objects and good ultrasound reflectors.

These two surface-plot images were produced using 40-kHz ultrasound under identical conditions. In the top figure, a handgun was suspended, at a range of 1.5 m, within inches in front of a human wearing a shirt and tie and standing behind a heavy sweatshirt. The bottom figure shows the identical image to the same scale after the handgun was removed from the scene. No frequency, brightness, or contrast filters, which would have altered heights in the surface plots, were applied.

CONCEALED WEAPONS RETURN MUCH LOUDER ECHOES THAN HUMANS

- IMAGE OF HANDGUN ON HUMAN BEHIND HEAVY SWEATSHIRT

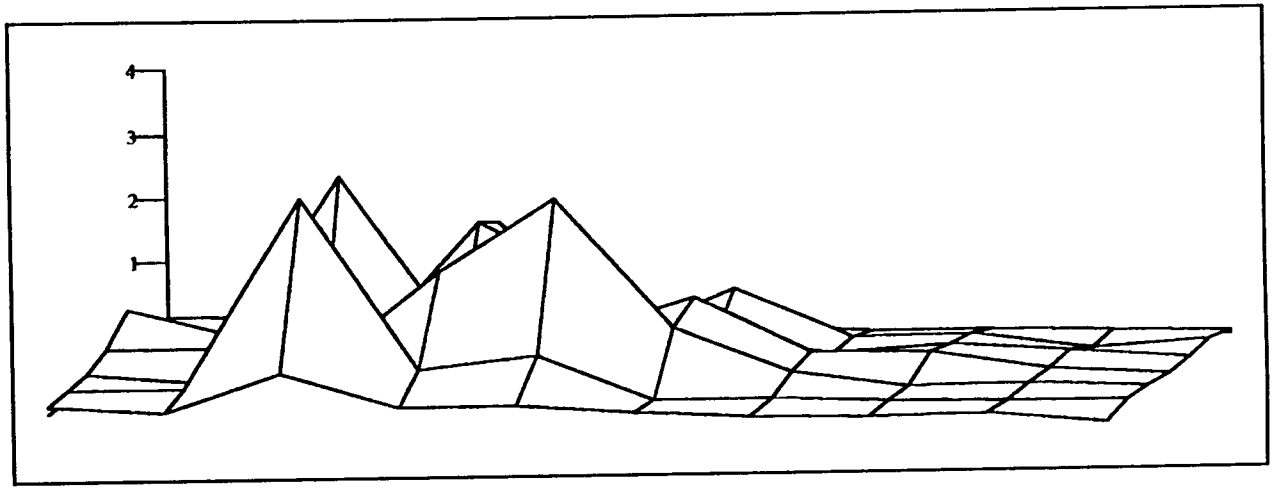

- IDENTICAL CONDITIONS, EXCEPT NO HANDGUN

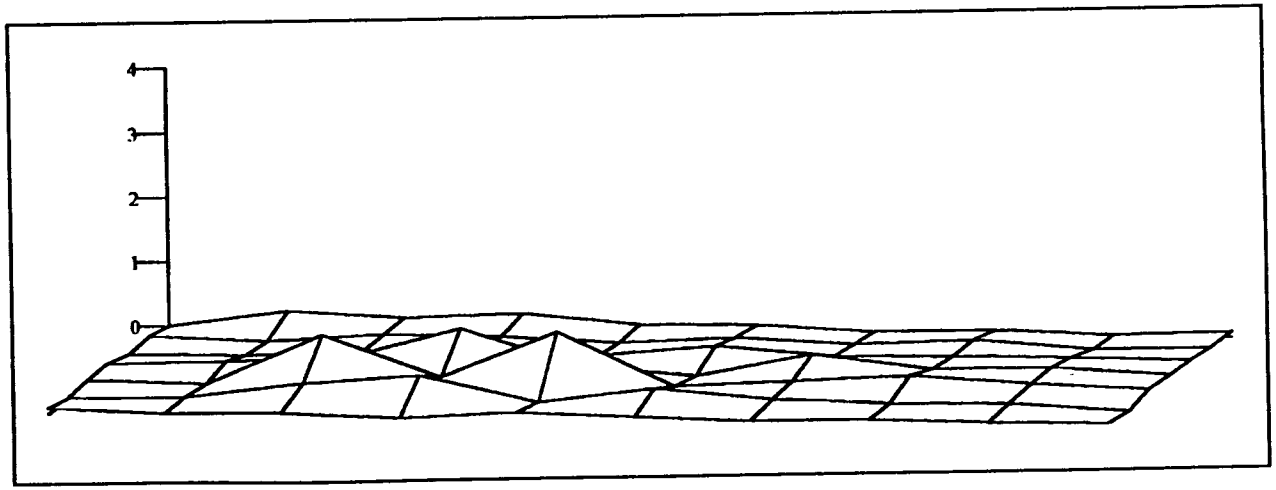

LEXAN KNIFE CONCEALED UNDER WOOL SWEATER ON HUMAN BODY

The image of a lexan knife shown in this chart is a good example of the capabilities of the ultrasound sensor to image nonmetallic concealed weapons. Both the lexan knife and the ultrasound image of the knife at 200 kHz are shown on the facing page in full scale. The lexan knife was concealed under a wool sweater on a human body at about 4 ft. from the ultrasound sensor. Details of this image will be discussed in the section on image processing. The image illustrates an advantage of ultrasound over certain other CWD techniques, in that ultrasound sees any hard object concealed under clothing and not just metallic weapons.

LEXAN KNIFE CONCEALED UNDER WOOL SWEATER ON HUMAN BODY

LEXAN KNIFE (SCALE 1:1)

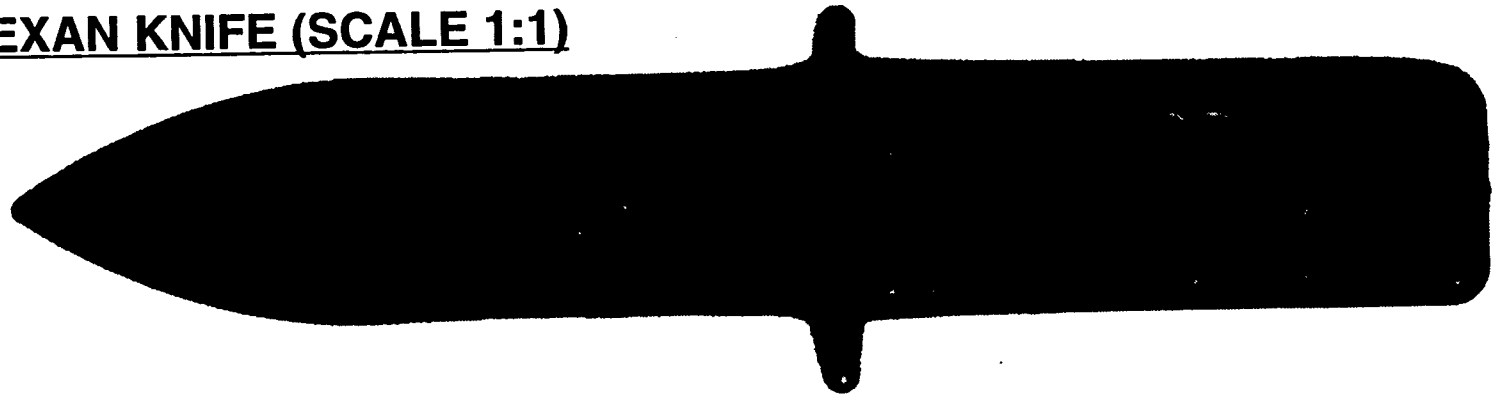

ULTRASOUND IMAGE AT 4 ft (SCALE 1:1)

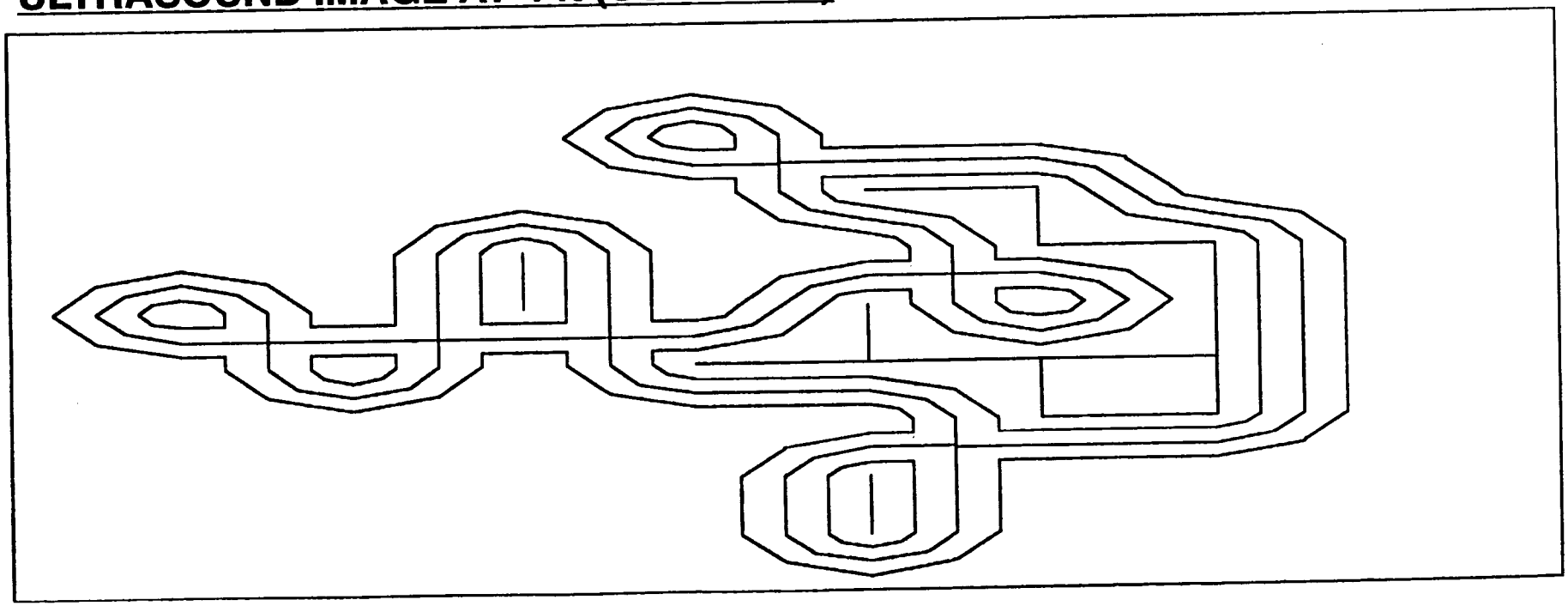

NO KNIFE CONCEALED UNDER WOOL SWEATER ON HUMAN BODY

When the lexan knife was removed from underneath the sweater immediately after the image on the preceding page was produced, a second image of the same body, in the same position, under the same conditions, and with the same processing and filtering showed no evidence of any concealed weapons under the sweater. Thus, the image of the lexan knife proved to be a true image, and not an artifact of the processing.

NO KNIFE CONCEALED UNDER WOOL SWEATER ON HUMAN BODY

SAME SWEATER, SAME BODY, SAME POSITION,
SAME CONDITIONS, SAME FILTERING,
SAME EVERYTHING, EXCEPT .....

..... NO KNIFE

ULTRASOUND IMAGE AT 4 ft (SCALE 1:1)

ULTRASOUND IMAGE OF CONCEALED HANDGUN OVERLAID ON HANDGUN

The handgun shown in this figure and the ultrasound image of the concealed handgun at 200 kHz are shown here at 1/2 scale. The handgun was concealed under a heavy sweatshirt on a human body. The image also shows two false-positive pixels. In general, the false-positive pixel rate for all of our ultrasound images was less than or about 2%, as it was here.

ULTRASOUND IMAGE OF CONCEALED HANDGUN OVERLAID ON HANDGUN

- HANDGUN CONCEALED ON HUMAN BODY UNDER HEAVY SWEATSHIRT SCALE 1:2

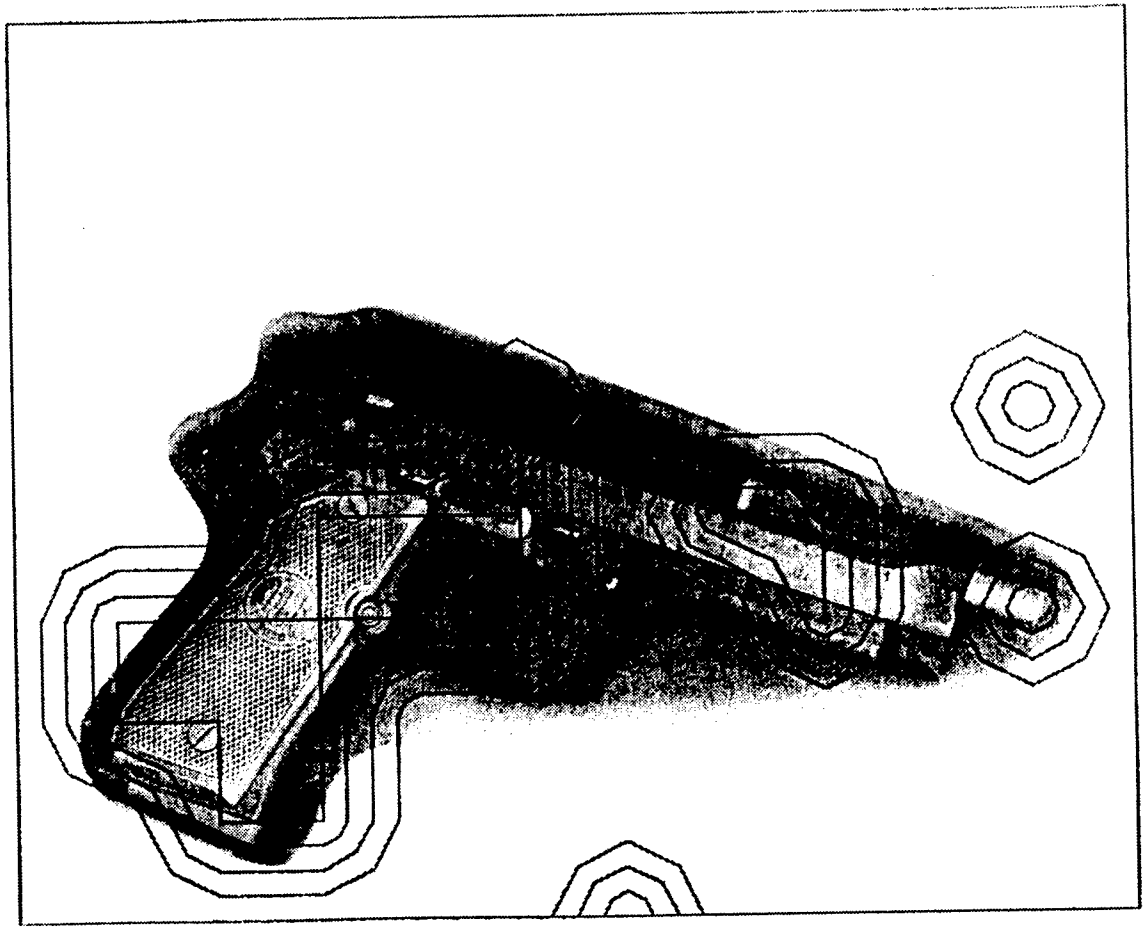

NO HANDGUN CONCEALED UNDER HEAVY SWEATSHIRT ON HUMAN BODY

When the handgun was removed from under the sweatshirt, the ultrasound image of the same body, in the same position, wearing the same clothing, under the same conditions and with the same processing and filtering produced the image shown here, containing one false-positive pixel. The false-positive pixel was determined to have come from a crimped seam in the sweatshirt. This image demonstrates again the marked distinction between images of bodies with concealed weapons and without.

NO HANDGUN CONCEALED UNDER HEAVY SWEATSHIRT ON HUMAN BODY

- ULTRASOUND IMAGE AT 4 FT (SCALE 1:2)

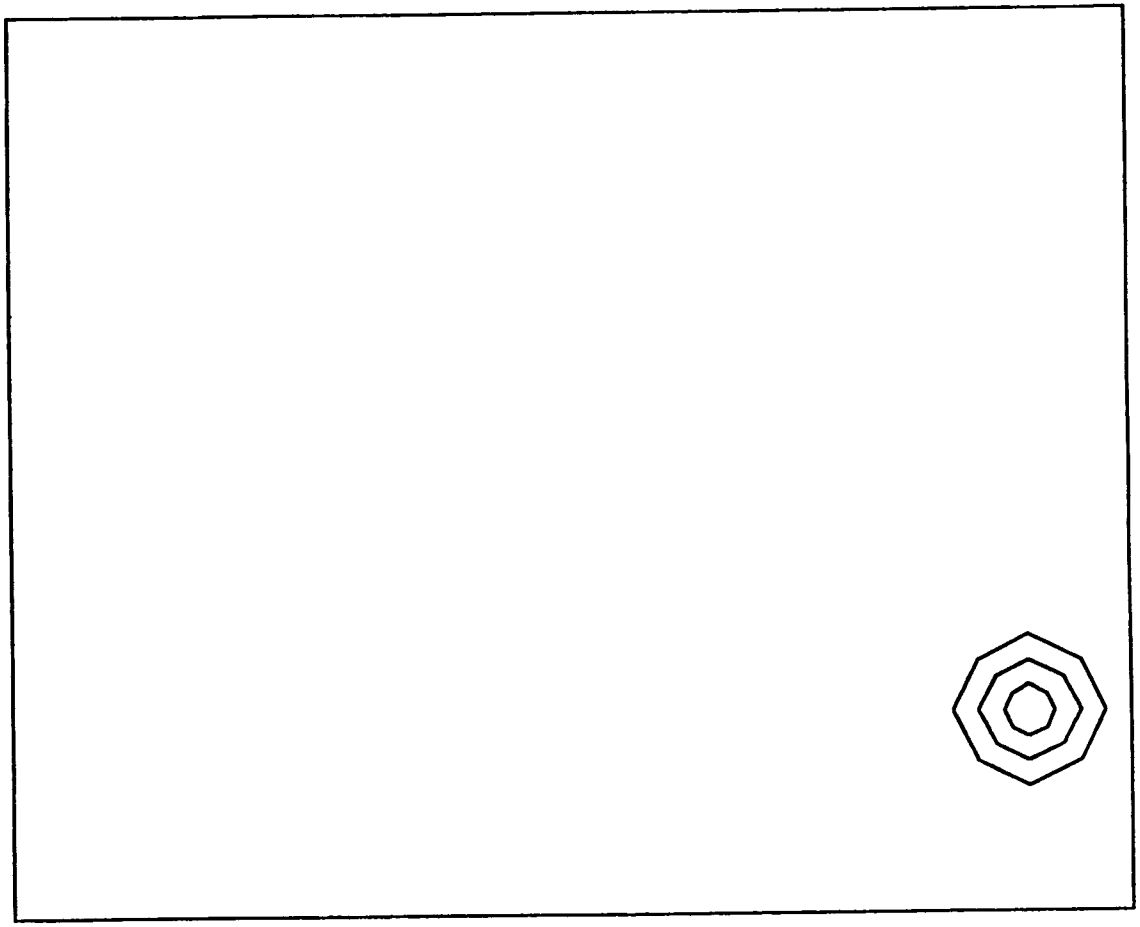

- SAME SWEATSHIRT, SAME BODY, SAME POSITION, SAME CONDITIONS, SAME FILTERING, SAME EVERYTHING, EXCEPT.... NO HANDGUN

IMAGING RANGE VS. ULTRASOUND FREQUENCY

Most of our ultrasound work in Phase 1 was concentrated at two frequencies, 40 and 200 kHz. At 40 kHz, we imaged a handgun at 15 ft. with 4-in. resolution using an 18-in. transmitter dish. We tested the ultrasound sensor to ranges of 25 ft., but were not able to produce images at that range. Most of the 200-kHz imaging was done at a range of 4 to 5 ft. The range at this higher frequency is limited by the attenuation of 200-kHz ultrasound in air, which we measured to be 9 dB/m. At all frequencies, we routinely achieved a resolution that was within a factor of two of the diffraction limit, despite using inexpensive focusing optics. Mostly, we used an 18-in. aluminum solar concentrator that costs about $30 from Edmund Scientific. Because even at 200 kHz the wavelengths are >1 mm, high resolution can be achieved easily and simply without rigorous tolerance requirements on surface figure or smoothness.

At 40 kHz, the attenuation in air is so low that it does not limit the range. Instead, the range at low frequencies is limited by the need to illuminate the target with a wide range of aspect angles. Ideally, the best illumination of the target by an active ultrasound source is omnidirectional. The closest approximation of this illumination with an active ultrasound source is a large diffuse transmitting dish. The range of aspect angles incident on the target shown in the figure on the facing page is the diameter of the diffuse dish divided by the range to the target.

IMAGING RANGE VS. ULTRASOUND FREQUENCY

Frequency (kHz)	Imaging Range (ft)	Resolution @ Range (in.)	Range-Limiting Factor
40	15	4	18-in. Transmitter
40	25	?	18-in. Transmitter
200	4	0.6	~10-dB/m Attenuation

- We routinely achieve diffraction-limited resolution at 40 and 200 kHz
- Transmitter aspect angle limits range at 40 kHz to about one foot of range per inch of diameter

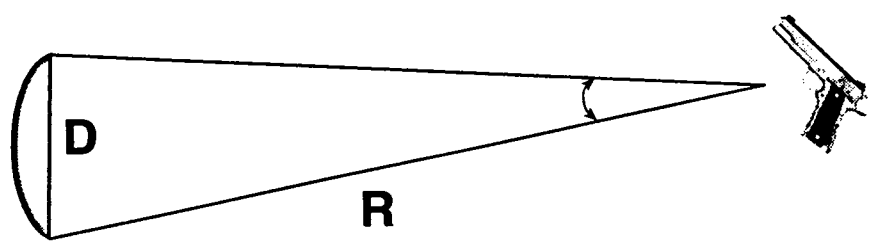

CONCEALED HANDGUN AT 15 FEET

The facing picture shows a handgun and ultrasound image at 40 kHz of the same handgun to the same scale. The resolution with 18-in. receiver dish, about 4 inches, is indicated by the scale. The six pixels of the image are probably representative of an image of a handgun with 4-in. resolution. It is a true image, however, as shown in the next chart.

CONCEALED HANDGUN AT 15 FEET

- HANDGUN CONCEALED ON HUMAN BODY UNDER WOOL SWEATER

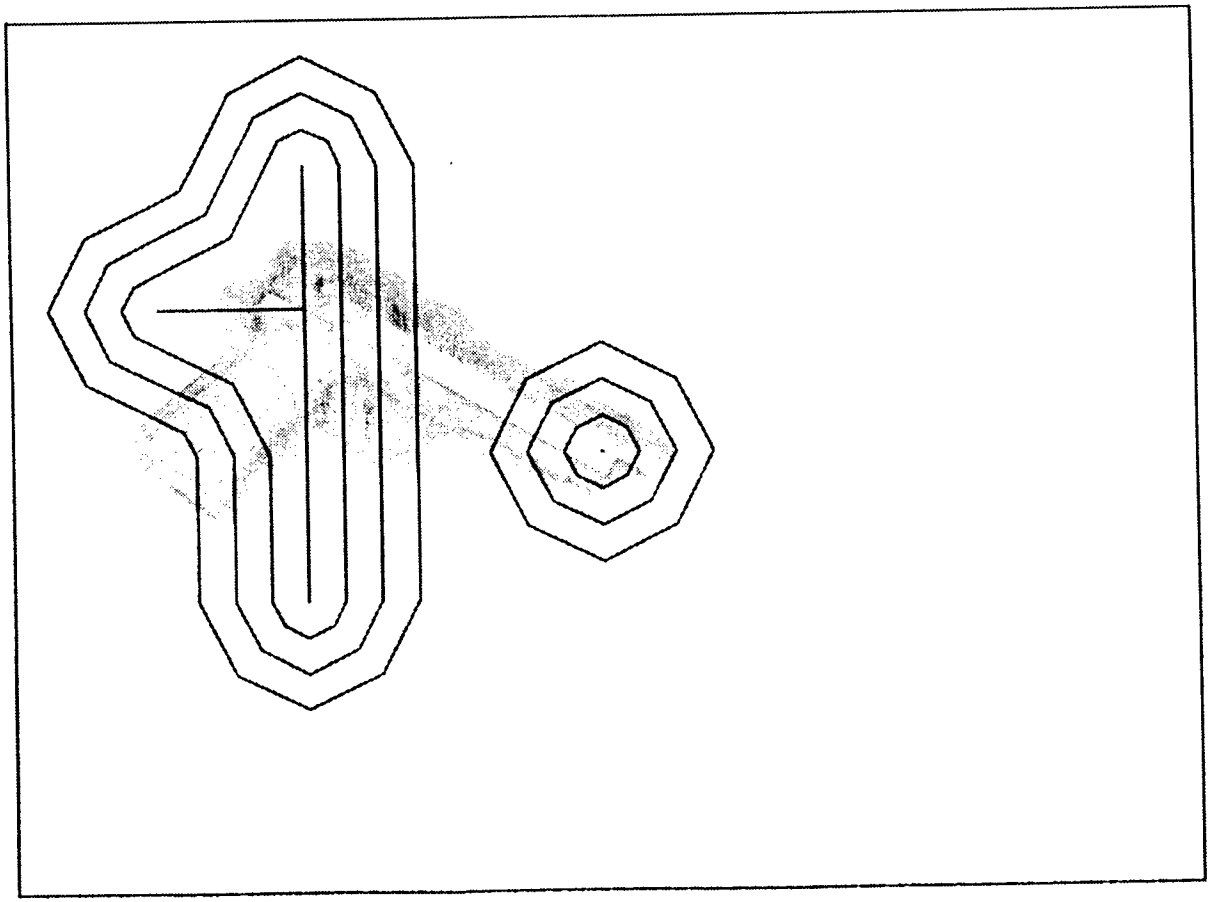

RESOLUTION

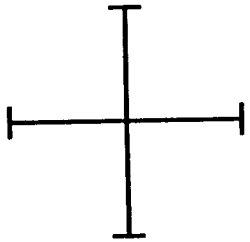

NO CONCEALED HANDGUN AT 15 FEET

When the handgun was removed from the under the sweater and an image of the same body, in the same position, wearing the same clothing, under the same conditions and with the same processing and filtering was taken, the result was no pixels above the brightness threshold, as shown in this figure. Even at a range of 15 ft., the marked difference between a concealed weapon and no concealed weapon persists.

NO CONCEALED HANDGUN AT 15 FEET

- SAME SWEATER, SAME BODY, SAME POSITION, SAME CONDITIONS, SAME FILTERING, SAME EVERYTHING, EXCEPT.... NO HANDGUN

JAYCOR MINE-DETECTION RADAR

This photograph shows the mine-detection radar that was used to detect concealed weapons at ranges over 10 m in Phase 1. Of course, the mine-detection radar needs to be mobile, even though a CWD radar does not. The one transmitter horn is in the middle and the stereo receiver horns are on the outside for azimuthal accuracy. The radar equipment fills most of the back of the jeep, but, as mentioned, will be made much more compact by Spring 1997 in the ongoing upgrade program.

JAYCOR MINE-DETECTION RADAR

RADAR SOFTWARE BLOCK DIAGRAM

The radar software has been optimized for mine detection from a moving vehicle, and not for CWD on moving targets. Nevertheless, the software was adapted for detecting concealed weapons on humans. The accuracy of the system that we tested in Phase 1, before the upgrade, gave the range to the concealed weapon within inches and the azimuth to within about 0.7 degrees, or about 5 in. at a 10-m range.

RADAR SOFTWARE BLOCK DIAGRAM

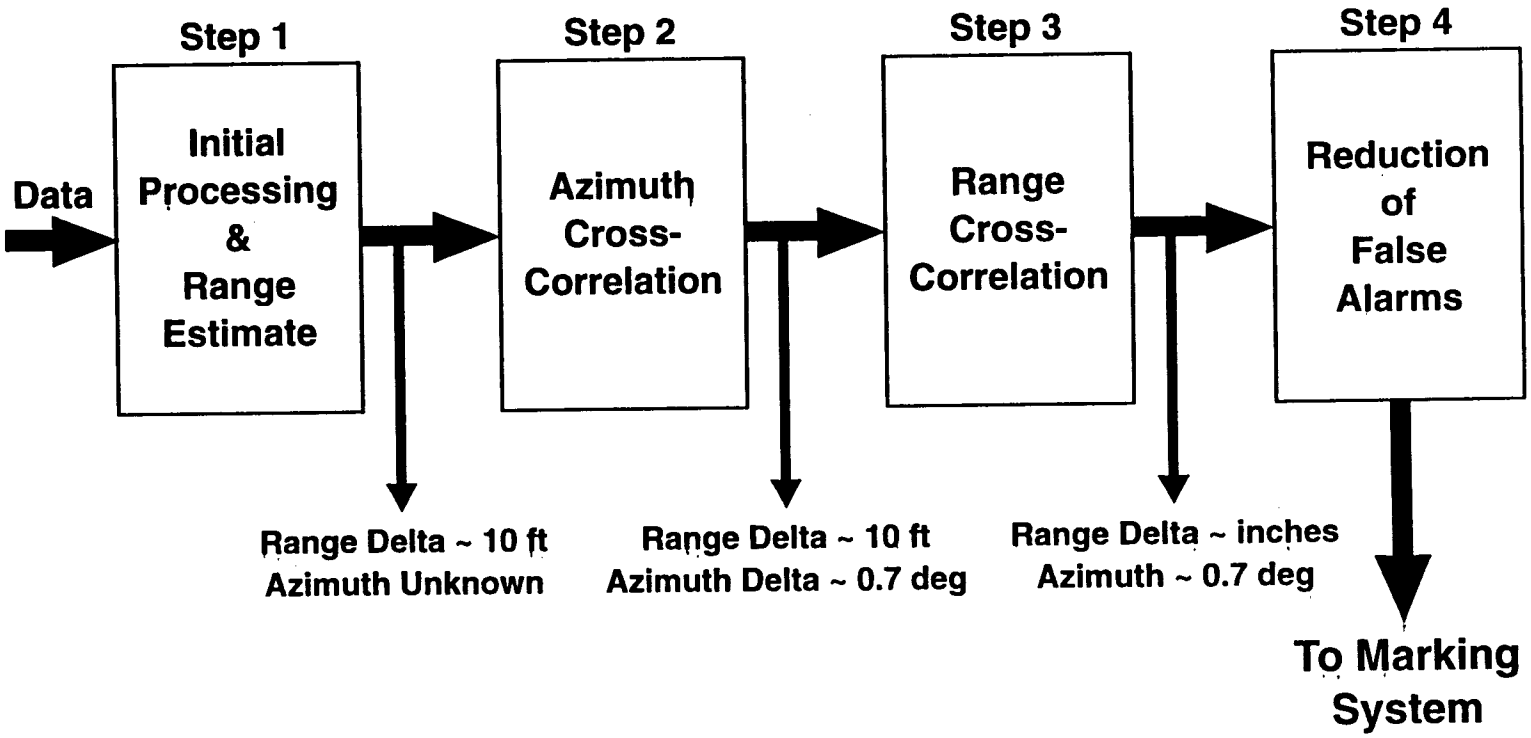

RADAR CWD TEST RESULTS

This figure is a typical example of spectral data of a person with and without a handgun at a range of 10 m. The radar measures returns at 100-MHz intervals between 0.5 and 4 GHz. The spike at about 3 GHz is characteristic of a person carrying a handgun, and is usually missing from the spectrum of same person without the handgun. More data of this type, which appears later in this report, suggests a probability of detection for the mine-detection radar, unoptimized for CWD, of about 80%.

RADAR CWD TEST RESULTS

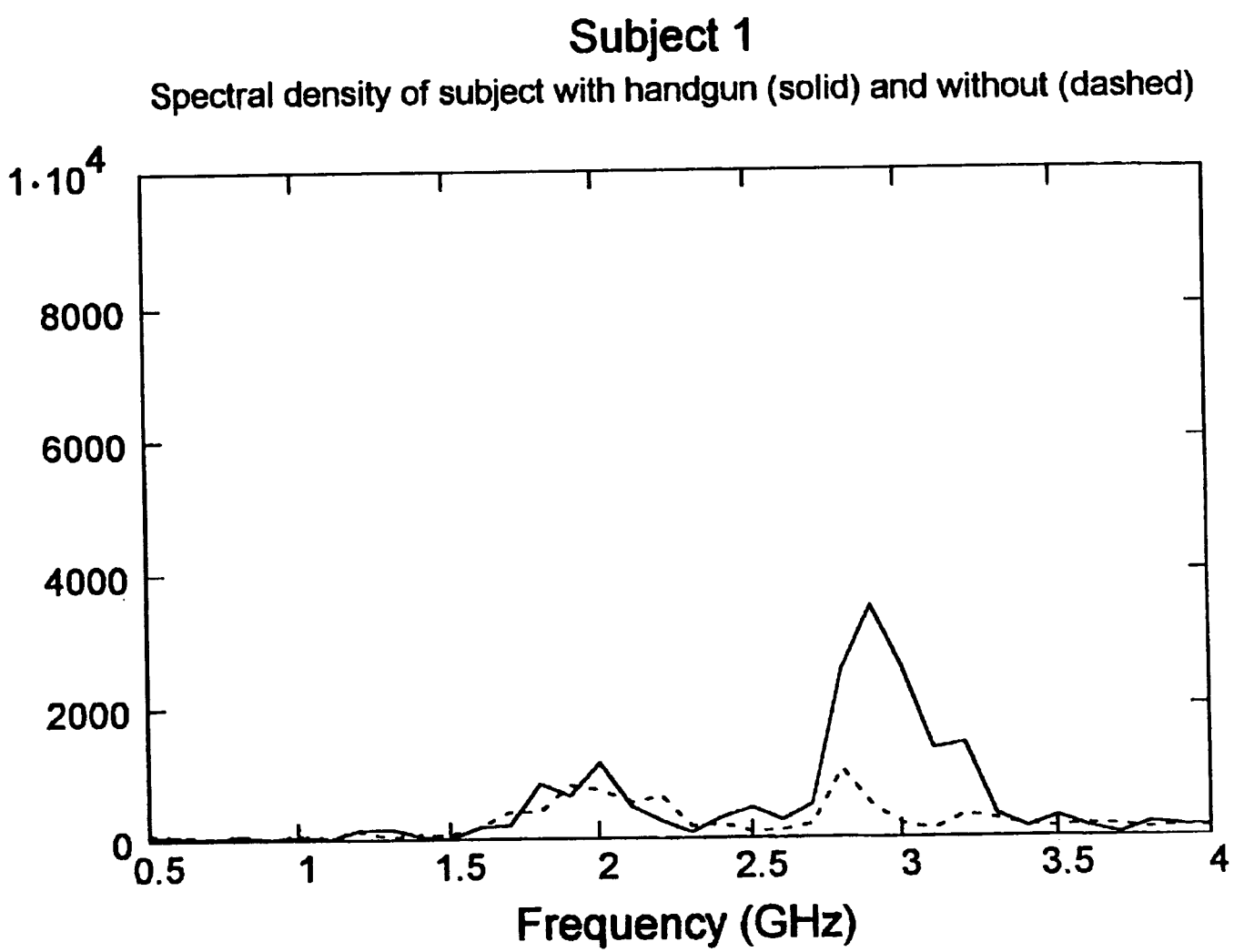

PHASE 1 RADAR CONCLUSIONS

The mine-detection radar has been used in the Phase 1 CWDT Program to locate moving humans in real time and to detect nonmetallic (plastic bars) and metallic concealed weapons at ranges up to 25 m. The challenge to the use of an active radar system, such as the mine-detection radar, for CWD is discriminating concealed weapons from their human carriers. Thus far, no filtering techniques specific to CWD have been implemented on the mine-detection radar. Neither have any hardware changes been made to the radar system specifically for CWD. In this report, we will point out certain hardware changes that might be made, such as from a vertical to a circular polarization, that might increase the probability of detection of concealed weapons on moving humans. The upgraded radar under the new Army program is now scheduled to be completed April 1997. The upgraded radar will have improved performance, including improved shot-to-shot reproducibility, and will be much more compact than the version we used in Phase 1.

PHASE 1 RADAR CONCLUSIONS

- JAYCOR mine-detection radar successfully locates moving humans and nonmetallic and metallic concealed weapons to 25 m

- Discrimination of concealed weapons requires

  — Improved shot-to-shot reproducibility
  — New filtering techniques
  — Hardware changes (lower frequencies, circular polarization, etc.)

- JAYCOR/Lockheed Army project anticipates new mine-detection radar with improved shot-to-shot reproducibility by December 1996

  — Improved technology will aid CWD

PHASE 2 ULTRASOUND UPGRADES

This table shows in the left column the characteristics of the ultrasound breadboard sensor that was developed and demonstrated in Phase 1, and in the right column the characteristics of the brassboard ultrasound sensor that we have proposed for Phase 2. Since the Phase 1 breadboard sensor uses only one detector at a time, images must be constructed by scanning the receiver dish pixel by pixel over the target area. Typically, it takes 30 minutes to produce an image of the order of 12 x 12 pixels in this manner. Since the breadboard ultrasound sensor operates at only one ultrasound frequency, it may be used either for detecting weapons at long ranges at low frequencies or for imaging weapons at close ranges using higher frequencies. The low frequencies are better for low-resolution distant detection of weapons, and the high frequencies are better for high-resolution close imaging. The breadboard sensor cannot offer both capabilities at the same time. Also, the breadboard sensor must acquire all of the data before the data is processed and filtered afterwards. The primary processing is by binary thresholding of individual pixels. That is, a brightness threshold is set for the image, depending on transmitted power, range, clothing concealment, and detector sensitivity. A spectral density above the brightness threshold appears as a positive pixel in the image, and one below does not.

Since the time required to collect the data for a single image is so long, we must first carefully map out the area to be imaged by the breadboard sensor. This is done with the aid of a laser pointer and an x-y translational stage with a controller for the motion of the receiver dish.

The resolution and the range of the breadboard ultrasound sensor are both limited by the sizes of the receiver and transmitter dishes, respectively. The diffraction-limited resolution is proportional to the diameter of the receiver dish, and the range of aspect angles that can be made to be incident on the target is proportional to the diameter of the diffuse-source transmitter dish.

The Phase 2 brassboard ultrasound sensor will operate at video frame rates of 30 ms per image. It will be equipped with Aerojet's ultrasound imaging array of about 50 x 50 pixels. We would expect the Phase 2 brassboard to operate at two frequencies, 40 kHz and 160 to 200 kHz. The dual frequencies would allow both distant detection at the lower frequency and close-range imaging at the higher frequencies. Since the ultrasound sensor should be capable of imaging concealed weapons in real time, it will have tuning and filtering knobs, probably as controls on a PC controller. Human factors considerations will be involved in the decisions on filtering and displaying the image data. Gray-scale pixels may improve recognition of concealed weapons by the users over binary thresholding. With dual frequencies, and the lower frequency used for distant detection, it should be possible to automatically centroid a concealed weapon by centering the sensor on the area of brightest return. The ultrasound image might even be superimposed on a low-intensity video camera image. The processor might even draw the user's attention to the area of a potential concealed weapon by presenting that area within a box on the monitor. A larger receiver dish and transmitter dish or array will also help improve the resolution and range of a Phase 2 ultrasound brassboard sensor.

PHASE 2 ULTRASOUND UPGRADES

Phase 1 Breadboard	Phase 2 Brassboard
30 minutes/image	30 milliseconds/image
12 x 12 pixel images	50 x 50 pixel images
Close imaging <u>or</u> distant detection	Close imaging <u>and</u> distant detection
Single frequency	Dual frequencies
Post-processed tuning/filtering	Real-time tuning/filtering knobs
Binary thresholding of pixels	Variable amplitudes of pixels
Laborious preframing of images	Automatic centroiding
Resolution limited (18" rcvr)	Improved resolution (30" rcvr)
Range limited (18" x-mtr)	Improved range (30" x-mtr)

PHASE 2 RADAR UPGRADES

This table shows in the left column the characteristics of the Phase 1 breadboard sensor tested for CWD and in the right column the characteristics of the brassboard radar sensor that we propose to build in Phase 2. The radar that we used in Phase 1 was optimized for detecting mines from moving vehicles. The 60-degree field of view (FOV) was adequate for detecting mines at ranges of tens of meters. The frame rate of 2 s per (spectral) image was adequate for slow motion (5 mph) through mine fields, and the 6 cu.ft. of equipment was adequate for the prototype device. The 36 frequencies produced by the radar from 0.5 to 4 GHz covered the range of resonance frequencies of buried metallic and nonmetallic mines. The vertical polarization of the radar also was ideal for finding mines.

A brassboard radar, dedicated to concealed weapons detection, will be built in Phase 2. The brassboard radar will use the hardware technologies of the Phase 1 radar and of the ongoing upgraded radar program, but will design the software specifically to be optimized for CWD. The radar will have the faster spectral image rate of 0.5 s per image of the upgraded radar, and will have the more compact 2 cu.ft. volume of the upgraded radar, but will have a wider FOV, which is valuable for the CWD mission. Also, to access the resonance frequencies of some longer concealed weapons, some frequencies below 500 MHz will be included in the radar spectrum. Lastly, since the orientation of a long concealed weapon is not known beforehand, circular polarization may be the best choice for CWD.

PHASE 2 RADAR UPGRADES

Phase 1 Breadboard	Phase 2 Brassboard
Mine-detection radar	Dedicated CWD radar
Optimized for moving radar/ stationary targets	Optimized for stationary radar/ moving targets
60° FOV	90° FOV
2 seconds/image	0.5 second/image
Radar 6 cu. ft.	2 cu. ft. with cooling
Frequencies (0.5 to 4 GHz) optimized for mines	Frequencies optimized for CWD
Vertical polarization for mines	Circular polarization for CWD

PHASE 1 BREADBOARD

Ultrasound Sensor Design and Operation

COMPUTER CONTROLLER

The 486 notebook PC in the breadboard ultrasound sensor performed three important functions: controlling the motor drive, data acquisition, and image processing. A software program called CWD was written to control the vertical scanning of the receiver dish in coordination with data acquisition. The CWD program stepped the motor drive controller pixel-by-pixel through vertical scans of the target area. At each pixel, the stepper motor paused long enough to allow the ultrasound pulses to be produced and received, and the data stored in the digitizing oscilloscope, before proceeding to the next pixel. The CWD program took each of the 512 data points from each pixel and placed them in an array containing data from all the n x m pixels of the image. The notation here is that each image had n horizontal rows of pixels and m vertical columns. After all 512 x n x m data points had been acquired in the digitizing oscilloscope by the CWD program, the data was read through a GPIB interface into the notebook computer. An image processing program, IMAGE, was written to process the data inside the computer and produce an image.

COMPUTER CONTROLLER

- Notebook PC configured to control stepper-motor and data acquisition
- Image Processing Software also installed to handle post-scan processing

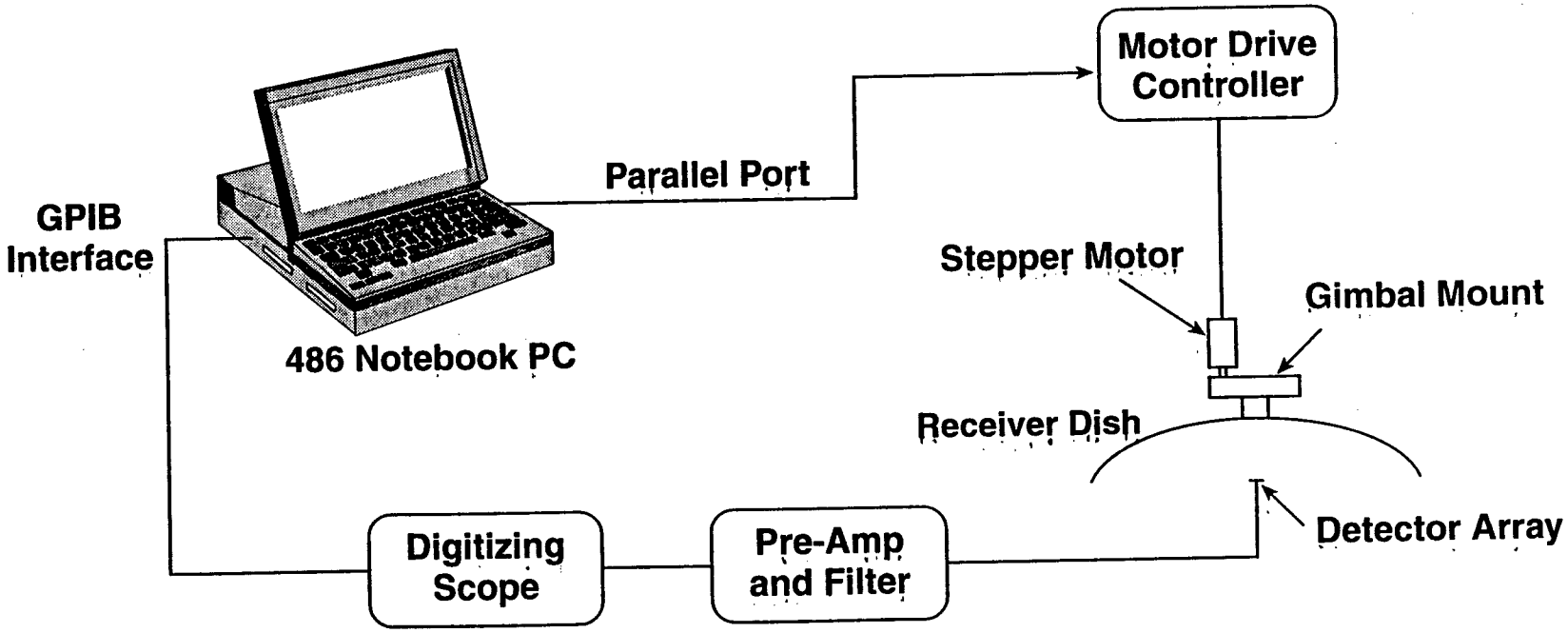

DETECTOR ELECTRONICS

In the Phase 1 breadboard ultrasound sensor, the detector signal was fed through a pre-amplifier to a tuned active bandpass filter/amplifier, and from there to the digitizing oscilloscope. The tuning and amplifying functions will be performed the on ultrasound focal plane array (FPA) in the Phase 2 brassboard sensor. A digitizing oscilloscope is not needed in the Phase 2 sensor, and will be replaced by a high-speed commercial processor chip.

DETECTOR ELECTRONICS

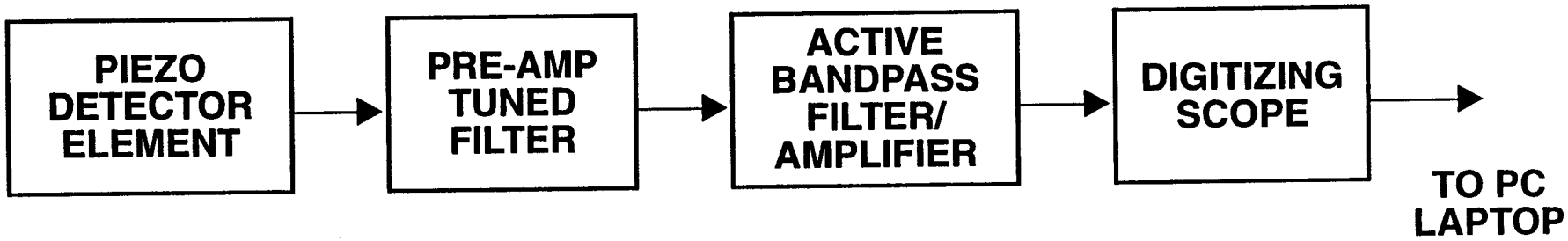

- Pre-amp, band-pass filter and amplifier stages to be consolidated into detector array
- Digitizing scope to be replaced with high-speed off-the-shelf array processor chip

CWD DATA ACQUISITION TEST SETTINGS

This chart shows a sample screen from the CWD data acquisition program. Inputs for the pixel array and size of pixels are provided before the automatic scanning sequence begins.

CWD DATA ACQUISITION TEST SETTINGS

(1)	Scope Channel	1
(2)	Pts to Acquire	512
(3)	Rows in Grid	12
(4)	Columns in Grid	12
(5)	X Spacing (turns)	1
(6)	Y Spacing (turns)	.5
(7)	File Name Prefix	0727
(8)	Auto Test Sequence	Yes
(C)	Continue	

Enter selection:

DATA ACQUISITION PROGRAM FOR CWD IMAGING

This chart shows another sample screen from the CWD program. Options are given for controlling the receiver dish, acquiring data, and finally converting the data to a format used by the image processing program.

DATA ACQUISITION PROGRAM FOR CWD IMAGING

1. Transfer waveform from scope
2. Convert data to Mathcad format
3. Motor control
4. Scope control
5. Reset test parameters
6. Exit to DOS

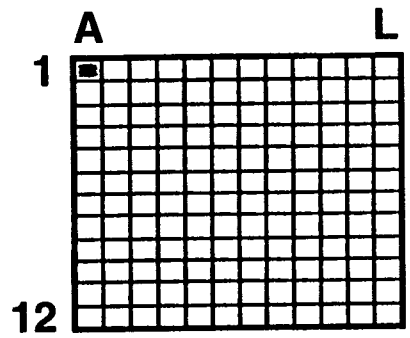

←→↑↓ CWD Grid
(M) Move Motor

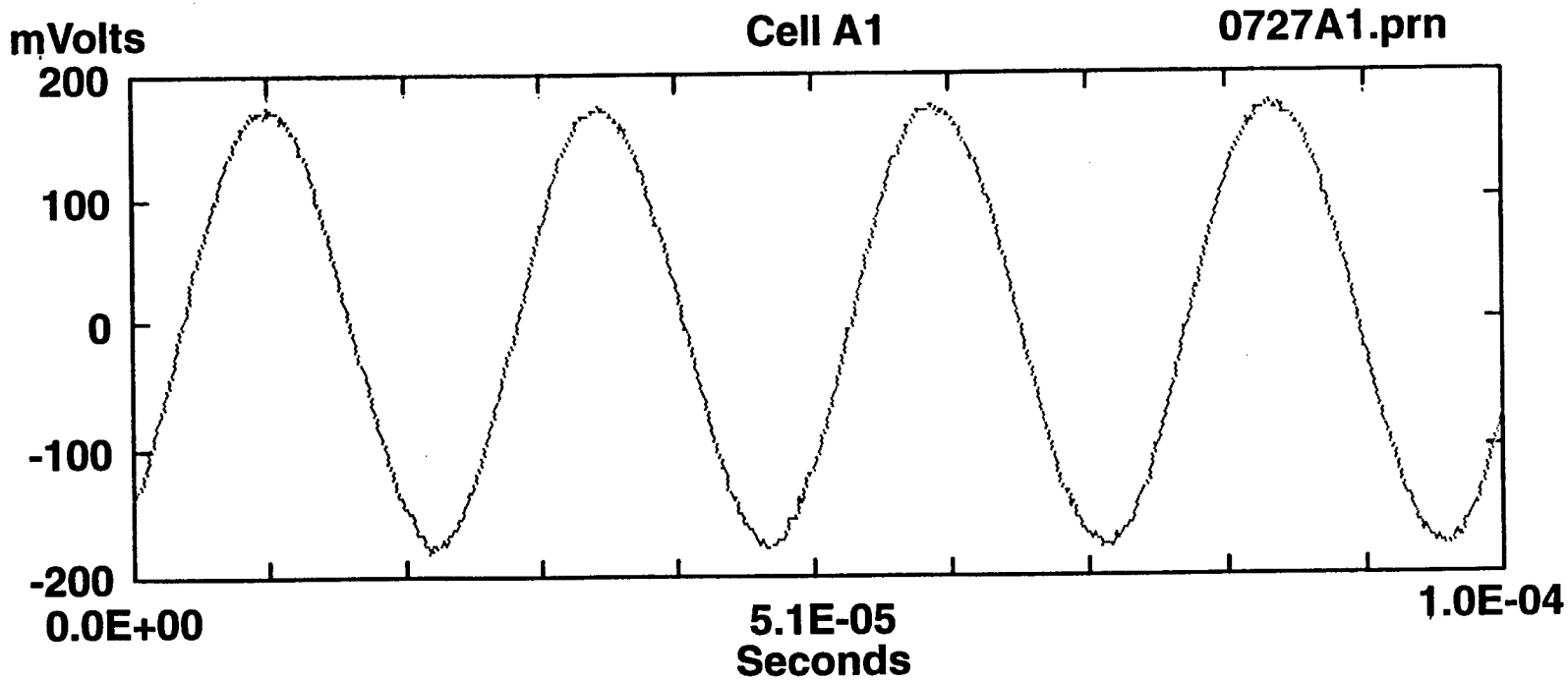

PHASE 1 BREADBOARD

Ultrasound Image Processing

ULTRASOUND SENSOR RESOLUTION

Ultrasound obeys the same wave diffraction and geometrical optics equations as light, but has a much longer wavelength. This means that near-diffraction-limited resolution can be achieved at ultrasound wavelengths of interest easily and cheaply. Finely polished optics are not needed for focusing ultrasound. In virtually all cases, the resolution of our images was limited by diffraction. Generally, though, the diffraction limit of resolution was not much different from the geometrical optics limit.

ULTRASOUND SENSOR RESOLUTION

- Ultrasound obeys same diffraction and geometrical optics equations as light
- Ultrasound resolution limited by:
  - Diffraction
  - Geometrical optics (ray-tracing)

  whichever is worse
- We routinely achieve diffraction-limited resolution at $\lambda = 1.7$ mm (200 kHz) and $\lambda = 8.5$ mm (40 kHz)

TEST STAND FOR MEASURING ULTRASOUND RESOLUTION

This figure shows a test we performed in which resolution was limited by geometrical optics rather than diffraction. The vertical post acts as a thin slit for diffraction, because at any angle of viewing, specular reflection from the post occurs only along a thin line on the post. The aperture on the detector blocks all ultrasound except that which is directly incident on the aperture. The geometrical-optics-limited resolution in this configuration at 200-kHz frequency is about 1.6 cm. The diffraction-limited resolution, calculated on the next page, is slightly higher at about 1.75 cm.

TEST STAND FOR MEASURING ULTRASOUND RESOLUTION

- Achieved theoretical-limit resolution

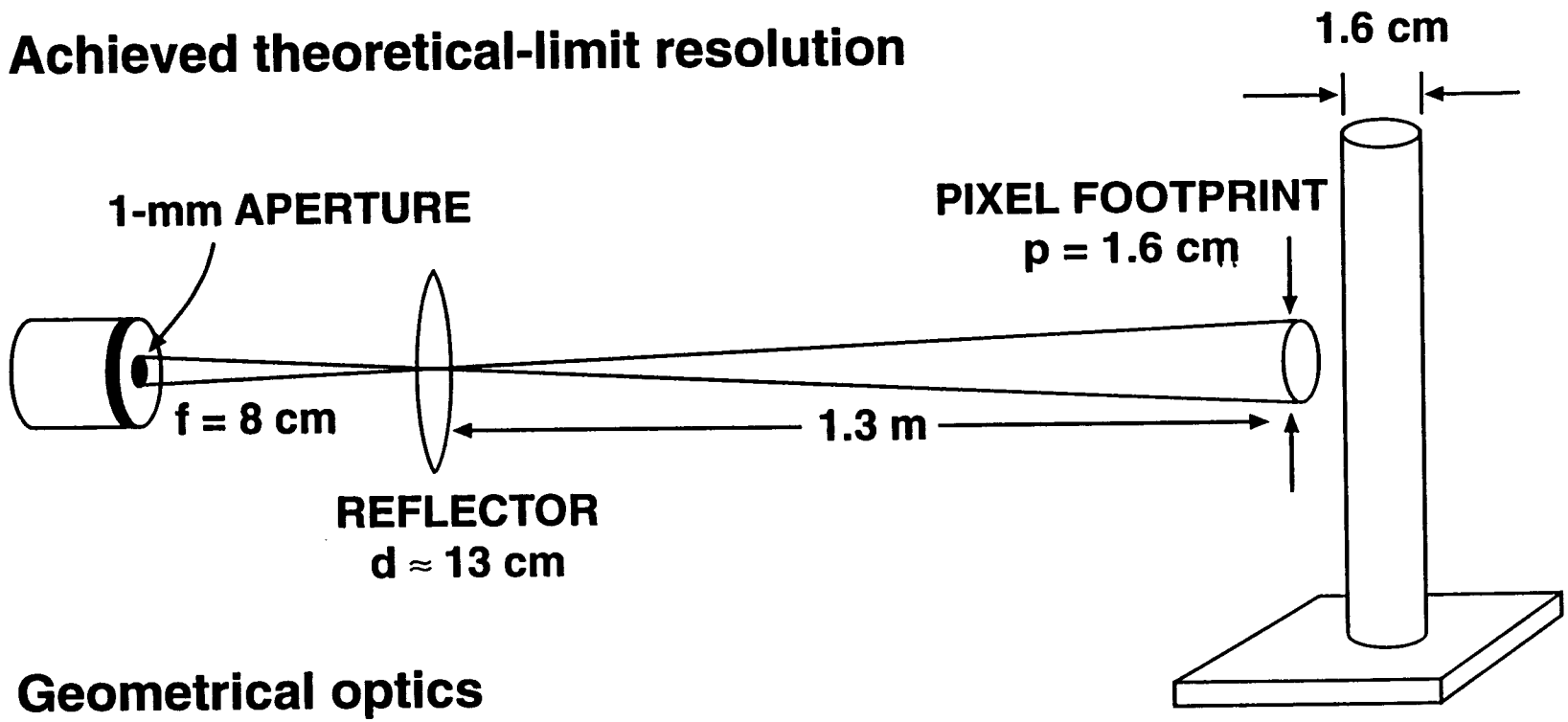

- Geometrical optics

$$p \approx \left(\frac{1\,\text{mm}}{8\,\text{cm}}\right) 1.3\,\text{m} \approx 1.6\,\text{cm}$$

- Aperture on transducer used in lieu of mm-sized detectors

ULTRASOUND RESOLUTION MEASUREMENT AT 200 kHz

This figure shows the data of an azimuthal scan of the ultrasound echo returning from the cylindrical post shown on the previous page. The full-width at half-maximum (FWHM) of the ultrasound intensity is about 1.6 cm which is about equal to the geometrical-optics-limited resolution and the diffraction-limited resolution of our test set-up. In general, virtually any configuration we used had a resolution within a factor of two of the diffraction limit.

ULTRASOUND RESOLUTION MEASUREMENT AT 200 kHz

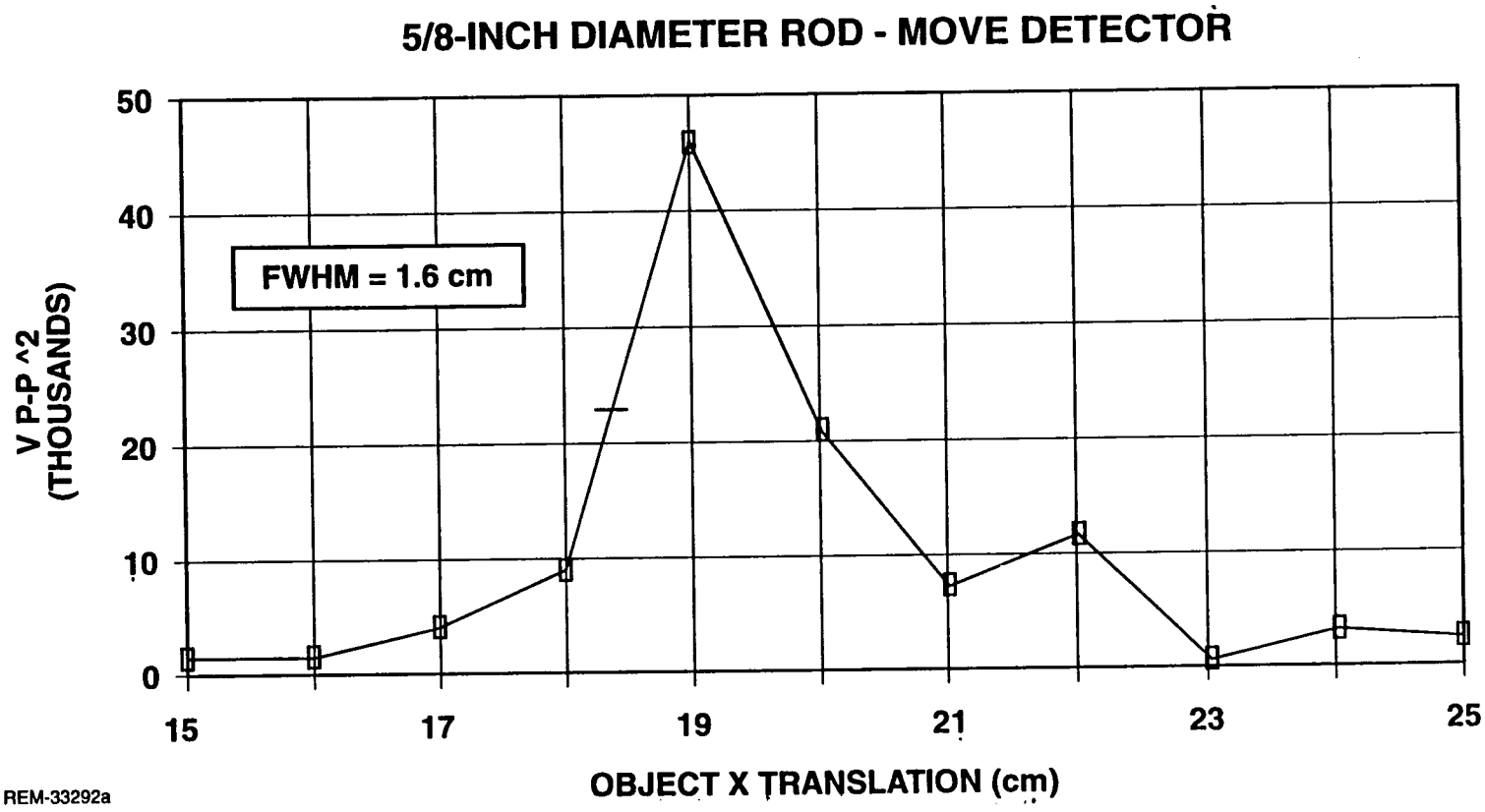

- $R_g \approx \frac{a}{f} r \approx \frac{1\,mm}{8\,cm} 1.3\,m \approx 1.6\,cm$
- $R_d \approx 1.03 \frac{\lambda}{d} r \approx 1.03 \frac{1.7\ mm}{13\ cm} 1.3\ m \approx 1.75\ cm$

LOW-FREQUENCY ULTRASOUND FOR LONG-RANGE DETECTION

At an ultrasound frequency of 40 kHz, the range of a CWD sensor is not limited by attenuation in air, which is only about 1 dB/m. Instead, the range at low frequency is limited by the diversity of aspect angles with which the target can be illuminated. The diversity of aspect angles, in turn, is limited by the diameter of the transmitter dish. Increasing the size of the transmitter not only increases the range by increasing the diversity of aspect angles illuminating the target, but also improves the resolution in proportion to the diameter of the dish. At 15 feet, we have measured the resolution at 40 kHz to be 3.4 inches using an 18-inch diameter dish. In Phase 2, we plan to increase the range and improve the resolution by using a 30- to 36-inch transmitter dish at 40 kHz. A 3-foot dish will give 2-inch resolution at 15 feet and 4-inch resolution at 30 feet.

LOW-FREQUENCY ULTRASOUND FOR LONG-RANGE DETECTION

- At 40 kHz, range of concealed weapons detection is limited only by size of transmitter dish to about 1 ft/in
  - Attenuation is only ~1 dB/m
- Diffraction-limited resolution of 18" dish

$$R_d = 1.03 \frac{\lambda}{d} r \approx 3.4'' \text{ at 15 ft}$$

- Measured resolution

$$R_d \approx 4'' \text{ at 15 ft}$$

- Can achieve 2" resolution at 15 ft and 4" resolution at 30 ft with 3-ft dish at 40 kHz

ULTRASOUND SIGNALS TRANSMITTED THROUGH CLOTHING

The transmission of ultrasound through clothing was tested for a wide variety of types of clothing at two different ultrasound frequencies, 40 and 200 kHz. The measurements were made by placing a pair of transducers 2 m apart and inserting articles of clothing between them. The numbers shown in this table are the voltage signal measured by the receiving transducer normalized to the voltage received when no clothing was between the transmitter and receiver. In general, clothing transmits 40 kHz better than 200 kHz, just as air does. A 50% transmitted voltage signal corresponds to a factor of 4 loss of intensity, or about 6 dB attenuation loss. By comparison, the dynamic range of our detector amplifier was 120 dB. That is, the amplifier saturated at 6 V, and the signal was lost in noise at 6 μV. At high signal strengths, disconnecting the amplifier added about another 25 dB to the dynamic range of the sensor. Even the least transmissive article of clothing tested, the down-filled winter coat with nylon shell, attenuated 40-kHz ultrasound by only 70 dB in a roundtrip through the coat, opening the possibility that a concealed weapon might even be detected under such an article of clothing.

ULTRASOUND SIGNALS TRANSMITTED THROUGH CLOTHING

Material	Transmitted Voltage Signal (%) @ 40 kHz	Transmitted Voltage Signal (%) @ 200 kHz
Baseline	100	100
Heavy Polyester Sweatshirt	69	44
Nylon/Polyester Shop Coat	67	55
Cotton Flannel Shirt	57	33
Acrylic Sweatshirt (folded double)	52	16
Wool Sweater	47	11
Wool Navy Pea Coat	34	11
Cotton Sweatshirt (folded double)	23	0.82
Wool Suit Coat #1	18	7.7
Wool Suit Coat #2	15	5.5
Wool Suit Coat #3	12	2.2
Down-Filled Winter Coat, Nylon Shell	1.4	0.11

IMAGE PROCESSING BY "IMAGE"

An image processing program, IMAGE, was written specifically to process the images produced by the Phase 1 ultrasound breadboard sensor. IMAGE was written as an interactive document on Mathcad® PLUS 6.0, a commercial math program. IMAGE was loaded onto the same notebook computer used for data acquisition and controlling the receiver dish. The IMAGE program prompts the user for inputs to enable it to read the image data files and to filter and process the ultrasound images. After reading the files, IMAGE first eliminates low-amplitude noise before tuning to the ultrasound frequency passband. The maxima in spectral density of each pixel are arranged in an n x m matrix corresponding to the pixel arrangement in the image. Then brightness and contrast filters are applied before displaying the images. This software program is only applicable for the Phase 1 breadboard sensor, and not for the Phase 2 brassboard sensor, which will do most of its processing on the focal plane.

IMAGE PROCESSING BY "IMAGE"

- Image processor is interactive document on Mathcad® PLUS 6.0, which operates in same notebook computer used for data acquisition

- IMAGE asks for inputs to enable it to

  — Read n x m data files
  — Eliminate low-amplitude noise
  — Tune to the ultrasound frequency
  — Arrange in-band pixel maxima as n x m matrix
  — Apply brightness and contrast filters
  — Display intermediate and final images

- IMAGE was developed for Phase 1 breadboard only, not for Phase 2

NOISE FLOOR SET AT 1.5 σ

The traces shown here and in the following figures are actual examples of data from the image of a lexan knife, showing how that image was developed.

The first processing step by the IMAGE program is to filter out low-amplitude noise. The program calculates the standard deviation σ of the signal in each pixel. Any of the 512 data points in a signal trace that has a magnitude $<1.5\ \sigma$ is set equal to 0. The signal in the upper left is filtered by this method to give the signal shown in the upper right figure. This signal is typical of the return from that part of the imaged area that conceals a weapon. The noise shown in the lower left figure is typical of the return from a part of the imaged area that does not conceal a weapon. When this typical noise trace is filtered with a 1.5-σ threshold, the result is shown in the lower right figure. When the noise is filtered by this method, the high-frequency content, within the passband of the frequency filter, is mostly lost. The filtered signal in the upper right figure, on the other hand, retains the high-frequency signal content for further processing.

NOISE FLOOR SET AT 1.5 σ

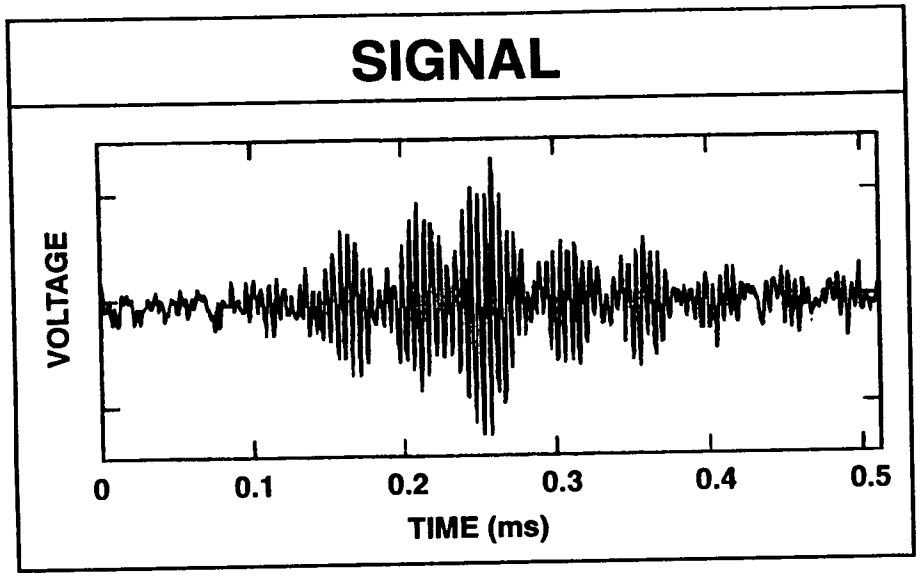

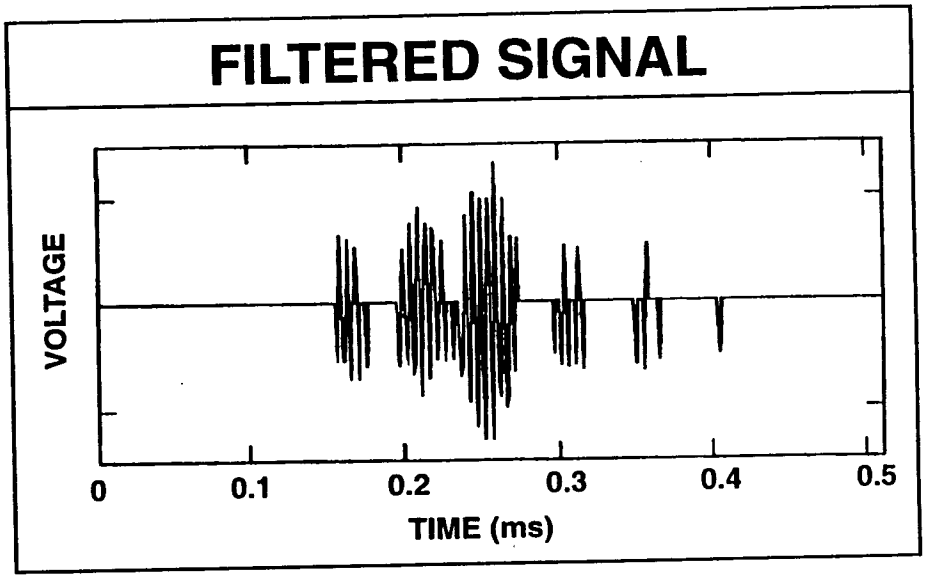

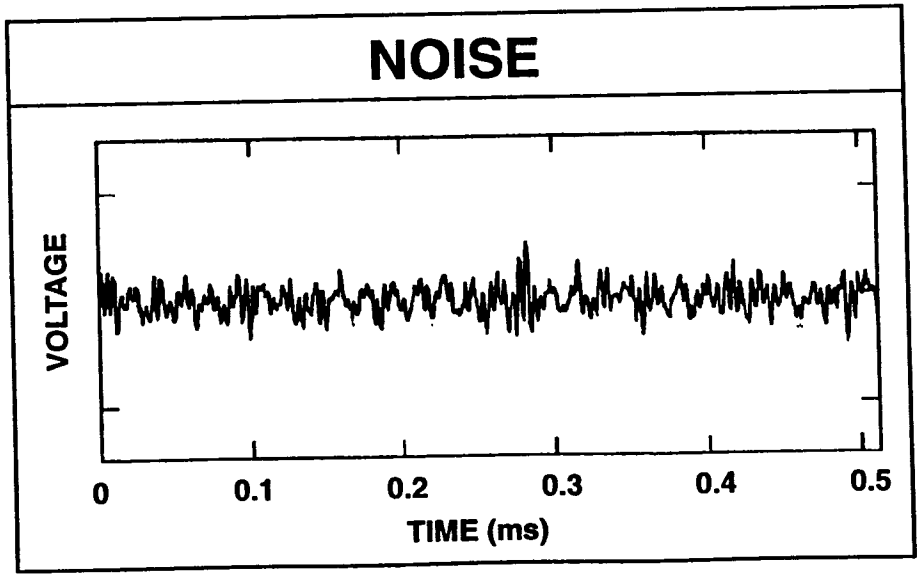

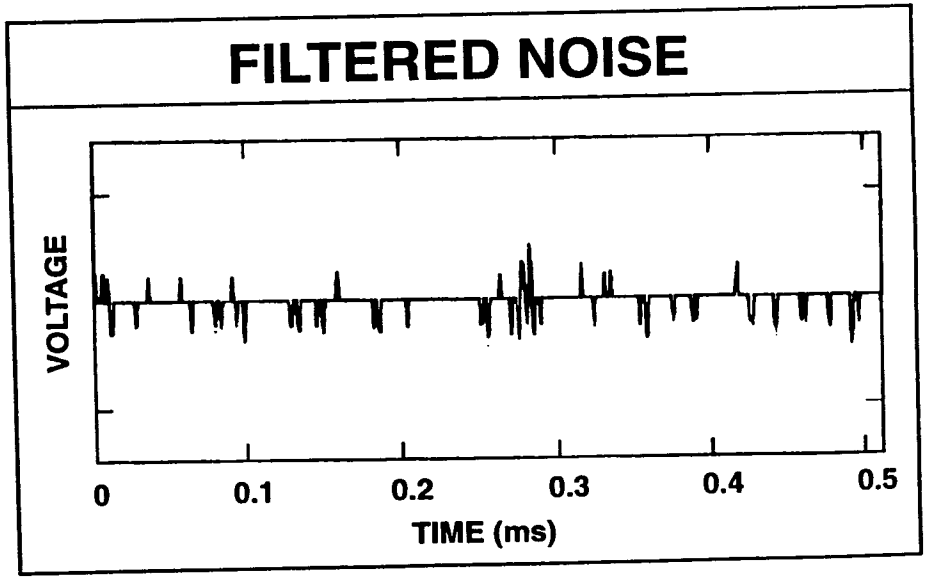

FREQUENCY FILTER SET AT 4%

After the signals and noise have been filtered for low-amplitude noise, the resulting traces are Fourier transformed to give the spectral density of the signal trace for each pixel. A typical spectral density for the filtered signal shown on the preceding page is shown below on the left. The IMAGE program numerically selects a frequency passband at the operating ultrasound frequency of the sensor. Typically the width of the passband is about 4%. Only one number is associated with each pixel. That number is the peak magnitude of the spectral density of the noise-filtered signal within the frequency passband. That is, in the facing figure on the right below, the peak amplitude of the spectral density spike within the frequency passband is saved.

FREQUENCY FILTER SET AT 4%

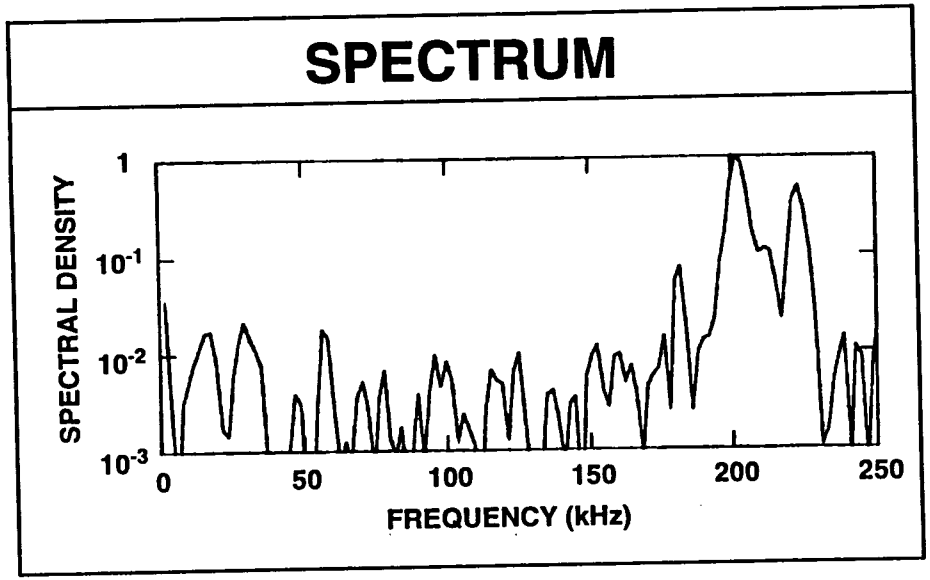

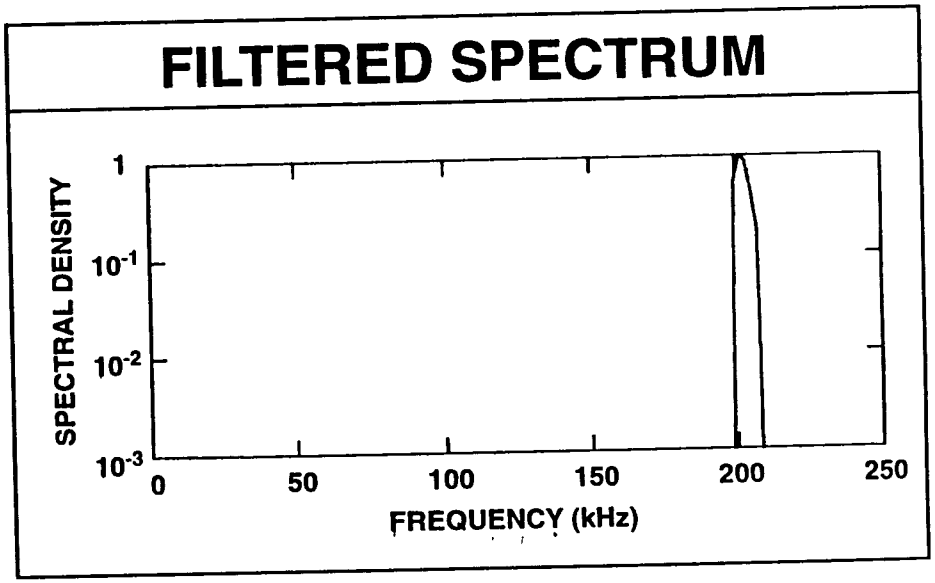

IMAGE ARRAYED AND FILTERED FOR BRIGHTNESS

The spectral density peaks for each pixel are associated with each pixel as in the upper-left facing figure. The IMAGE program arrays these spectral density peaks into a 2-D matrix corresponding to the scanned image, as shown in the upper-right figure. The surface plot is also recorded as a contour plot, as in the lower-left figure. The contour plot is then filtered for brightness, to remove the small spectral-density maxima that survived the noise filtering. The brightness-filtered contour image is shown in the lower-right figure. The last processing step of the IMAGE program is to filter for contrast. The brightness filter set a floor, below which any amplitudes were set equal to 0. The contrast filter sets a ceiling, above which any amplitudes are set equal to the ceiling. The contrast filtering removes the bright ultrasound glints and gives a better cosmetic appearance to the image, as shown on the next page. We have found that for this particular image processing program, the best image appearance is achieved for a contrast filter set at 1% above the brightness filter.

IMAGE ARRAYED AND FILTERED FOR BRIGHTNESS

SPECTRAL DENSITY MAXIMA

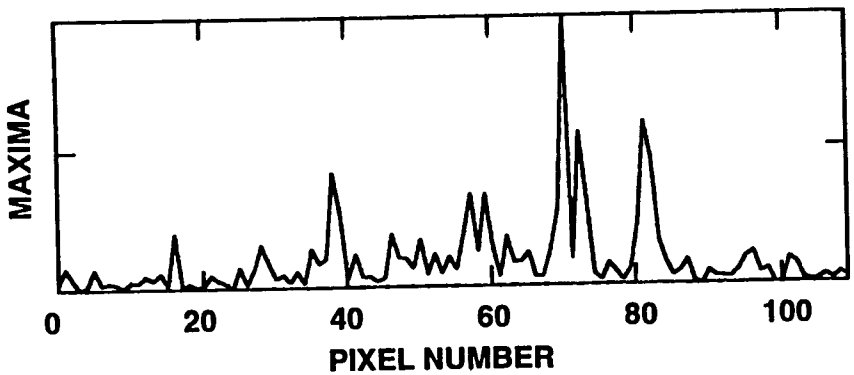

IMAGE MATRIX

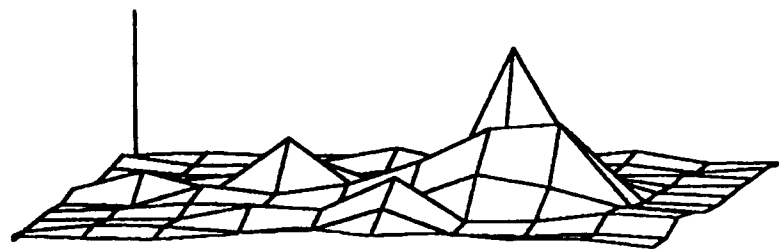

CONTOUR PLOT

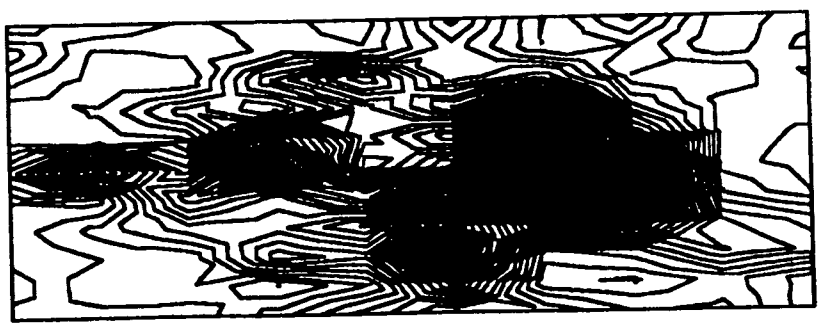

BRIGHTNESS FILTERED

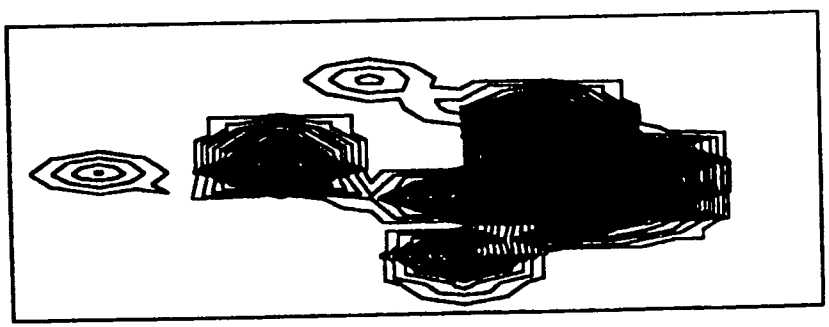

LEXAN KNIFE CONCEALED UNDER WOOL SWEATER OF HUMAN BODY

The image of a lexan knife shown in this chart is a good example of the capabilities of the ultrasound sensor to image nonmetallic concealed weapons. Both the lexan knife and the ultrasound image of the knife are shown on the facing page in full scale. The lexan knife was concealed under a wool sweater on a human body at about 4 ft. from the ultrasound sensor. Details of this image will be discussed in the section on image processing. The image illustrates an advantage of ultrasound over certain other CWD techniques, in that ultrasound sees any hard object concealed under clothing and not just metallic weapons.

LEXAN KNIFE CONCEALED UNDER WOOL SWEATER ON HUMAN BODY

LEXAN KNIFE (SCALE 1:1)

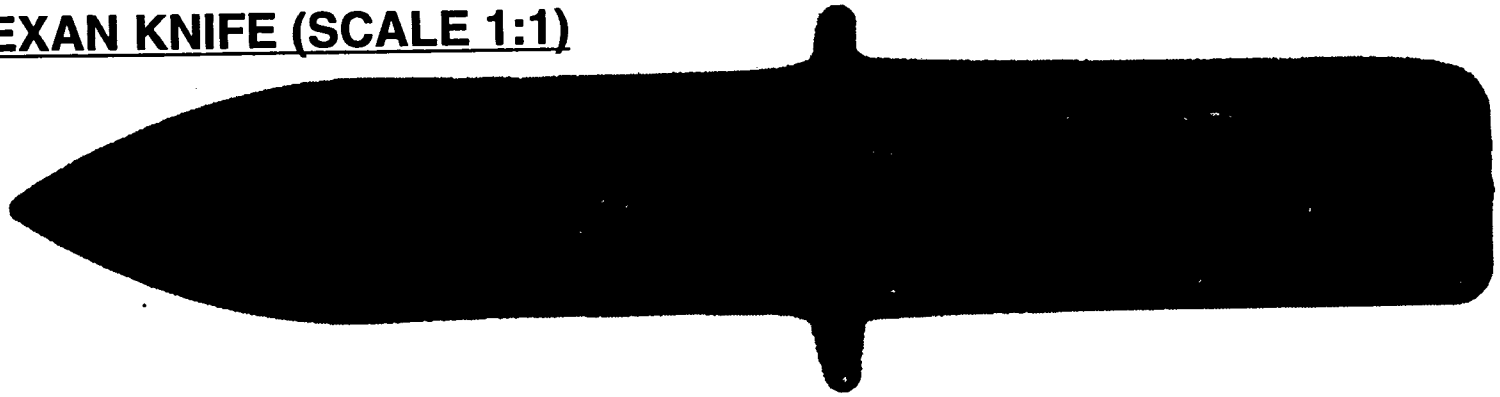

ULTRASOUND IMAGE AT 4 ft (SCALE 1:1)

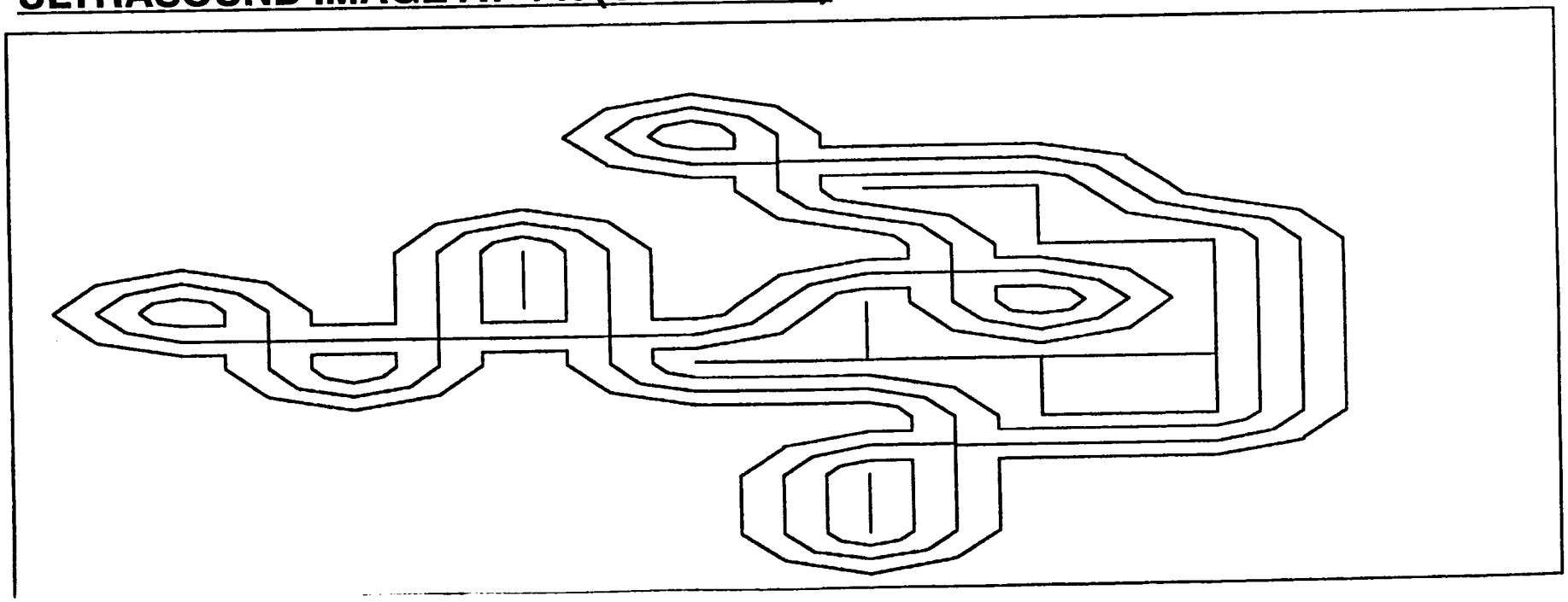

IMAGE PROCESSING PROGRAM

The IMAGE processing program is shown in completeness on the following three pages. The program is a document written for Mathcad® PLUS 6.0. The IMAGE program reads a file created by the CWD data-acquisition program. It then processes the file, as described in the preceding pages. On these pages, the IMAGE program develops the image of the lexan knife shown on the preceding page. A copy of the IMAGE program has been delivered to Rome Laboratory.

IMAGE 0image.mcd for Mathcad Plus 6.0 F. Felber JAYCOR 14 May 1996

Filters, Fourier analyzes, and binary-thresholds an array of detector signal traces to produce an image.

$S := \mathrm{READPRN}(\mathrm{aacwd})$ $N := \mathrm{rows}(S)$ $i := 0..N-1$ $K := \mathrm{cols}(S)-1$ $k := 0..K$ $\mu s := 10^{-6}$ $kHz := 10^{3}$

S is a matrix of $\mathrm{cols}(S) = 110$ and $\mathrm{rows}(S) = 512$

1. INPUT the number of rows in the image $R := 11$

2. INPUT the number of columns in the image $C := 10$

3. CHECK that this quantity equals zero $R \cdot C - \mathrm{cols}(S) = 0$ If not, change R or C.

4. INPUT 0 for top-down scan, 1 for switchback $s := 1$ Default is 1

5. INPUT the oscilloscope sampling time in μs $\Delta t := 1 \cdot \mu s$

6. INPUT the standard-deviation filter factor $\alpha := 1.5$ Default is 1.5

$r := R-1$ $c := C-1$ $m := 0..r$ $n := 0..c$ $t_i := i \cdot \Delta t$ $j := 1..\frac{N}{2}$ $f_j := \frac{j}{(N-1)\cdot \Delta t}$

Frequency resolution is $f_1 = 1.957 \cdot kHz$

Noise filter:

```
S := | k ← 0
     | for k ∈ 0..K
     |   | σ ← stdev(S^<k>)
     |   | i ← 0
     |   | for i ∈ 0..N-1
     |   |   | A ← S_i,k
     |   |   | P_i,k ← 0  if |A| < α·σ
     |   |   | P_i,k ← A  otherwise
     | P
```

View any of the $\mathrm{cols}(S) = 110$ noise-filtered waveforms by changing the second index of S in this graph:

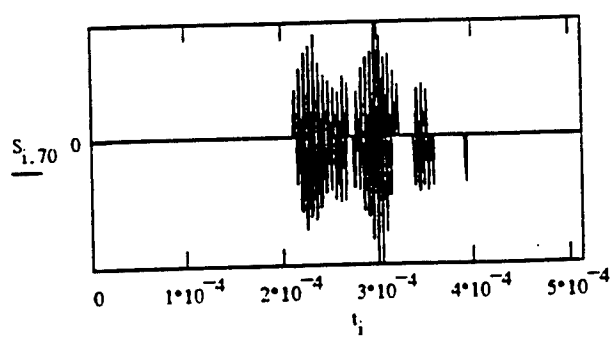

Fourier transform of waveforms:

```
fl := | k ← 0
      | for k ∈ 0..K
      |   | FS ← fft(S^<k>)
      |   | AFS ← |FS|
      |   | AFS_0 ← 0
      |   | M ← max(AFS)
      |   | j ← 0
      |   | while AFS_j < M
      |   |   j ← j + 1
      |   | fl_k,0 ← f_j
      |   | fl_k,1 ← M^2
      | fl
```

$fm_k := fl_{k,0}$ $I_k := fl_{k,1}$

$Max1 := \max(I)$ $K1_k := \mathrm{if}(Max1 = I_k, k, 0)$ $kmax := \max(K1)$

Max FT signal is in pixel number $kmax = 70$

Max FT signal in that pixel is $Max1 = 1.94 \cdot 10^{-3}$

Max FT signal occurs at frequency $fm_{kmax} = 201.566 \cdot kHz$

View frequencies at which FT signal maxima occur vs. pixel number

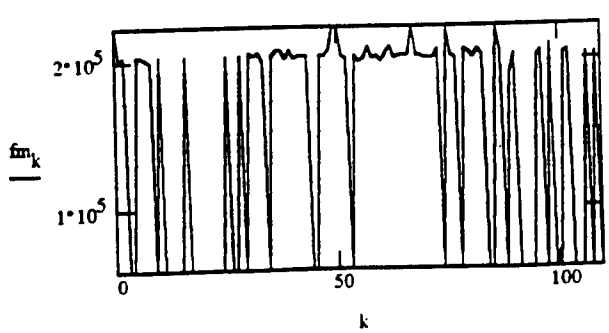

Select lower and upper bounds of frequency filters between 0 kHz and $\text{floor}\left(10^{-3}\cdot f_{\frac{N}{2}}\right) = 500$ kHz

7. INPUT lower bound of frequency filter $\text{lower} = 198\cdot\text{kHz}$

8. INPUT upper bound of frequency filter $\text{upper} = 208\cdot\text{kHz}$

$\text{low} = \text{floor}(\text{lower}\cdot(N-1)\cdot\Delta t)$ $\quad \text{up} = \text{ceil}(\text{upper}\cdot(N-1)\cdot\Delta t)$ $\quad \text{low} = 101$ $\quad \text{up} = 107$

Apply frequency filter to FT:

```
fl := | k ← 0
      | for k ∈ 0..K
      |   | FS ← fft(S^<k>)
      |   | AFS ← |FS|
      |   | m ← 0
      |   | while m ≤ low
      |   |   | AFS_m ← 0
      |   |   | m ← m + 1
      |   | n ← N/2
      |   | while n ≥ up
      |   |   | AFS_n ← 0
      |   |   | n ← n − 1
      |   | M ← max(AFS)
      |   | j ← 0
      |   | while AFS_j < M
      |   |   j ← j + 1
      |   | fl_k,0 ← f_j
      |   | fl_k,1 ← M^2
      | fl
```

$Q = \text{reverse}(\text{sort}(I))$ $\quad Q_0 = 1.94\cdot 10^{-3}$

Linear Array —> Matrix

```
I := | n ← 0
     | for n ∈ 0..c
     |   | m ← 0
     |   | for m ∈ 0..r
     |   |   I_m,n ← I_m+n·R
     | I
```

View surface plot before brightness and contrast filtering:

After frequency filtering:

$\text{fm}_k = \text{fl}_{k,0}$ $\quad I_k = \text{fl}_{k,1}$

$\text{Max1} = \max(I)$ $\quad \text{K1}_k = \text{if}(\text{Max1} = I_k, k, 0)$ $\quad \text{kmax} = \max(\text{K1})$

Max FT signal is in pixel number $\quad \text{kmax} = 70$

Max FT signal in that pixel is $\quad \text{Max1} = 1.94\cdot 10^{-3}$

Max FT signal occurs at frequency $\quad \text{fm}_{\text{kmax}} = 201.566\cdot\text{kHz}$

Mean of frequencies at which FT maxima occur in each pixel $\quad \text{mean}(\text{fm}) = 203.825\cdot\text{kHz}$

View frequencies at which FT signal maxima occur vs. pixel no.

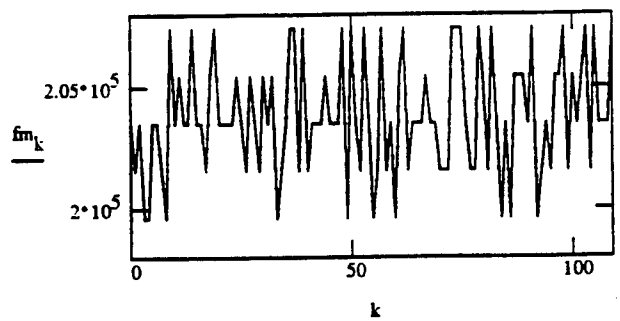

View FT signal maxima vs. pixel number

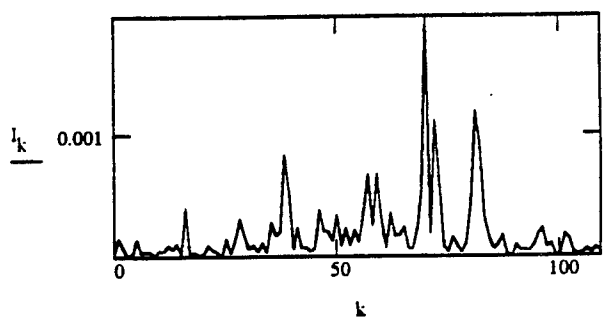

$I(m,n) = I_{m\cdot(1-s)+s\cdot\left[\frac{r}{2}+(-1)^{n+1}\cdot\left(\frac{r}{2}-m\right)\right],n}$ $\quad I_{m,n} = I(m,n)$

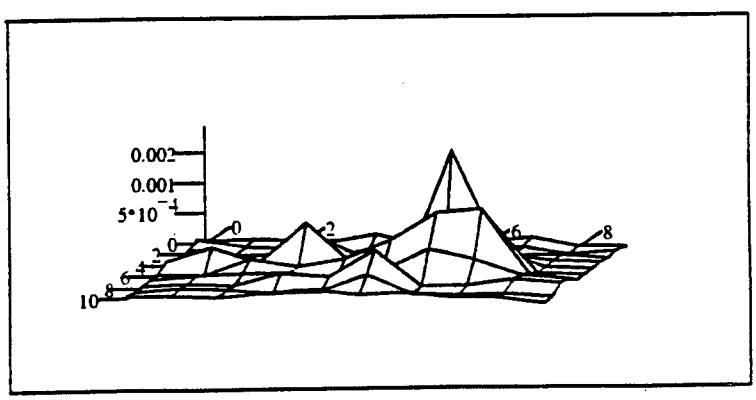

I

9(a). INPUT number of pixels that should exceed brightness filter threshold $p := 19$

$Min := Q_p \qquad Min = 2.904 \cdot 10^{-4}$

9(b). Or **INPUT** brightness filter threshold directly (untoggle this equation) $Min := ■■$

Contrast filter is set 1% above brightness filter: $Max := 1.01 \cdot Min$

$$I(m,n) := \begin{cases} I_{m,n} & \text{if } I_{m,n} \le Max \\ Max & \text{otherwise} \end{cases} \qquad I_{m,n} := I(m,n) \qquad I(m,n) := \begin{cases} I_{m,n} & \text{if } I_{m,n} > Min \\ Min & \text{otherwise} \end{cases} \qquad I_{n,r-m} := I(m,n)$$

10. To **SET GRID** on this contour plot,
(a) click on plot,
(b) click on Graphics,
(c) click on 3D Plot Format
(d) click on Axes.
(e) under X-Axis, set No. of Grids and Max. Val. equal to $c = 9$
(f) under Y-Axis, set No. of Grids and Max. Val. equal to $r = 10$

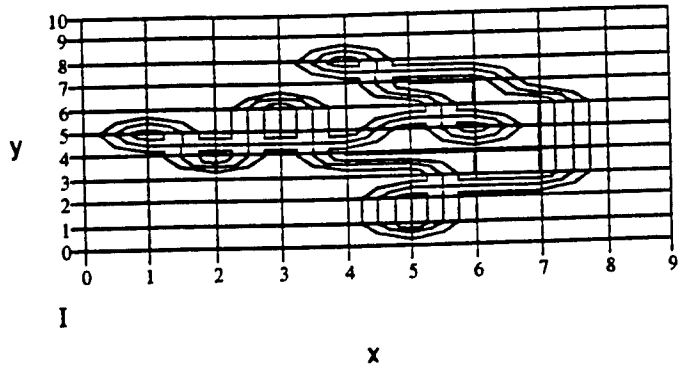

To transform the grid points (x,y) above to pixel numbers k (starting at 0), and vice versa, use these:

To transform (x,y) to k: $x := 0 \quad y := 10 \quad k := R \cdot x + r - y \cdot (-1)^{s \cdot x}$ $\qquad k = 0$

To transform k to (x,y): $k := 70 \qquad x := \mathrm{floor}\left(\frac{k}{R}\right) \quad y := \frac{r}{2} - \left(R \cdot x - \frac{r}{2} - k\right) \cdot (-1)^{s \cdot x} \qquad x = 6 \quad y = 6$

11. SCALE BORDER of final processed image to dimensions of imaged area. Corners of border correspond to centers of corner pixels.

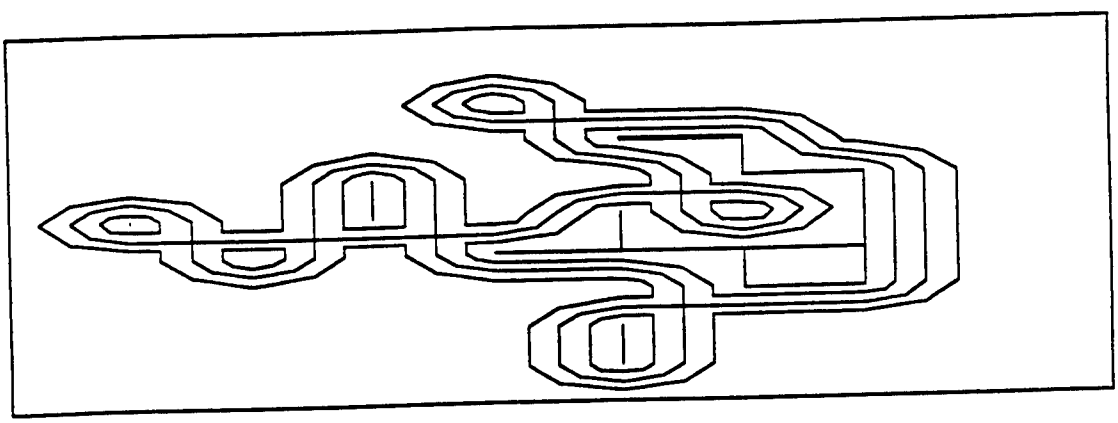

I

PHASE 1 BREADBOARD

Radar CWD
Test Results

PHASE 1 RADAR

The radar used for CWD in Phase 1 is a successful mine-detection radar. It is the only radar in the world capable of standoff detection of buried mines at ranges of tens of meters. For that reason the Army has awarded JAYCOR a program to upgrade the radar performance and to make it a compact 2 cubic feet by April 1997. Since it can detect metallic and nonmetallic mines up to 25 m, it can also detect concealed metallic and nonmetallic weapons at ranges up to 25 m very easily.

PHASE 1 RADAR

- Has been successfully tested by Army for mine detection in extensive tests (July 1996)
  - Under very adverse conditions it proved to be <u>only</u> standoff radar capable of mine detection
  - Found metallic and non-metallic buried mines at 25 m
  - Forward rate of travel: 3 km/hr
- Tested for CWD
- Radar development costs of $1.7 million paid by Army
- Army has announced award of new $7 million contract to JAYCOR/Lockheed Martin

APPLICATION OF RADAR TO WEAPONS DETECTION

The radar was tested for CWD in Phase 1 for its potential as a concealed-weapons bell ringer. That is, the much greater detection range of the radar could alert an imaging ultrasound sensor to the precise location of potential concealed weapons. This early warning function is particularly important in crowded areas, where an imaging sensor would not have time to scan each individual. The dual-sensor concept is to have the radar hand over the locations of potential concealed weapons to the imaging ultrasound sensor for positive identification. The radar can be easily integrated with an imaging ultrasound sensor to perform this handover function. The radar might also monitor the passage of individuals through corridors or portals, because the motion of humans on the 2-D cross-correlation display of the radar is easily observed.

APPLICATION OF RADAR TO WEAPONS DETECTION

- Bell ringer
  - — Early warning
  - — General area location
- Easily integrated with ultrasound system
  - — VME based, ethernet port
  - — No radio interference
- Usable in several configurations
  - — Scan a crowd
    - Location important
    - Pass location to ultrasound system
  - — Monitor passage through controlled corridor
    - Bell ringer
    - Alert ultrasound operator
    - One antenna application

TYPICAL 2-D CROSS-CORRELATION DISPLAY

This display is seen on a monitor in real time as the radar observes a scene. The motion of a human walking through the FOV of the radar is easily seen as the motion of a prominent cluster of peaks across this cross-correlation display. The prominent peaks can be color-coded to draw attention to the motion of the humans.

TYPICAL 2-D CROSS-CORRELATION DISPLAY

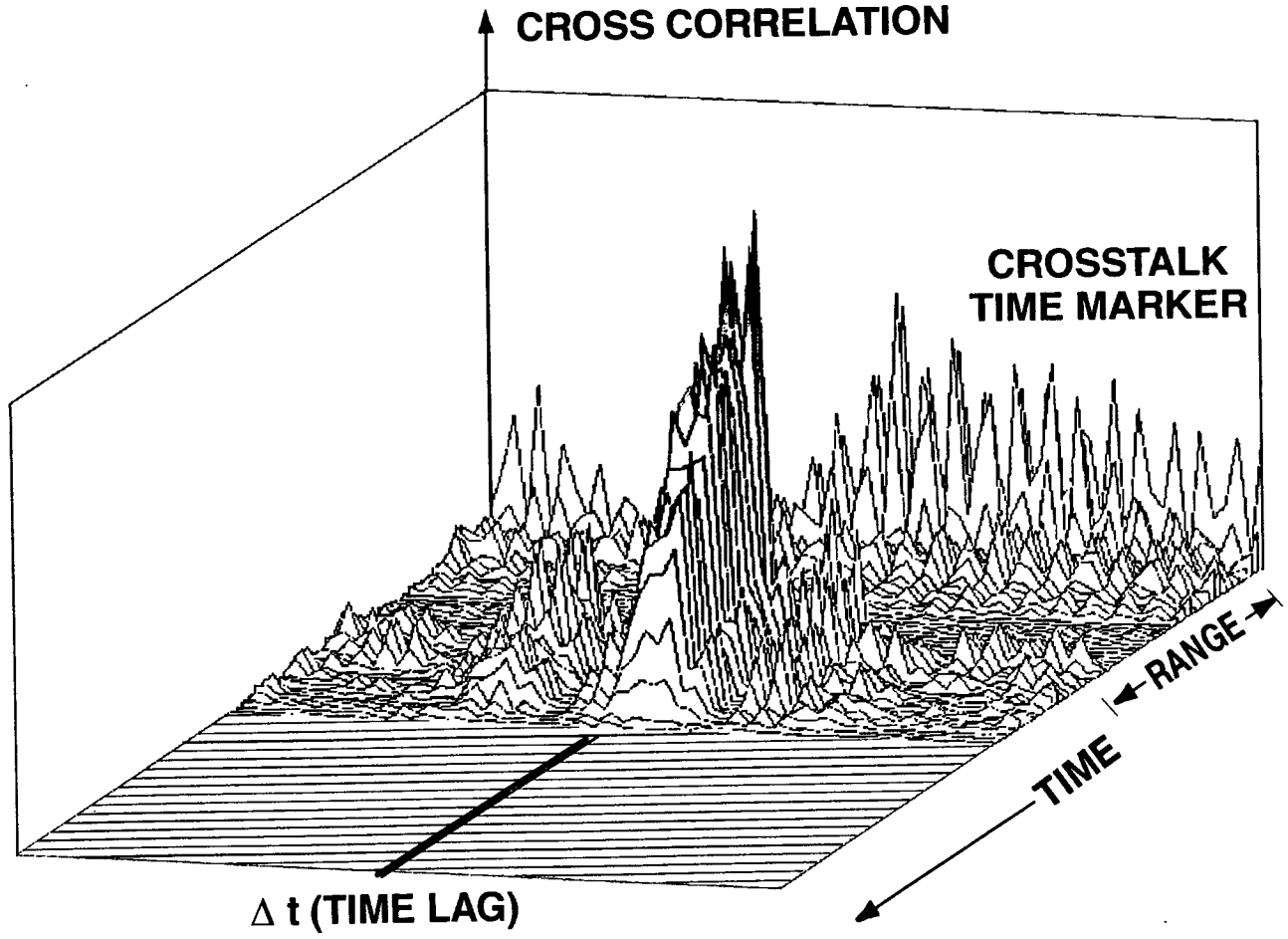

PHASE 1 RADAR CWD TESTS

The mine-detection radar was tested for CWD on several occasions. The first set of tests was invalid because the radar was too sensitive. Even at 10-m range, the signals from the human and concealed weapons saturated the amplifiers. Attenuators were added to reduce the sensitivity and range of the radar, and further tests were performed in July 1996. In these tests the radar looked at a handgun, a long pair of scissors, a plastic bar, a glass bottle, all under jacket and shirt concealments. The radar had no trouble seeing nonmetallic and metallic objects at ranges well over 10 m. These tests, however, showed no real evidence that the concealed weapons could be discriminated from their human carriers.

Later tests, shown for the first time in the following pages, suggest that even the unoptimized radar software might be capable of about 80% probability of detection of concealed weapons. (A detection seemed evident in 12 out of 15 trials, compared to a control spectral image.) The mine-detection software of the radar will be optimized for CWD in Phase 2.

PHASE 1 RADAR CWD TESTS

- Tested in Albuquerque July 23, 24
- 20 shots
  - Baselines
  - 44 Magnum
  - Long scissors
  - Plastic object
  - Bottle
  - Jacket and shirt concealments
- Conclusions
  - Easily locates nonmetallic and metallic objects and people at long ranges (25 m)
  - Additional filtering is needed to discriminate weapons

RADAR CWD TESTS

The following pages show the results of the most recent CWD tests using the mine-detection radar. The tests were performed in pairs on fifteen subjects, each standing facing the radar. For each subject, a spectrum was taken with the subject armed with a 9-mm handgun, and another spectrum taken of the same subject in the same position, but unarmed. When armed, some of the male subjects had the handgun in their front waistbands, and some in their side pockets. The females held the handgun by their sides. In all cases, the handgun was pointed down at the ground.

Each of the spectra comprises 36 data points, representing radar returns at 100-MHz intervals from 0.5 to 4.0 GHz. The spectra of Subjects 1 through 12 show marked enhancements of the armed subjects at 2 or 3 GHz. The spectra of subjects 13 through 15 do not. It is not known how these results will change when the subjects are moving. The following table categorizes the 15 subjects by body type.

Subject Number	Sex	Size	Subject Number	Sex	Size
1	M	Short	9	M	Short
2	F	Large	10	M	Short
3	M	Tall	11	M	Large
4	M	Medium	12	M	Medium
5	M	Medium	13	F	Tall
6	F	Short	14	M	Short
7	M	Short	15	M	Medium
8	M	Medium			

RADAR CWD TESTS

Subject 1

Spectral density of subject with handgun (solid) and without (dashed)

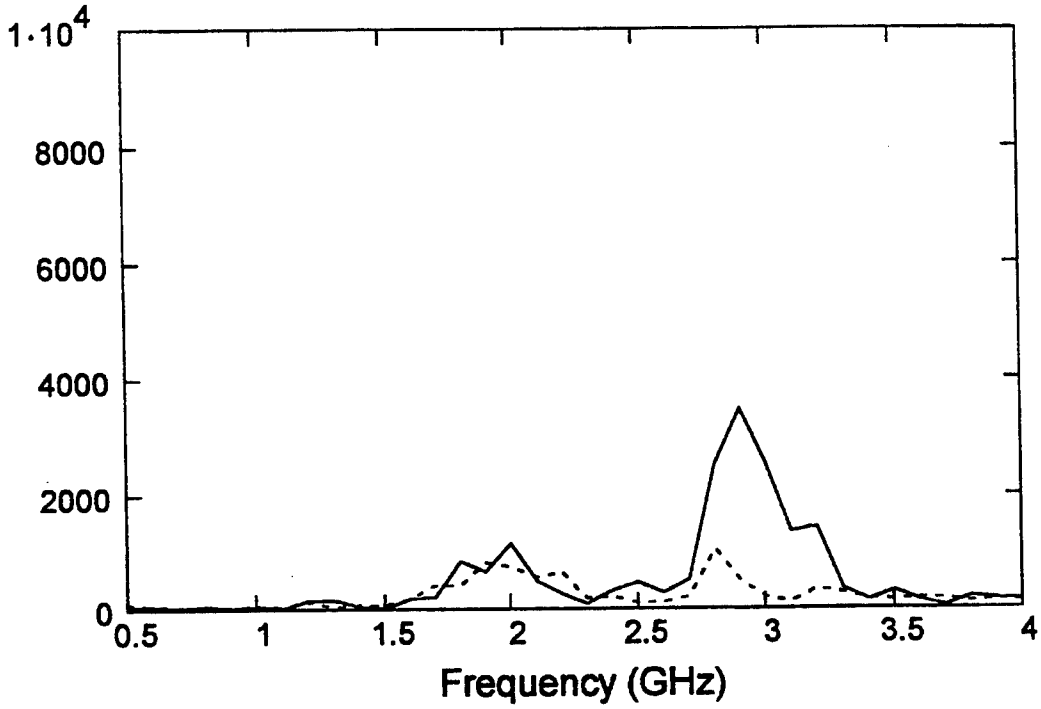

Subject 2

Spectral density of subject with handgun (solid) and without (dashed)

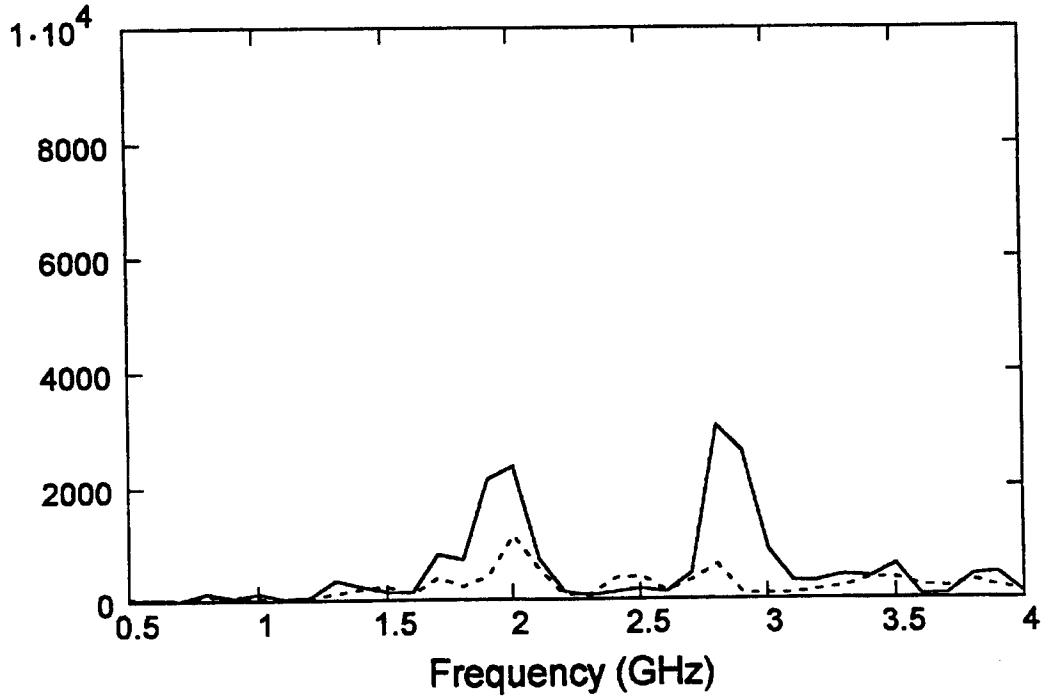

RADAR CWD TESTS (Continued)

Subject Number	Sex	Size	Subject Number	Sex	Size
1	M	Short	9	M	Short
2	F	Large	10	M	Short
3	M	Tall	11	M	Large
4	M	Medium	12	M	Medium
5	M	Medium	13	F	Tall
6	F	Short	14	M	Short
7	M	Short	15	M	Medium
8	M	Medium			

RADAR CWD TESTS (CONT.)

Subject 3

Spectral density of subject with handgun (solid) and without (dashed)

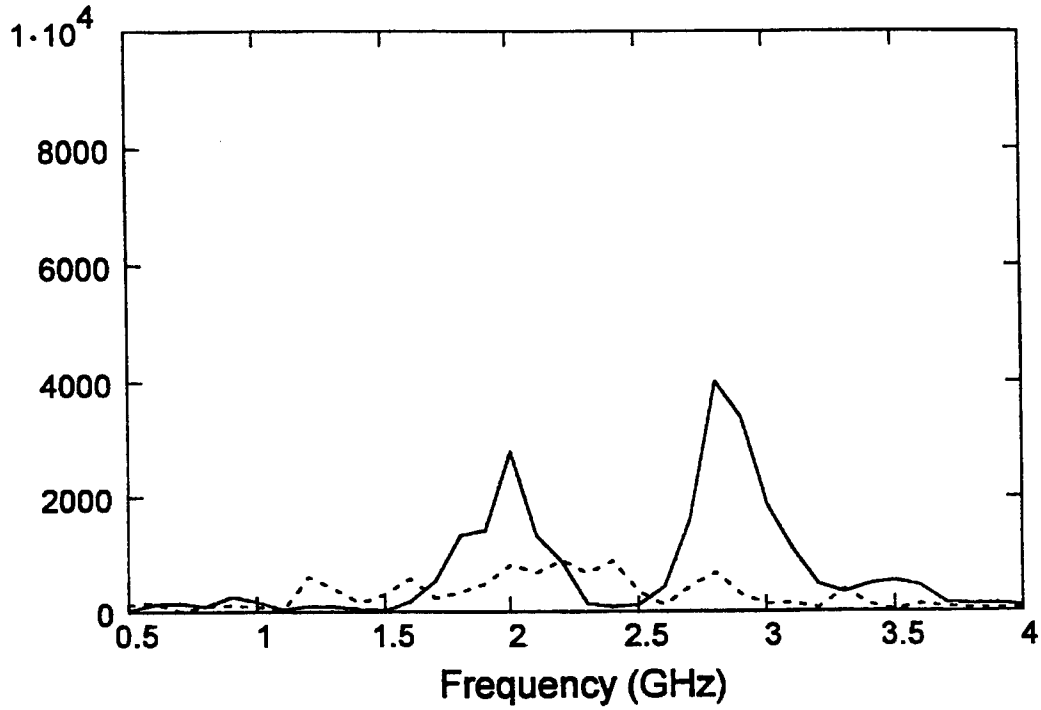

Subject 4

Spectral density of subject with handgun (solid) and without (dashed)

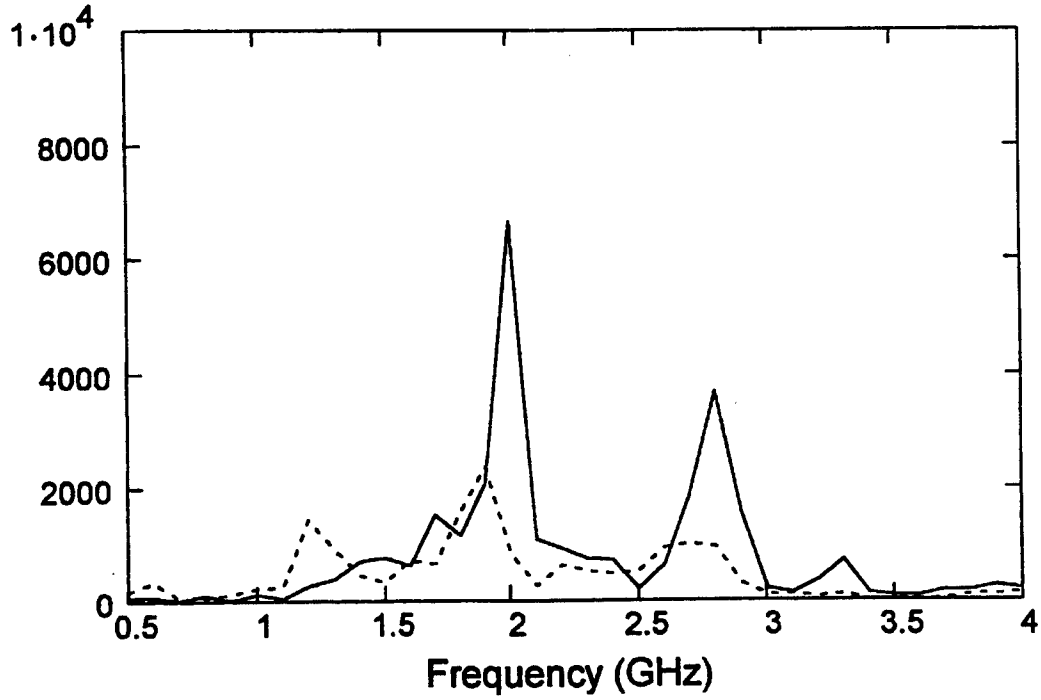

RADAR CWD TESTS (Continued)

Subject Number	Sex	Size	Subject Number	Sex	Size
1	M	Short	9	M	Short
2	F	Large	10	M	Short
3	M	Tall	11	M	Large
4	M	Medium	12	M	Medium
5	M	Medium	13	F	Tall
6	F	Short	14	M	Short
7	M	Short	15	M	Medium
8	M	Medium			

RADAR CWD TESTS (CONT.)

Subject 5

Spectral density of subject with handgun (solid) and without (dashed)

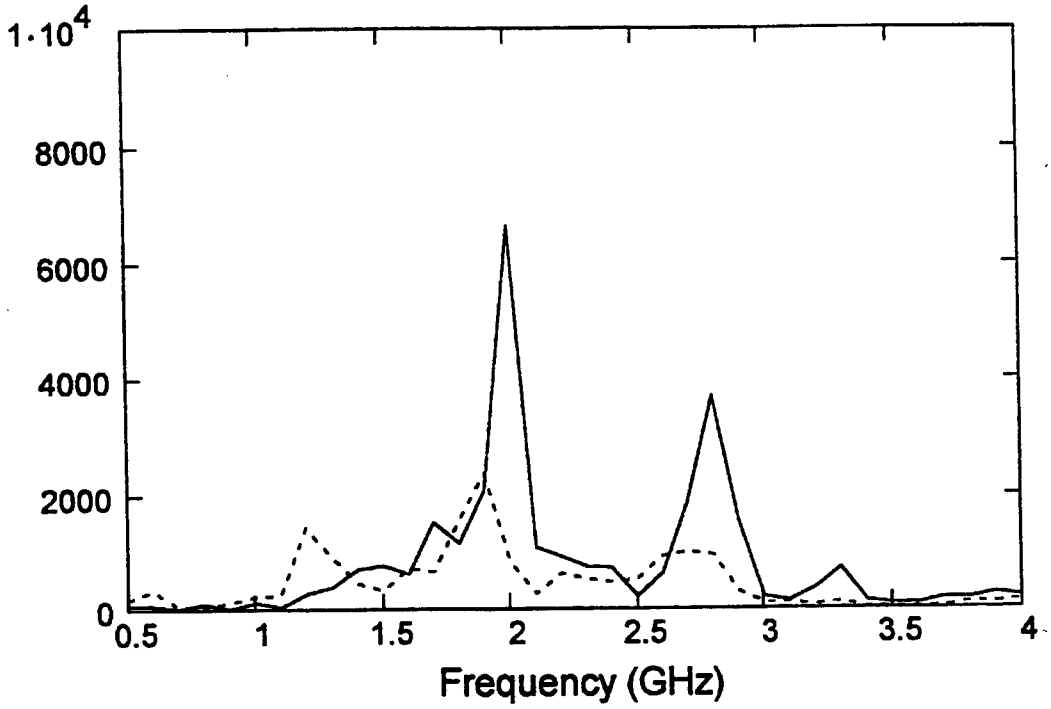

Subject 6

Spectral density of subject with handgun (solid) and without (dashed)

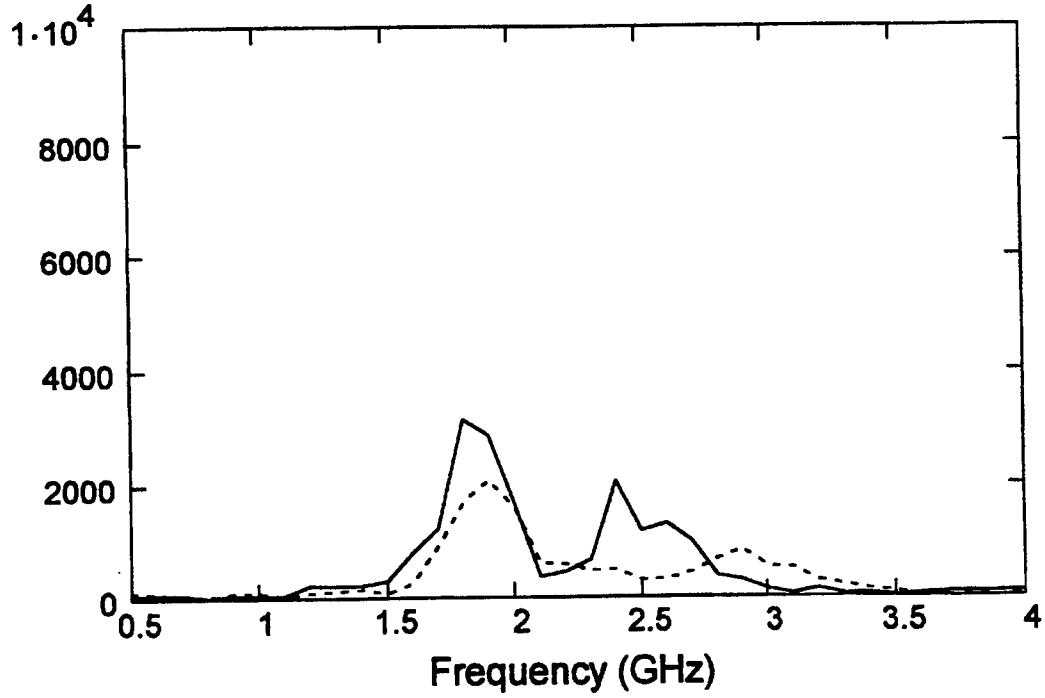

RADAR CWD TESTS (Continued)

Subject Number	Sex	Size	Subject Number	Sex	Size
1	M	Short	9	M	Short
2	F	Large	10	M	Short
3	M	Tall	11	M	Large
4	M	Medium	12	M	Medium
5	M	Medium	13	F	Tall
6	F	Short	14	M	Short
7	M	Short	15	M	Medium
8	M	Medium			

RADAR CWD TESTS (CONT.)

Subject 7

Spectral density of subject with handgun (solid) and without (dashed)

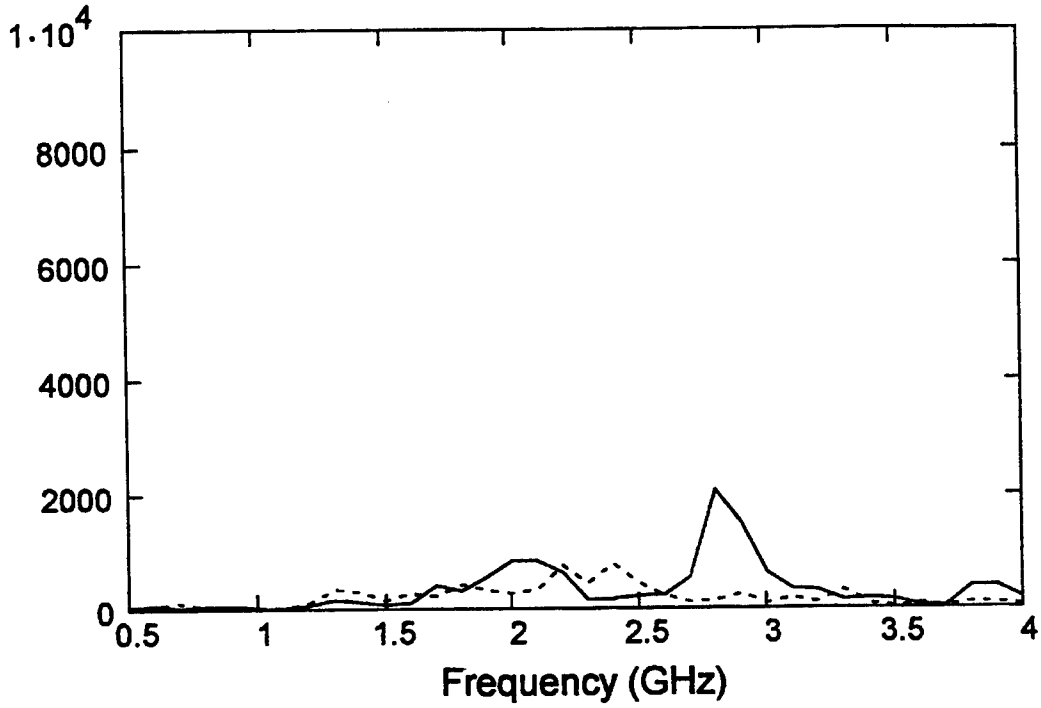

Subject 8

Spectral density of subject with handgun (solid) and without (dashed)

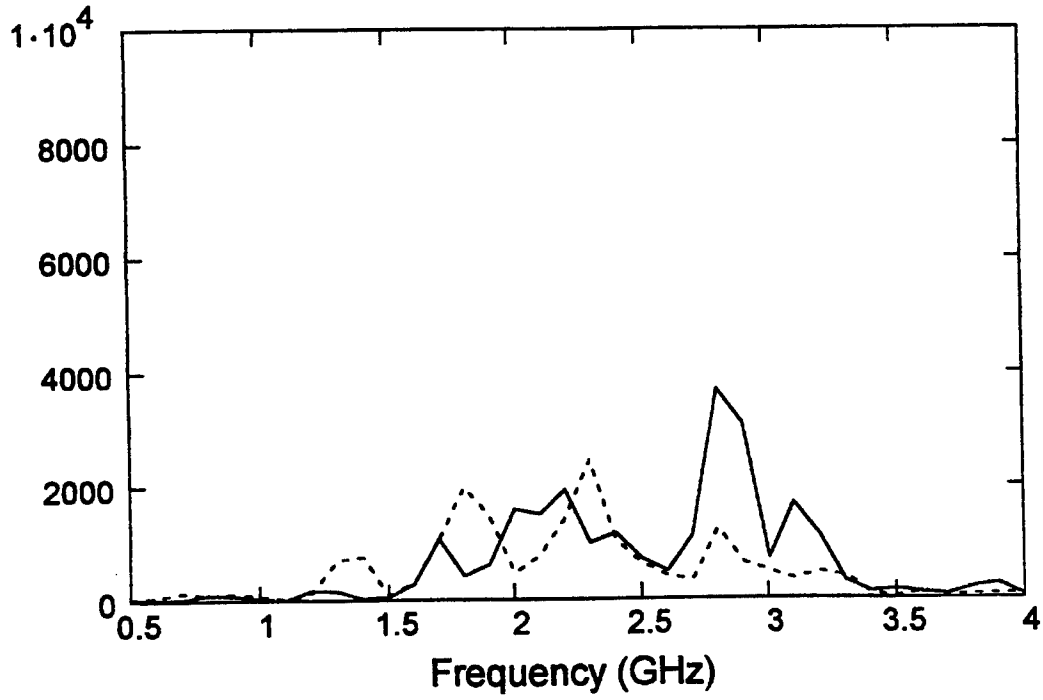

RADAR CWD TESTS (Continued)

Subject Number	Sex	Size	Subject Number	Sex	Size
1	M	Short	9	M	Short
2	F	Large	10	M	Short
3	M	Tall	11	M	Large
4	M	Medium	12	M	Medium
5	M	Medium	13	F	Tall
6	F	Short	14	M	Short
7	M	Short	15	M	Medium
8	M	Medium			

RADAR CWD TESTS (CONT.)

Subject 9

Spectral density of subject with handgun (solid) and without (dashed)

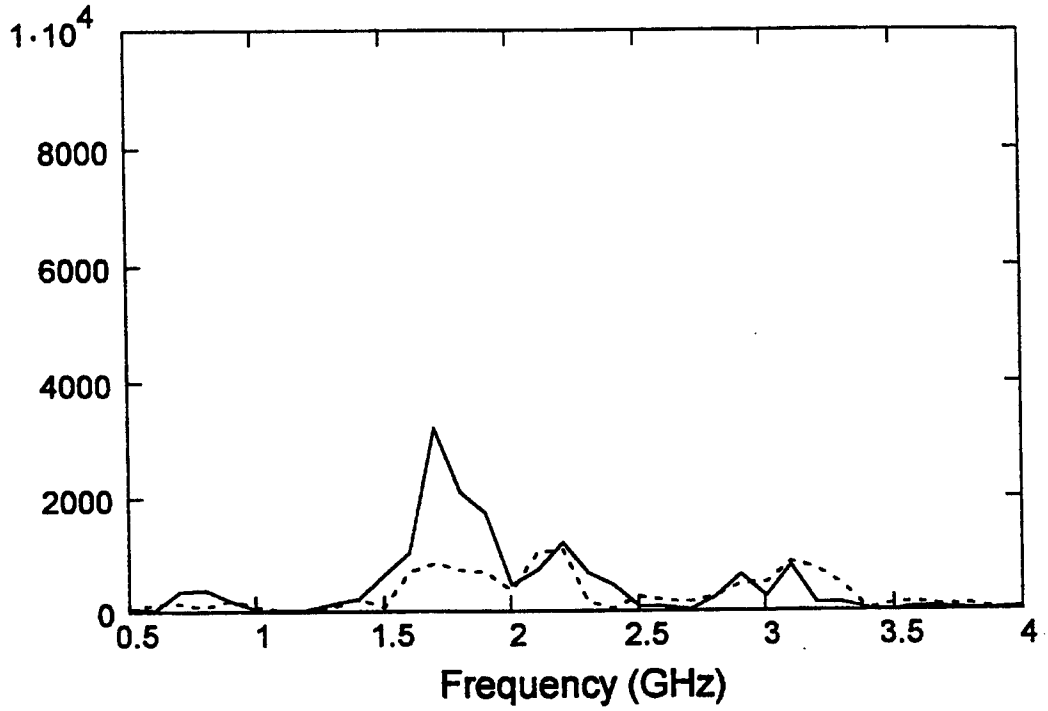

Subject 10

Spectral density of subject with handgun (solid) and without (dashed)

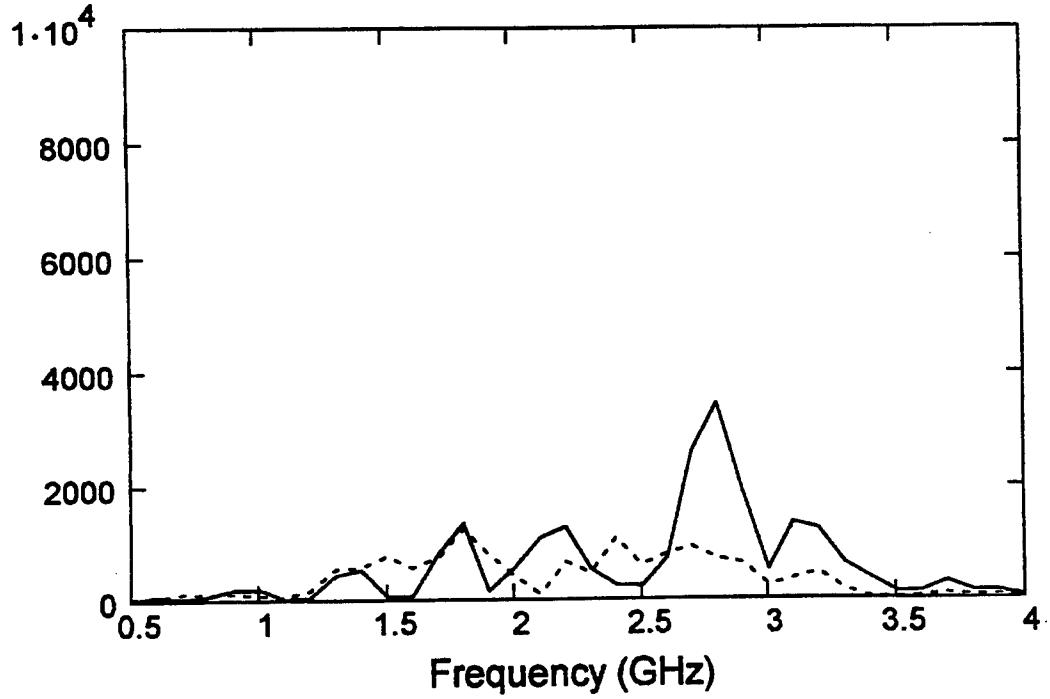

RADAR CWD TESTS (Continued)

Subject Number	Sex	Size	Subject Number	Sex	Size
1	M	Short	9	M	Short
2	F	Large	10	M	Short
3	M	Tall	11	M	Large
4	M	Medium	12	M	Medium
5	M	Medium	13	F	Tall
6	F	Short	14	M	Short
7	M	Short	15	M	Medium
8	M	Medium			

RADAR CWD TESTS (CONT.)

Subject 11

Spectral density of subject with handgun (solid) and without (dashed)

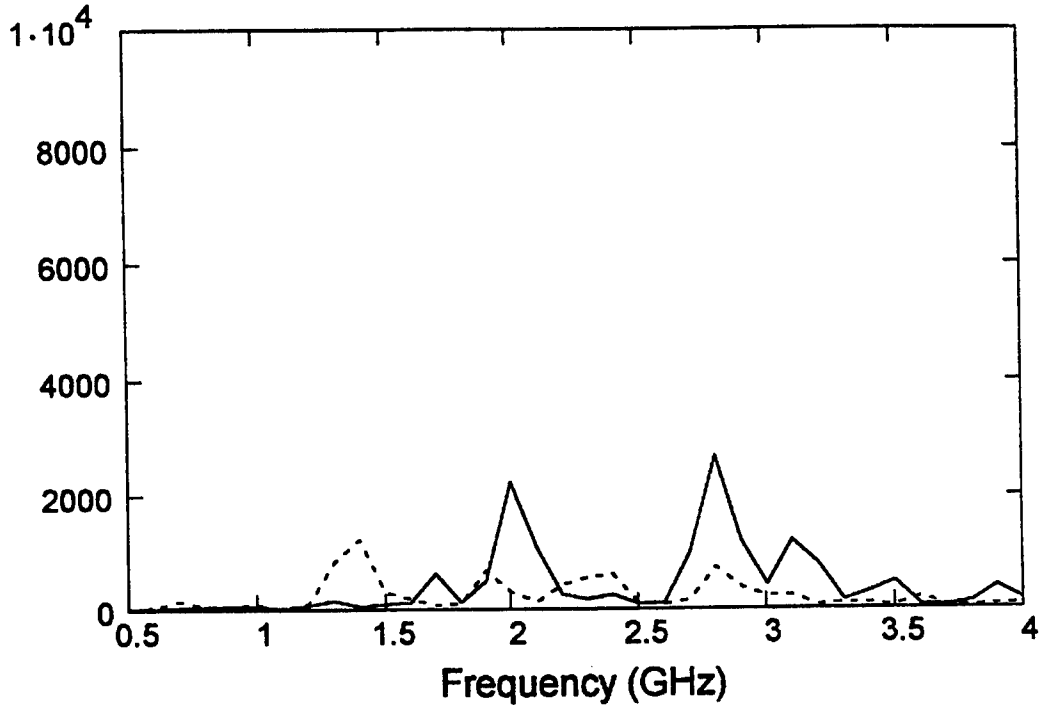

Subject 12

Spectral density of subject with handgun (solid) and without (dashed)

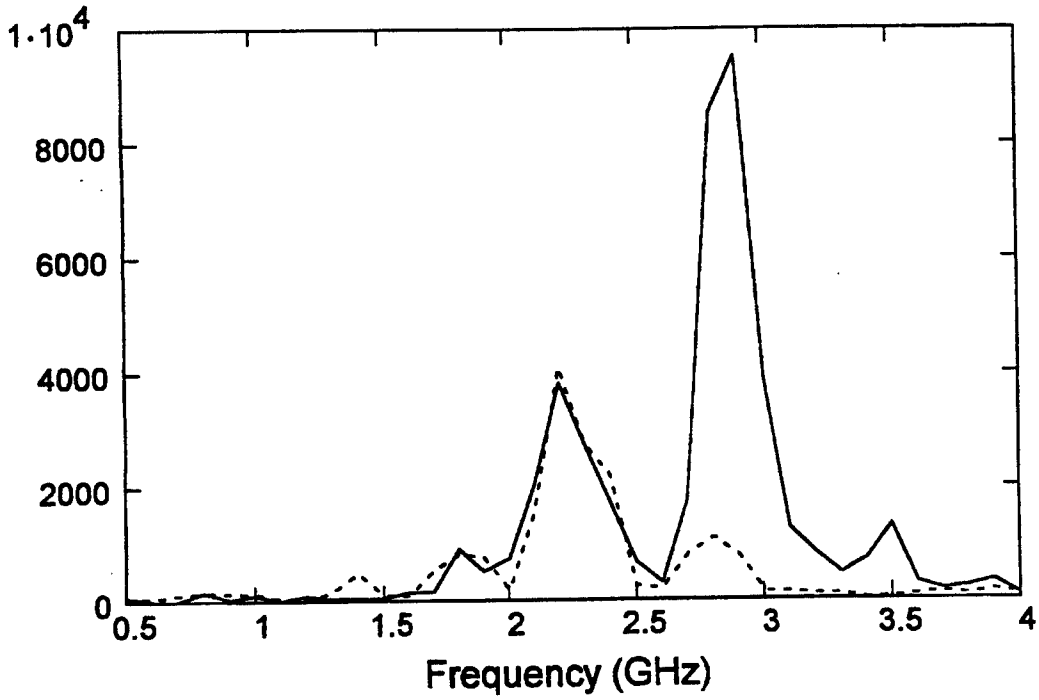

RADAR CWD TESTS (Continued)

Subject Number	Sex	Size	Subject Number	Sex	Size
1	M	Short	9	M	Short
2	F	Large	10	M	Short
3	M	Tall	11	M	Large
4	M	Medium	12	M	Medium
5	M	Medium	13	F	Tall
6	F	Short	14	M	Short
7	M	Short	15	M	Medium
8	M	Medium			

RADAR CWD TESTS (CONT.)

Subject 13

Spectral density of subject with handgun (solid) and without (dashed)

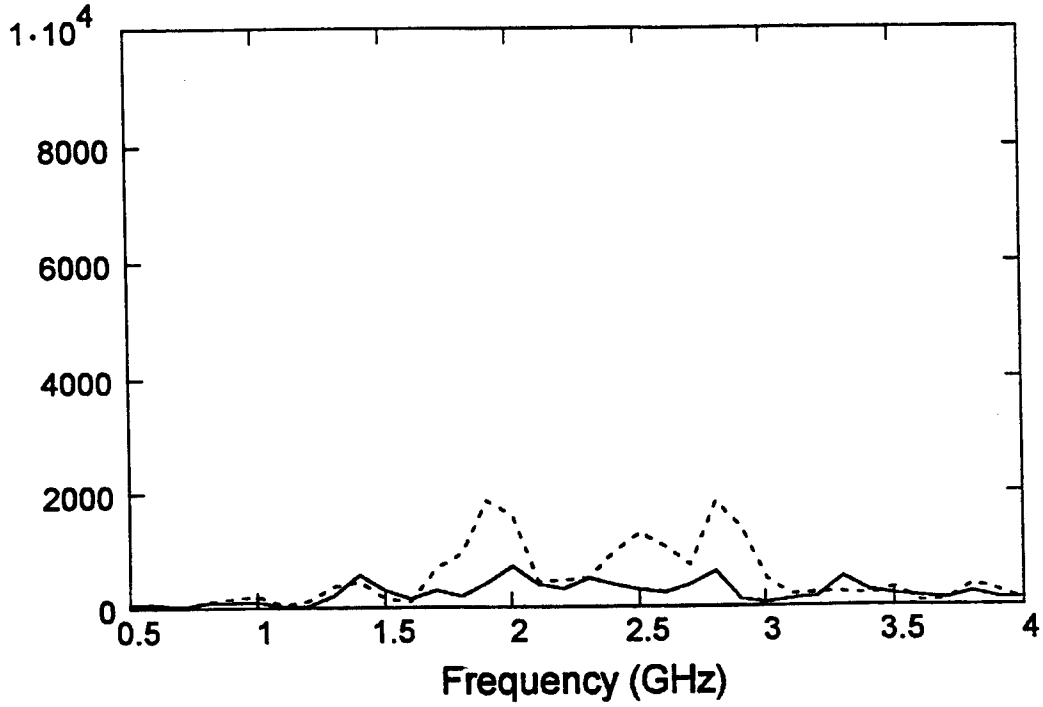

Subject 14

Spectral density of subject with handgun (solid) and without (dashed)

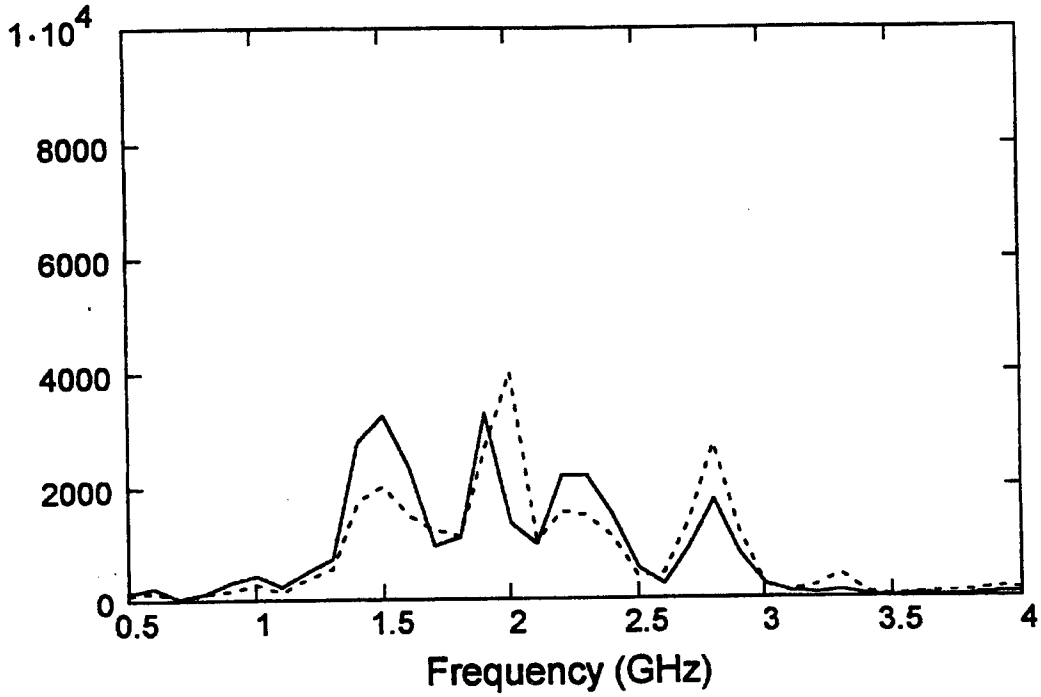

RADAR CWD TESTS (Continued)

Subject Number	Sex	Size	Subject Number	Sex	Size
1	M	Short	9	M	Short
2	F	Large	10	M	Short
3	M	Tall	11	M	Large
4	M	Medium	12	M	Medium
5	M	Medium	13	F	Tall
6	F	Short	14	M	Short
7	M	Short	15	M	Medium
8	M	Medium			

RADAR CWD TESTS (CONT.)

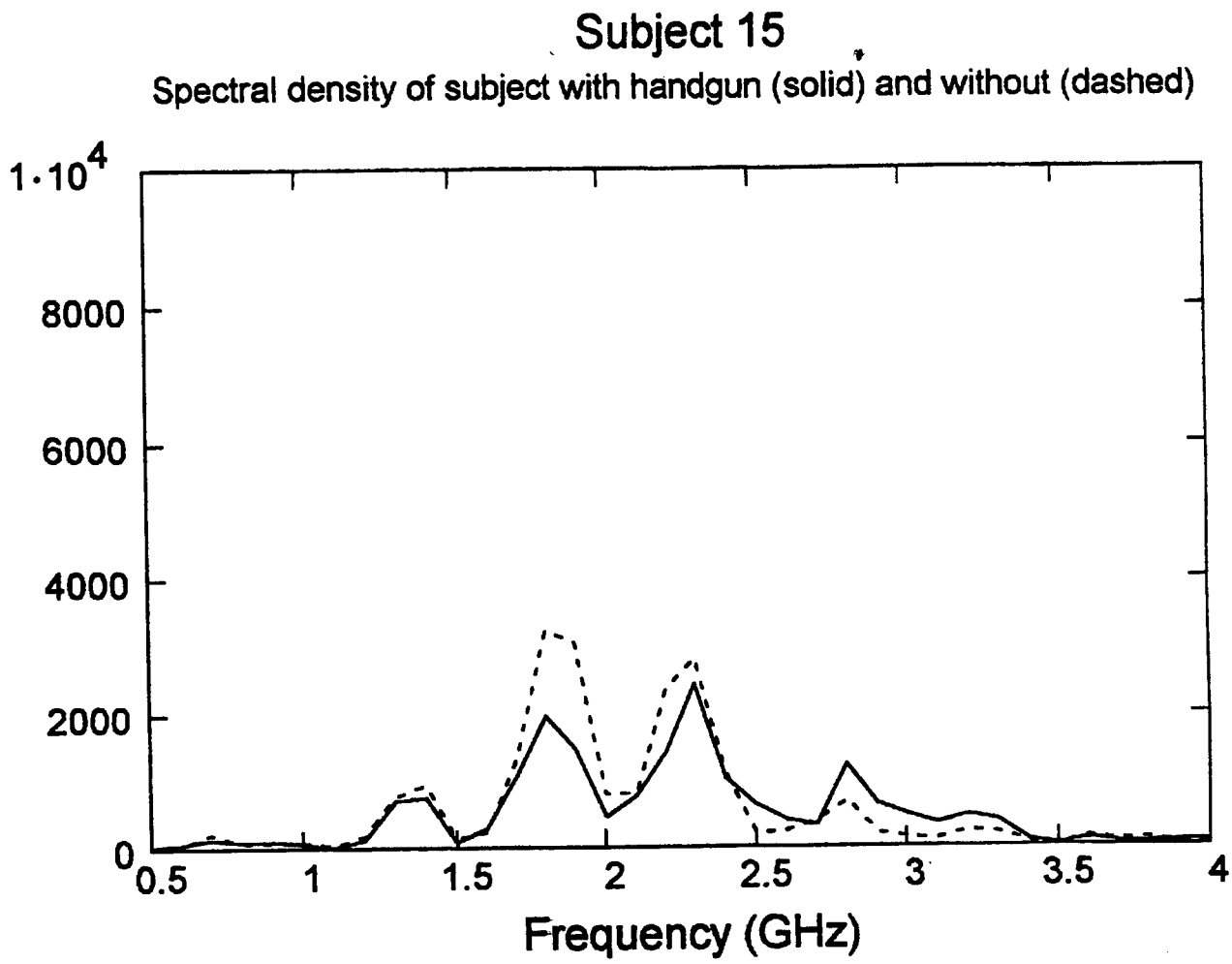

PHASE 1 RADAR CONCLUSIONS

The mine-detection radar has been used in the Phase 1 CWDT Program to locate moving humans in real time and to detect nonmetallic (plastic bars) and metallic concealed weapons at ranges up to 25 m. The challenge to the use of an active radar system, such as the mine-detection radar, for CWD is discriminating concealed weapons from their human carriers. Thus far, no filtering techniques specific to CWD have been implemented on the mine-detection radar. Neither have any hardware changes been made to the radar system specifically for CWD. In this report, we will point out certain hardware changes that might be made, such as from a vertical to a circular polarization, that might increase the probability of detection of concealed weapons on moving humans. The upgraded radar under the new Army program is now scheduled to be completed in April 1997. The upgraded radar will have improved performance, including improved shot-to-shot reproducibility, and will be much more compact than the version we used in Phase 1.

PHASE 1 RADAR CONCLUSIONS

- JAYCOR mine-detection radar successfully locates moving humans and nonmetallic and metallic concealed weapons to 25 m

- Discrimination of concealed weapons requires

  — Improved shot-to-shot reproducibility
  — New filtering techniques
  — Hardware changes (lower frequencies, circular polarization, etc.)

- JAYCOR/Lockheed Army project anticipates new mine-detection radar with improved shot-to-shot reproducibility by December 1996

  — Improved technology will aid CWD

PHASE 2 BRASSBOARD

Conceptual Design

ARTIST'S CONCEPT OF CWD SY1STEM AT BUILDING ENTRANCE

This figure illustrates how a complete CWD system might be deployed at a public building. In this conceptual sketch an active radar detects concealed weapons at long ranges in a crowd of people. The radar hands over the location of the potential concealed weapon to the ultrasound sensor, which images the concealed weapon at closer ranges. A human operator monitors a screen showing the ultrasound images at video frame rates superimposed on a video image of the scene. The sizes of the radar and ultrasound sensors in this illustration are representative of the expected sizes of fixed-site CWD sensors in practice. The radar sensor should be reduced to a compact 2 cubic feet by April 1997. The ultrasound sensor shown in this figure will probably be about the size of the box that is shown, but the dish might be somewhat larger, and there might be a lightweight array of transmitting transducers with the receiving dish.

ARTIST'S CONCEPT OF PROTOTYPE CWD SYSTEM DEPLOYED AT PUBLIC BUILDING ENTRANCE

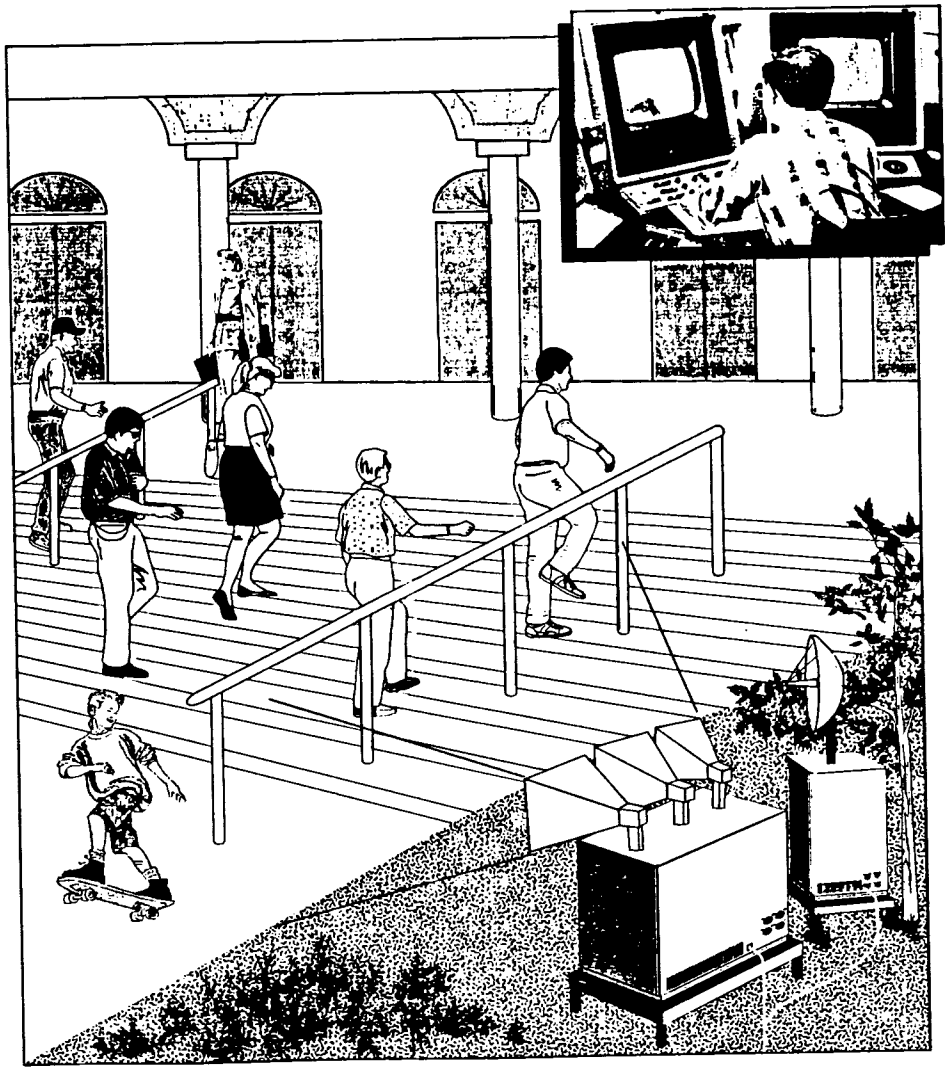

COMPLEMENTARY ADVANTAGES OF RADAR/ULTRASOUND SENSOR

The radar and ultrasound sensors complement each other for the fixed-site CWD mission. The radar has long range, but it only detects and locates concealed weapons and does not image them. The ultrasound sensor has shorter range, but the ability to image weapons with sufficient resolution for positive identification. If the ultrasound sensor has dual frequencies, then the lower-frequency sensor can be used for longer-range detection at lower resolution, and the higher-frequency sensor can be used for high-resolution images at close ranges. Both the radar and ultrasound sensors can be configured for fixed-site or mobile CWD. The ultrasound sensors have the further capability of detecting concealed weapons in handheld configurations. A radar can perform surveillance of a crowd over 90-degree azimuthal FOV without any motion. The ultrasound sensors will need to be directed by the radar to particular locations where weapons might potentially be concealed. A 40-kHz sensor at resolutions from 2 to 10 cm has a FOV at ranges up to 8 m about the size of a human body. The higher-resolution, higher-frequency ultrasound sensor has a narrower FOV of about 1 m, corresponding about to the length of a human torso. Both the radar and ultrasound sensors have excellent penetration of clothing and excellent capability of detecting nonmetallic concealed weapons. Both types of sensors are safe for use by human operators and safe for the public. The public has no problems accepting the safety of ultrasound sensors. The American National Standards Institute (ANSI) has no safety standards for ultrasound sensors, the way it does for electromagnetic sensors, such as radar. The radar sensor will probably be perceived by the public the same as a radar speed gun, which has comparable power output.

COMPLEMENTARY ADVANTAGES OF RADAR/ULTRASOUND SENSOR

Property	Radar	Ultrasound @ 40 kHz	Ultrasound @ 200 kHz
Range	From 3 to 15 m	From 2 to 8 m	From 1 to 3 m
Resolution	N/A	2 to 10 cm	1 to 2 cm
Frequency	0.5-4 GHz	40 kHz	200 kHz
Aperture	50 cm	90 cm	90 cm
Potential configurations	Fixed site, mobile	Fixed site, mobile, handheld	Fixed site, mobile, handheld
FOV	Crowd	Body	Torso
Penetration	Excellent	Excellent	Excellent
Nonmetallic CWD	Excellent	Excellent	Excellent
Safety	Excellent	Excellent	Excellent
Social acceptance	Satisfactory	Excellent	Excellent

RADAR-ULTRASOUND CONCEALED WEAPONS DETECTION SYSTEM

This figure shows schematically how an ultrasound sensor can be coupled to a radar sensor, so that the radar sensor can hand over location information to the ultrasound sensor for use by a system operator.

RADAR-ULTRASOUND CONCEALED WEAPONS DETECTION SYSTEM

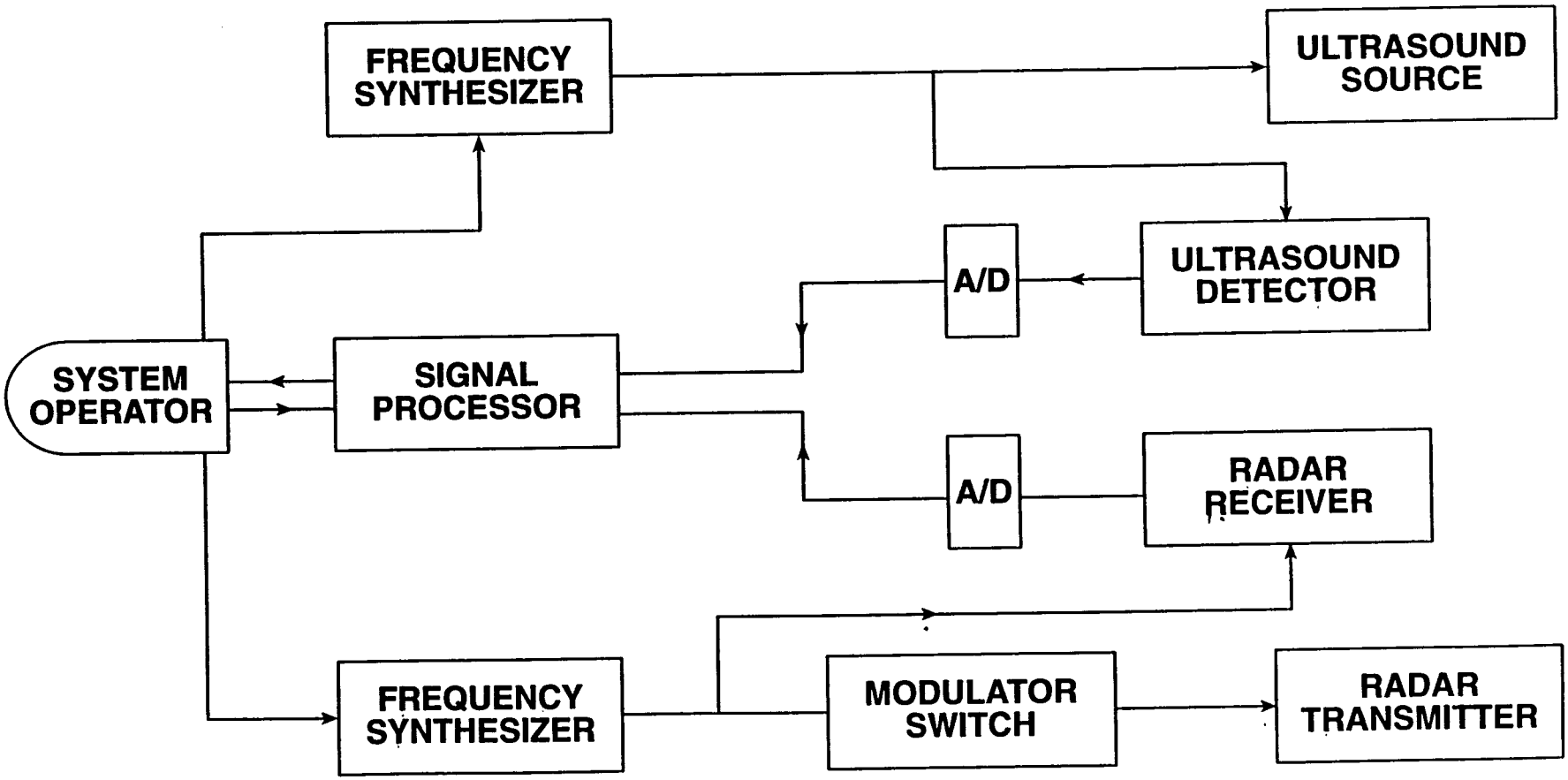

POTENTIAL SENSOR AND SIGNAL PROCESSING INTERFACE LINKAGES

This figure shows how the processing functions of the radar and ultrasound sensors can be linked together and the output displayed in various formats.

POTENTIAL SENSOR AND SIGNAL PROCESSING INTERFACE LINKAGES

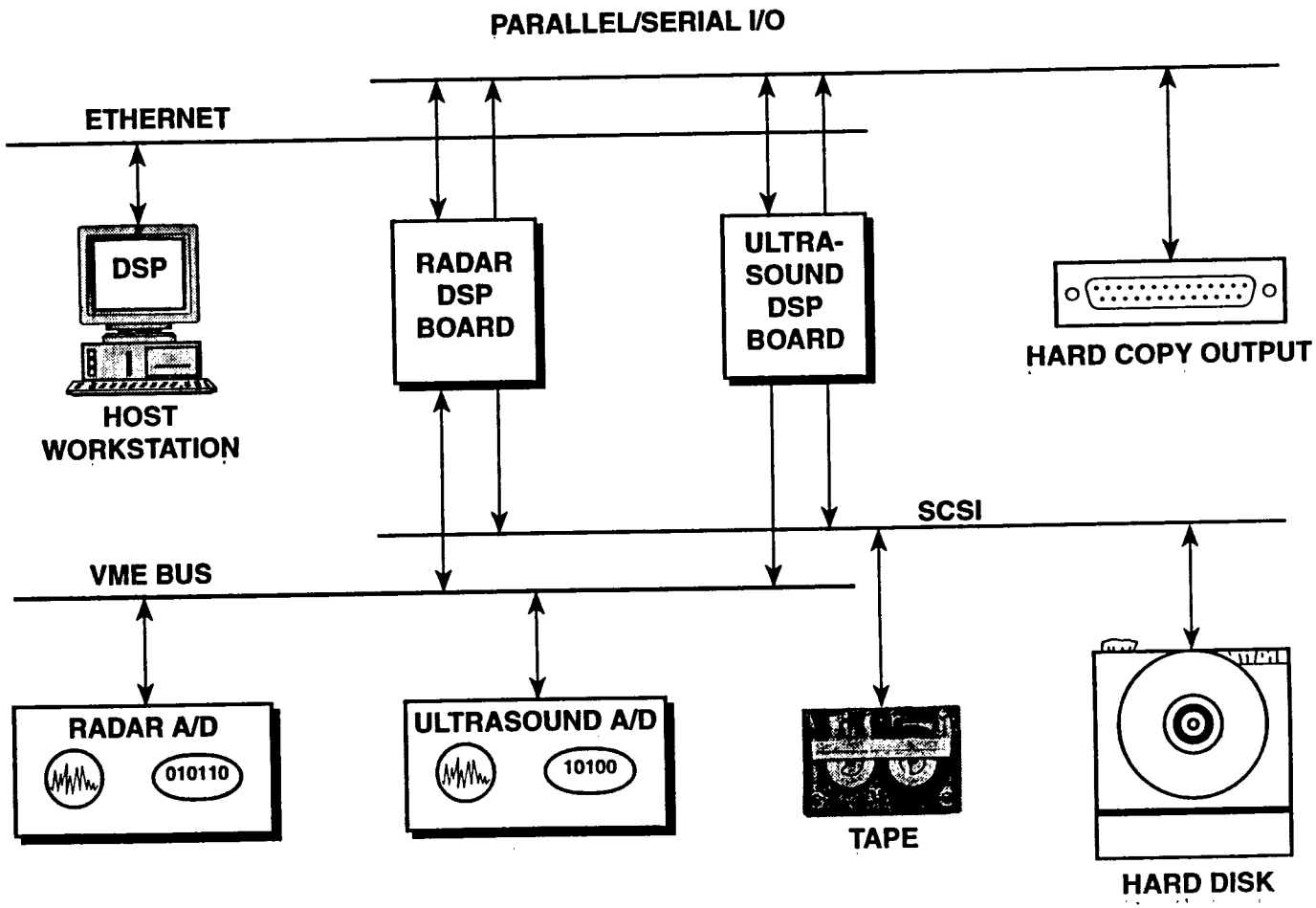

PHASE 2 ULTRASOUND UPGRADES

This table shows in the left column the characteristics of the ultrasound breadboard sensor that was developed and demonstrated in Phase 1, and in the right column the characteristics of the brassboard ultrasound sensor that we have proposed for Phase 2. Since the Phase 1 breadboard sensor uses only one detector at a time, images must be constructed by scanning the receiver dish pixel by pixel over the target area. Typically, it takes 30 minutes to produce an image of the order of 12 x 12 pixels in this manner. Since the breadboard ultrasound sensor operates at only one ultrasound frequency, it may be used either for detecting weapons at long ranges at low frequencies or for imaging weapons at close ranges using higher frequencies. The low frequencies are better for low-resolution distant detection of weapons, and the high frequencies are better for high-resolution close imaging. The breadboard sensor cannot offer both capabilities at the same time. Also, the breadboard sensor must acquire all of the data before the data is processed and filtered afterwards. The primary processing is by binary thresholding of individual pixels. That is, a brightness threshold is set for the image, depending on transmitted power, range, clothing concealment, and detector sensitivity. A spectral density above the brightness threshold appears as a positive pixel in the image, and one below does not.

Since the time required to collect the data for a single image is so long, we must first carefully map out the area to be imaged by the breadboard sensor. This is done with the aid of a laser pointer and an x-y translational stage with a controller for the motion of the receiver dish.

The resolution and the range of the breadboard ultrasound sensor are both limited by the sizes of the receiver and transmitter dishes, respectively. The diffraction-limited resolution is proportional to the diameter of the receiver dish, and the range of aspect angles that can be made to be incident on the target is proportional to the diameter of the diffuse-source transmitter dish.

The Phase 2 brassboard ultrasound sensor will operate at video frame rates of 30 ms per image. It will be equipped with Aerojet's ultrasound imaging array of about 50 x 50 pixels. We would expect the Phase 2 brassboard to operate at two frequencies, 40 kHz and 160 to 200 kHz. The dual frequencies would allow both distant detection at the lower frequency and close-range imaging at the higher frequencies. Since the ultrasound sensor should be capable of imaging concealed weapons in real time, it will have tuning and filtering knobs, probably as controls on a PC controller. Human factors considerations will be involved in the decisions on filtering and displaying the image data. Gray-scale pixels may improve recognition of concealed weapons by the users over binary thresholding. With dual frequencies, and the lower frequency used for distant detection, it should be possible to automatically centroid a concealed weapon by centering the sensor on the area of brightest return. The ultrasound image might even be superimposed on a low-intensity video camera image. The processor might even draw the user's attention to the area of a potential concealed weapon by presenting that area within a box on the monitor. A larger receiver dish and transmitter dish or array will also help improve the resolution and range of a Phase 2 ultrasound brassboard sensor.

PHASE 2 ULTRASOUND UPGRADES

Phase 1 Breadboard	Phase 2 Brassboard
30 minutes/image	30 milliseconds/image
12 x 12 pixel images	50 x 50 pixel images
Close imaging <u>or</u> distant detection	Close imaging <u>and</u> distant detection
Single frequency	Dual frequencies
Post-processed tuning/filtering	Real-time tuning/filtering knobs
Binary thresholding of pixels	Variable amplitudes of pixels
Laborious preframing of images	Automatic centroiding
Resolution limited (18" rcvr)	Improved resolution (30" rcvr)
Range limited (18" x-mtr)	Improved range (30" x-mtr)

FREQUENCY SCALING OF AEROJET DETECTORS

The ideal detectors for imaging in air are bender detectors. These are thin plates that produce a radial stress when bent in the vertical direction. These detectors have the greatest response sensitivity and fabricability in arrays. Each bender detector acts as a thin plate, rather than a membrane under tension. The tension in the bender detectors is negligible compared to the intrinsic tension of the material, which is the product of the Young's modulus and plate thickness. The electrical voltage is produced in bender detectors by the piezoelectric response to the radial stresses. Since each individual bender detector will be fastened to the focal plane at the edges of their respective apertures in the focal plane, each detector acts as an edge-clamped thin plate, obeying the fourth-order thin-plate equation of motion, which has the dispersion equation shown in this chart. In Phase 1, Aerojet fabricated several 4 x 4 arrays of detectors, each about 2-mm square. The detectors were made of about 4-mil thick piezoelectric films. The calculated resonant frequencies of the Aerojet detector arrays are shown in this chart. The actual fundamental frequency was somewhat lower than the calculated frequency. The resonances were measured at about 40 to 50 kHz. The discrepancy may be due to the array fabrication process or to parasitic mass on the piezoelectric film. The higher order modes, such as f_{22} or f_{13}, are candidates for amplification in a dual-frequency ultrasound sensor.

FREQUENCY SCALING OF AEROJET DETECTORS

- Each detector is edge-clamped square or circular thin plate
  - Thin-plate tension << Yd $\approx (2 \times 10^9\ N/m^2)(10^{-4}\ m) \approx 10^5\ N/m$

- Fourth-order thin-plate equation of motion for square detector has dispersion equation

$$f_{nm} \approx \frac{\pi dc}{4\sqrt{3}} \left[\left(\frac{n + 1/2}{L_x} \right)^2 + \left(\frac{m + 1/2}{L_y} \right)^2 \right] \text{ where } n, m = 1, 2, 3, \ldots$$

- For $A = L_x L_y = 4\ mm^2$, $c = 1.06$ km/s, $d = 110\ \mu m$, the first few resonant frequencies are

$f_{11} = 2.06\ dc/A = 60$ kHz

$f_{12} = 3.86\ dc/A = 110$ kHz

$f_{22} = 5.67\ dc/A = 170$ kHz

$f_{13} = 6.58\ dc/A = 190$ kHz

$f_{23} = 8.39\ dc/A = 240$ kHz

$f_{14} = 10.21\ dc/A = 300$ kHz

DUAL-FREQUENCY BENDER DETECTORS

In Phase 1, the simplest detector worked the best. The simplest bender detector was a single film layer of polyvinylideneflouride (PVDF). A teflon-copolymer, also sold commercially, may have slightly better properties for performance as an ultrasound detector. Aerojet found that the film used in the detector array needs to be taut, but high tension is not needed, as it is in tensioned membrane detectors. If circular detectors are used, instead of square detectors, then the second symmetric resonant frequency is conveniently about four times the fundamental frequency. (Non-symmetric resonant frequencies exist between the first two symmetric resonant frequencies.) For a dual-frequency sensor, this means that the two frequencies of operation could be, for example, 50 Hz and 194 Hz. Aerojet can make detector arrays with square or circular detectors equally easily.

DUAL-FREQUENCY BENDER DETECTORS

- Single film layer — PVDF or teflon-copolymer
- Edge-clamped film should be taut, but high tension not needed
- Second symmetric resonant frequency of circular film is 3.88 times fundamental
  - Example: 50 kHz and 194 kHz

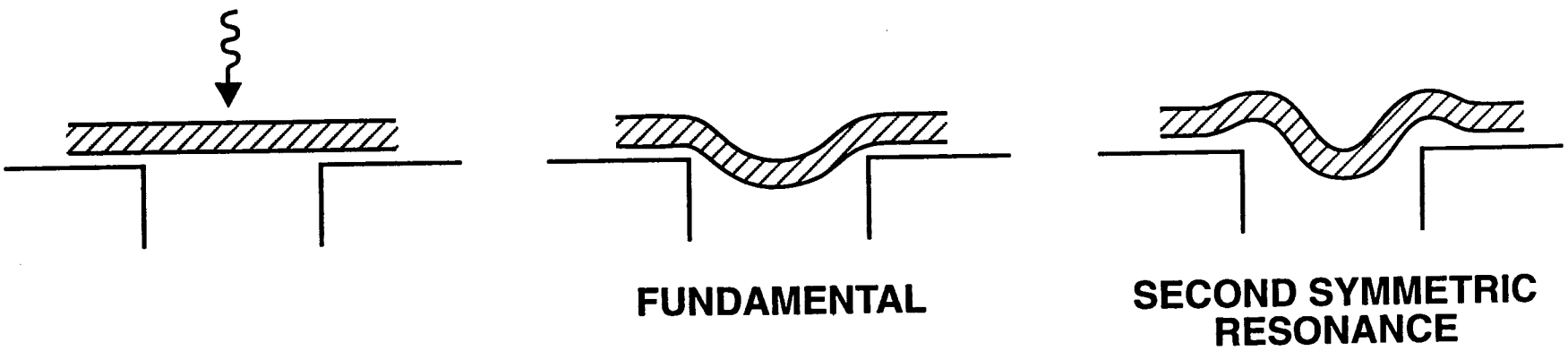

PHASE 2 ULTRASOUND IMAGE PROCESSING

The real-time image processing of the Phase 2 ultrasound brassboard sensor will differ substantially from the post-processing of images done in Phase 1. In Phase 2, Aerojet will fabricate a detector array of approximately 50 x 50 detectors. Some of the processing, such as pre-amplification and other analog processing, will be done on the focal plane. A VME crate will contain the analog-to-digital (AD) converter, the digital signal processing board, and the video card that controls the video display. The processor will accept filtering inputs from a notebook computer via an ethernet card. The brightness and contrast can be controlled, for example, by moving a trackball on the notebook computer. The digital signal processor will perform whatever digital filtering is needed to produce a viable image. Examples of processing techniques that can be built into the DSP board include nonuniformity correction, suppression of background, oversampling and averaging, spatial filtering, and thresholding. For example, the spatial filtering might filter out all apparent objects that are smaller or larger than typical concealed weapon sizes of, say, 3 inches to 15 inches.

PHASE 2 ULTRASOUND IMAGE PROCESSING

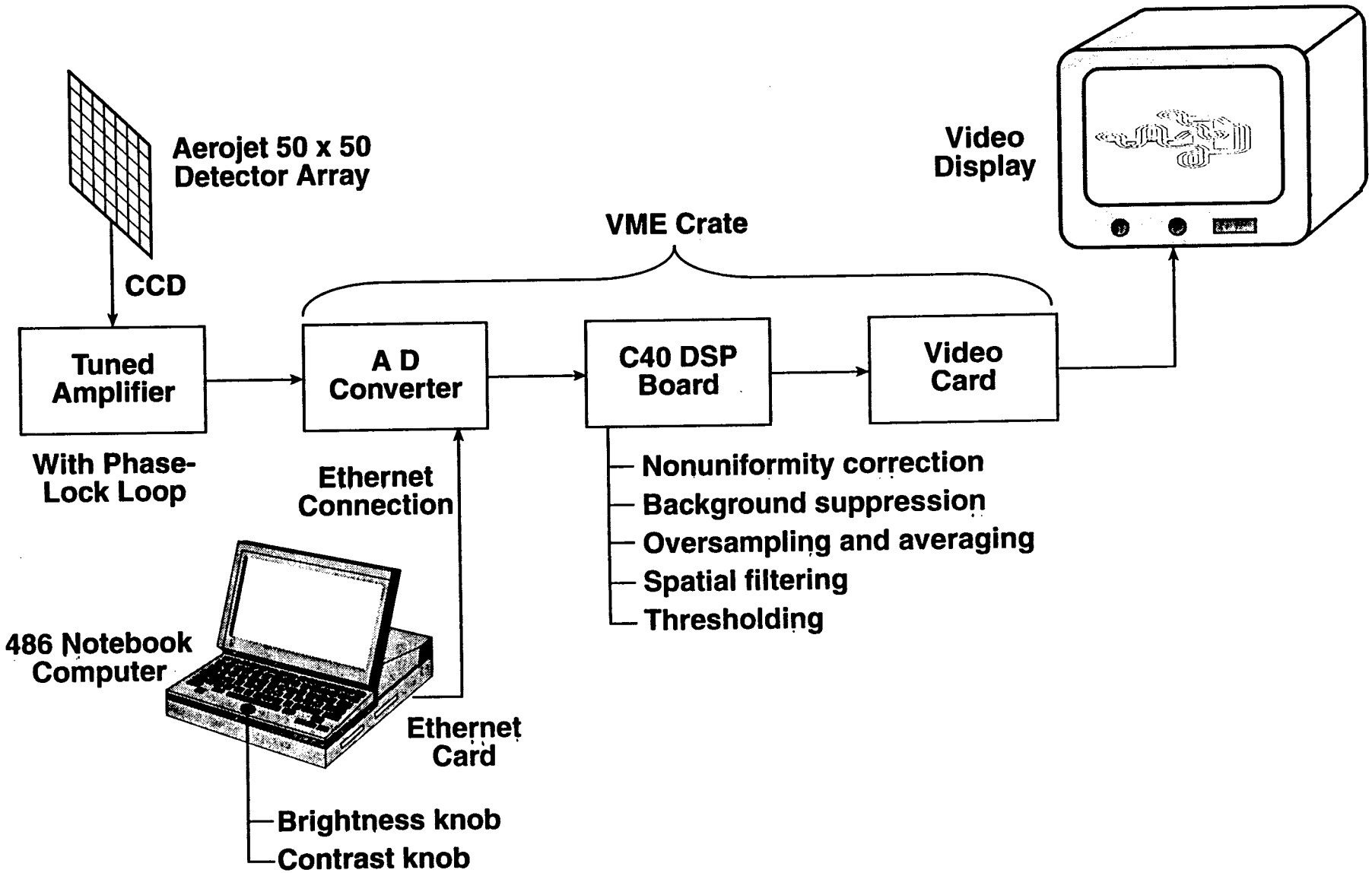

PHASE 2 ULTRASOUND SIGNAL PROCESSING

At video frame rates of 30 frames per second, a 50 x 50 array of detectors requires 75,000 pixels per second to be processed. Estimates have been made of the number of operations per pixel to suppress the background, filter the image pixels and display the image on a video monitor. These estimates are gives the table on this chart. Multiplying the pixel rate by the number of operations required per pixel gives the number of operations per second required of the signal processor.

PHASE 2 ULTRASOUND SIGNAL PROCESSING

Throughput Analysis for 30 Frames/s, 50 x 50 Array			
Algorithm	Pixels/s	OPS/pixel	MOPS
Background Suppression	75,000	60	4.5
Filtering	75,000	40	3
Video Display	75,000	10	.75

PHASE 2 ULTRASOUND SIGNAL PROCESSING APPROACH

The estimates on the preceding chart are displayed here along with the conclusion that approximately 8 million operations per second are needed for real-time image processing with the Phase 2 ultrasound brassboard sensor. This throughput can be handled easily with a single C40 DSP card.

PHASE 2 ULTRASOUND SIGNAL PROCESSING APPROACH

Throughput Analysis Summary

- 30 Frames/s of ultrasound data
  - — 50 x 50 detector array size
  - — 75,000 pixels/s

• Background suppression:	4.5 MOPS
• Filtering:	3 MOPS
• Video display:	750 KOPS
• Total:	~8 MOPS or <1 C40 DSP

PHASE 2 BRASSBOARD

Dedicated
CWD Radar

PHASE 2 CWD RADAR BRASSBOARD

This figure illustrates how a radar sensor might be implemented for CWD. The operator is looking at a color-coded video display of the 2-D cross-correlation map. The radar system used in Phase 1 for CWD testing could easily detect humans walking across the FOV of the radar on the cross-correlation display. The height of the peaks in the cross-correlation display is related to the probability of a concealed weapon at the resonant frequencies of the radar sensor. Instead of representing the cross-correlation as a 2-D surface plot, the amplitudes can very easily be color coded to alert the operator to the probability of concealed weapons.

PHASE 2 CWD RADAR BRASSBOARD

PHASE 2 RADAR UPGRADES

This table shows in the left column the characteristics of the Phase 1 breadboard sensor that was tested for CWD and in the right column the characteristics of the brassboard radar sensor that we propose to build in Phase 2. The radar that we used in Phase 1 was optimized for detecting mines from moving vehicles. The 60 degree field of view (FOV) was adequate for detecting mines at ranges of tens of meters. The frame rate of 2 s per (spectral) image was adequate for slow motion (2 mph) through mine fields, and the 6 cu.ft. of equipment was adequate for the prototype device. The 36 frequencies produced by the radar from 0.5 to 4 GHz covered the range of resonance frequencies of buried metallic and nonmetallic mines. The vertical polarization of the radar also was ideal for finding mines.

A brassboard radar, dedicated to concealed weapons detection, will be built in Phase 2. The brassboard radar will use the hardware technologies of the Phase 1 radar and of the ongoing upgraded radar program, but will design the software specifically to be optimized for CWD. The radar will have the faster spectral image rate of 0.5 s per image of the upgraded radar, and will have the more compact 2 cu.ft. volume of the upgraded radar, but will have a wider FOV, which is valuable for the CWD mission. Also, to access the resonance frequencies of some longer concealed weapons, some frequencies below 500 MHz will be included in the radar spectrum. Lastly, since the orientation of a long concealed weapon is not known beforehand, circular polarization may be the best choice for CWD.

PHASE 2 RADAR UPGRADES

Phase 1 Breadboard	Phase 2 Brassboard
Mine-detection radar	Dedicated CWD radar
Optimized for moving radar/ stationary targets	Optimized for stationary radar/ moving targets
60° FOV	90° FOV
2 seconds/image	0.5 second/image
Radar 6 cu. ft.	2 cu. ft. with cooling
Frequencies (0.5 to 4 GHz) optimized for mines	Frequencies optimized for CWD
Vertical polarization for mines	Circular polarization for CWD

PHASE 2 RADAR SIMPLIFICATIONS

The range of frequencies used in the mine-detector radar is intended to cover the range of resonant frequencies of a wide variety of buried metallic and nonmetallic mines. The mine-detection radar types mines by their characteristic spectra. Typing concealed weapons is virtually impossible because of the infinite variety of possible sizes and shapes. Therefore, the spectral signature is not that important for CWD, which means that fewer frequencies need to be sampled. Also, the range of sizes of concealed weapons is limited, which means that only a relatively narrower range of frequencies needs to be sampled for detecting concealed weapons. The relaxed frequency sampling requirements means fewer oscillators in the synthesizer and fewer and cheaper amplifiers. The processing and data acquisition requirements are similarly reduced.

Mines need to be located to within inches. The requirements for locating humans who may be carrying concealed weapons are less rigorous. The radar will only need to distinguish the location of one human from a nearby human. The reduced range accuracy requirement again means less data processing and less hardware.

The radar used in Phase 1 CWD testing was far more sensitive and had far greater range than was required. The power of the radar could be reduced from 10 to 1 W, which would substantially reduce the cost of amplifiers from about $20K to $1K. The reduction of power is made possible not only because the greater range is not needed, but the radar targets have greater cross sections than buried mines and the radar penetrates clothing more easily than it penetrates soil.

PHASE 2 RADAR SIMPLIFICATIONS

- Fewer frequencies because of narrower range of concealed weapon sizes
  - Fewer oscillators in the synthesizer
  - Less data acquisition and analysis
  - Fewer and cheaper amplifiers
- Less accurate range information
  - Less data processing
  - Less hardware
    - Do not need to sample outgoing pulse
- Reduce power from 10 W to 1 W
  - Larger target cross section and better penetration
  - Fewer and cheaper amplifiers ($20K → $1K)

BLOCK DIAGRAM

This figure is a schematic diagram of the major components of the Phase 2 CWD brassboard radar sensor. Like the radar used in Phase 1, it has stereo reception and only a single transmit antenna. The stereo receive antennas are for azimuthal direction finding. The Phase 2 CWD radar is substantially simpler and cheaper than the mine-detection radar used in Phase 1 for the reasons given on the preceding page.

BLOCK DIAGRAM

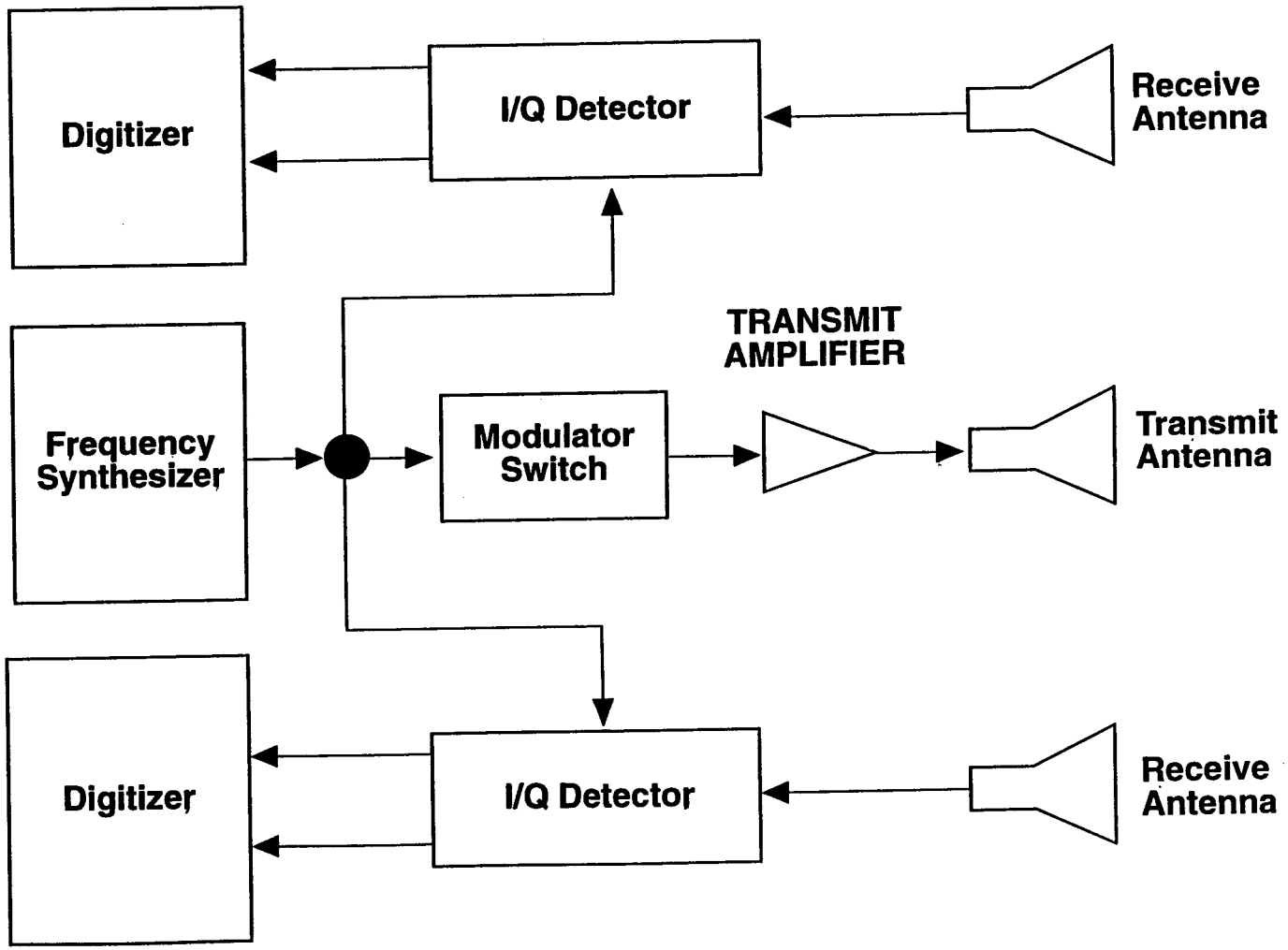

COMPUTER CONFIGURATION

The computer configuration for the Phase 2 CWD radar is shown schematically in this diagram. After processing, the outputs are sent via VME bus to the ultrasound sensor. The processed outputs of the radar sensor will control the direction in which the ultrasound transmit and receive dishes are pointed.

COMPUTER CONFIGURATION

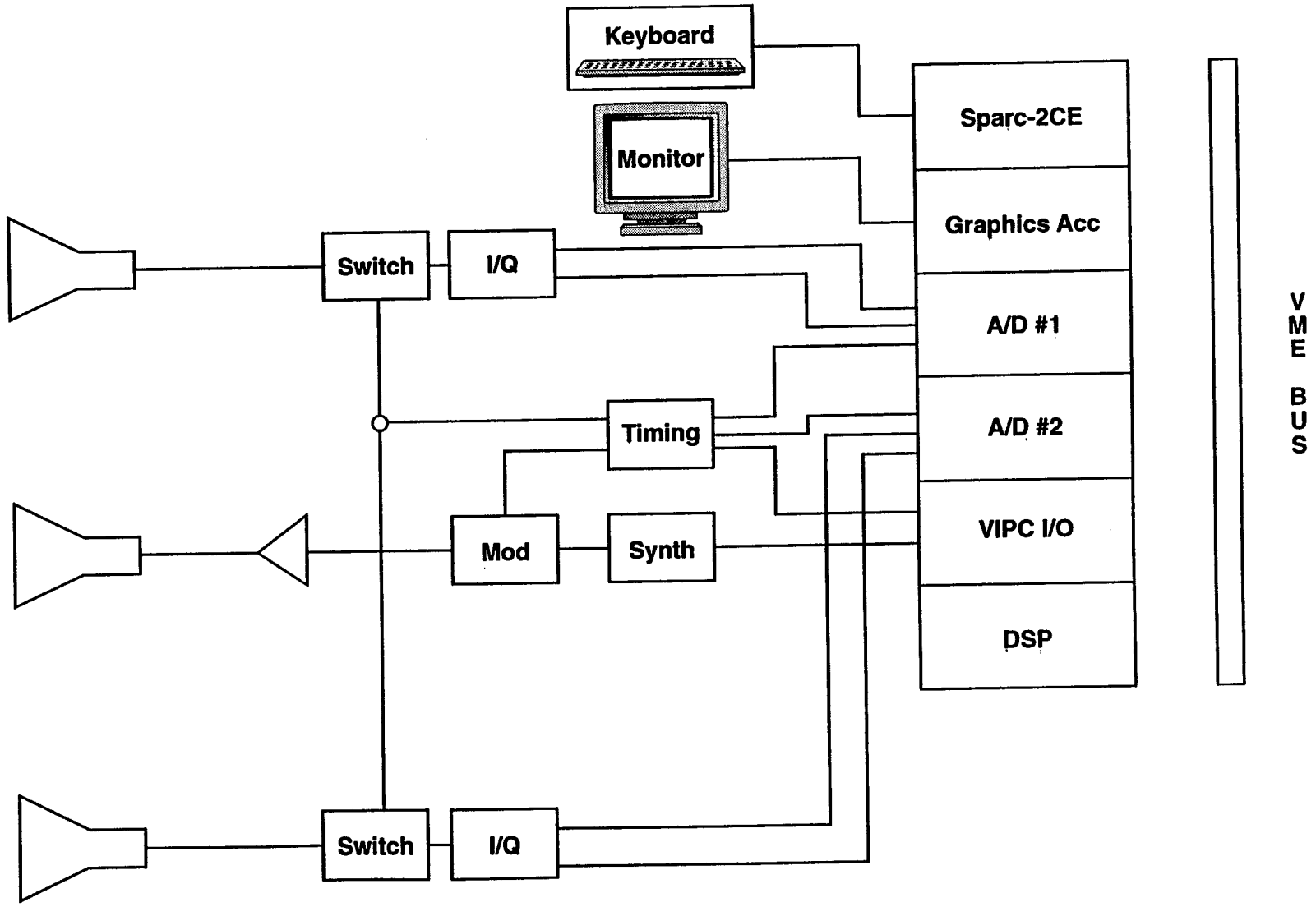

PHASE 2 RADAR FREQUENCIES

Concealed weapons are not too different in size from buried mines. Therefore, the range of frequencies used in the mine-detection radar is almost the same as the range that would be needed for a CWD radar. Since most concealed weapons behave as monopoles, the range of frequencies for the half-wave resonance for typical weapons is about 0.3 to 2 GHz. Long, edged weapons and long-barreled handguns will resonate at the lower frequencies which are not currently sampled by the existing mine-detection radar. Although we may wish to extend the range of a CWD radar to lower frequencies, fewer frequencies will be needed all told, since attempts will not be made to type the concealed weapons by their spectral signatures, but only to detect them. Fewer frequencies will result in lower costs and simpler and faster systems.

PHASE 2 RADAR FREQUENCIES

- Most concealed weapons behave as monopoles
  - — Half-wave resonance
  - — Typical weapon lengths 6-12 inches
    - ⇒ 0.3 to 2 GHz
- Lower frequencies needed for larger weapons
- Fewer frequencies needed
  - — Cheaper synthesizer
  - — Simplifies and speeds
    - Data collection
    - Data analysis

PHASE 2 RADAR PROCESSING UPGRADES

The mine-detection radar is currently being upgraded under an Army program. Much of the radar processing upgrading that will be done under the ongoing program will also be applicable and valuable to a Phase 2 CWD radar. For example, the upgraded radar will be able to detect mines from vehicles moving faster than the current allowable speed of 3 km/hr. The sensitivity of the radar has been greatly improved. And of course, reducing the volume of the upgraded mine-detection radar to 2 cubic feet will be a valuable improvement for the Phase 2 CWD brassboard radar as well.

In Phase 1, the mine-detection algorithms and software were not substantially changed to optimize them for the CWD mission. In Phase 2, new algorithms will need to address the CWD mission, which is very different than the mine-detection mission. For example, the display will be of a moving individual, rather than of a stationary mine from a moving vehicle. The display will be designed for the operator of a CWD system. The sensor might provide audible alarms along with color-coded measures of the radar returns from each moving object. As with the ultrasound sensor, the color-coded cross-correlation data may be superimposed on a video camera view of the scene to help correlate alarms with specific individuals in a crowd.

PHASE 2 RADAR PROCESSING UPGRADES

- Reduction of static background
- Visual and audio binary-thresholding alarms
- Display moving coordinates of suspect
- Able to handle speeds up to 10 km/hr
  - — Must track suspect to do time delay and integration (TDI)
- Reduce conversion time in digitizer by orders of magnitude (under Army contract)

PHASE 2 RADAR SOW

In Phase 2 the radar brassboard sensor will be built from scratch. In most details it will resemble the upgraded mine-detection radar that will be completed in April 1997. The radar antennas will needed to be mounted at about 6-ft. height for fixed-site applications, since the radar is designed to point slightly downwards at targets of interest. The radar will have simplified hardware optimized for the CWD mission. The existing mine-detection code, MDET is suitable for observing stationary targets from a moving platform. The MDET code will need to be modified for surveillance of moving targets. The detection algorithms in the code will also need to be modified specifically for the CWD mission. Different filtering algorithms will be needed as well. After the hardware and software has been prepared for the Phase 2 brassboard radar, the system will be calibrated for detection of concealed weapons and tested under wide ranges of operating conditions.

PHASE 2 RADAR SOW

- Build radar brassboard from scratch
  - Resembling most details of mine detection radar
  - Stationary 6' mount
  - Optimized frequency range
- Processing algorithms
  - Modify MDET code for moving targets (but not system controls)
  - Modify detection algorithms in MDET for weapon on person
- System calibration
  - Different sensitivity from mine detection
- System test
  - Vary humans, weapons, ranges, concealments, orientations, motion, etc.

APPENDIX A

Fusion of radar and ultrasound sensors for concealed weapons detection

F. S. Felber, H. T. Davis III, C. Mallon, and N. C. Wild

JAYCOR
P. O. Box 85154, San Diego, CA 92186

ABSTRACT

An integrated radar and ultrasound sensor, capable of remotely detecting and imaging concealed weapons, is being developed. A modified frequency-agile, mine-detection radar is intended to specify with high probability of detection at ranges of 1 to 10 m which individuals in a moving crowd may be concealing metallic or nonmetallic weapons. Within about 1 to 5 m, the active ultrasound sensor is intended to enable a user to identify a concealed weapon on a moving person with low false-detection rate, achieved through a real-time centimeter-resolution image of the weapon. The goal for sensor fusion is to have the radar acquire concealed weapons at long ranges and seamlessly hand over tracking data to the ultrasound sensor for high-resolution imaging on a video monitor.

We have demonstrated centimeter-resolution ultrasound images of metallic and non-metallic weapons concealed on a human at ranges over 1 m. Processing of the ultrasound images includes filters for noise, frequency, brightness, and contrast.

A frequency-agile radar has been developed by JAYCOR under the U. S. Army Advanced Mine Detection Radar Program. The signature of an armed person, detected by this radar, differs appreciably from that of the same person unarmed.

Keywords: Sensor, sensor fusion, concealed weapon, concealed weapons detection, radar, ultrasound, imaging, image processing.

1. INTRODUCTION

An integrated ultrasound and radar sensor, which will be capable of remotely detecting and imaging concealed weapons, is being developed. A scenario for the use of such an integrated sensor in law enforcement might be the following. From an unobtrusive site more than 10 m away, a frequency-agile radar will specify with a high probability of detection (P_D) which individuals in a moving crowd may be concealing metallic or nonmetallic weapons. The radar will hand over the location tracking data on the concealed weapon to the ultrasound sensor. At ranges up to a few meters, the active ultrasound sensor will enable a guard to identify the concealed weapon on a moving person with a low false-detection rate, achieved through a real-time centimeter-resolution image of the weapon on a video monitor. The high resolution and anticipated low false-detection rate of the ultrasound sensor complement Fourth Amendment bans of unreasonable searches and seizures.

Both the radar and ultrasound sensors will detect not only metal guns and knives, but also such nonmetallic weapons as ceramic handguns, sharpened stakes, and bottles of caustic or flammable fluids. The frequency-agile radar has been developed by JAYCOR and tested for mine detection under the U. S. Army Advanced Mine Detection Radar Program. In field tests it has successfully detected and located 100% of buried plastic and metal mines at ranges up to 15 m. The radar finds plastic mines, and might also find nonmetallic weapons, by differences in the dielectric constant. The radar and controlling software will be modified to detect, screen, and locate concealed weapons at 10 m in a moving crowd.

For accurate identification of concealed weapons, the radar will provide acquisition data on detected weapons to the active ultrasound sensor. Handheld, battery-operated ultrasound rangefinders, available in hardware stores, have over a 10-m range at low (40 kHz) ultrasound frequencies. High-resolution imaging of concealed weapons with higher frequency (200 kHz) ultrasound requires high effective radiated power (ERP) and sensitive detectors. We have developed and demonstrated a novel repetitive and efficient source of high-power, coherent ultrasound radiation suitable for remote imaging in air. With sensitive ultrasound detectors and high-gain transceivers, this advance makes possible the centimeter-resolution ultrasound imaging of concealed weapons at ranges of several meters.

2. SENSOR FUSION

When operated together in an integrated system, the ultrasound and radar sensors will provide for detection at 10 m and unambiguous identification of concealed weapons up to 3 to 5 m. We expect to achieve high probability of detection (P_D > 95%), while maintaining an acceptably low false-detection rate. The radar-based weapons detector will serve as a bell-ringer by alerting the operator and the ultrasound subsystem to a possible concealed weapon at a particular location in the radar field of view (FOV) up to 10 m away. The ultrasound transmitter and receiver will then slew to the suspected location and provide finer details of concealed objects in its narrower FOV up to 3 to 5 m away. Figure 1 shows the main components of the integrated sensor system.

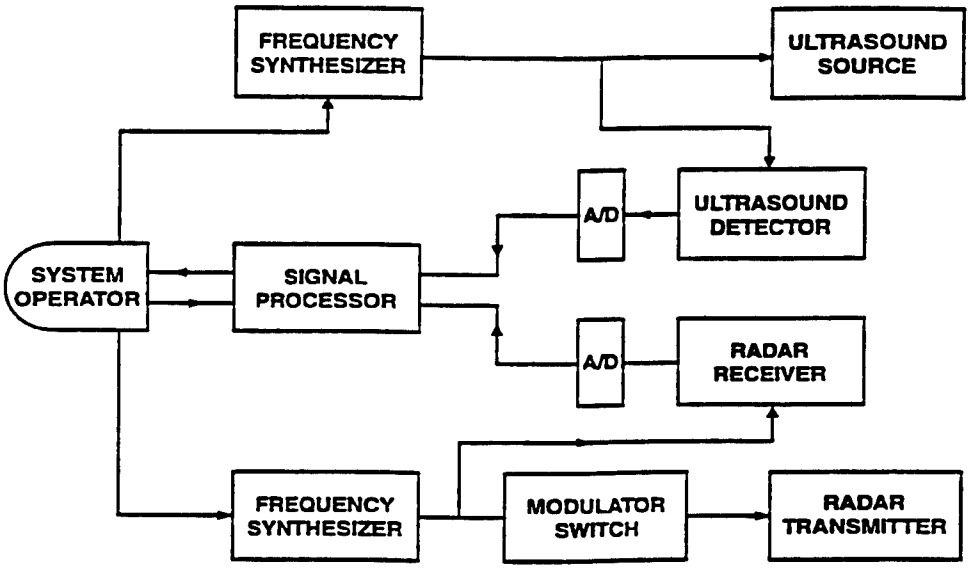

Figure 1. Block diagram of concealed weapons detection system and components.

The need for a system that can detect and image concealed weapons in real time has driven the design to include two complementary sensor technologies. These proven technologies, radar and ultrasound, should provide for high P_D and low occurrence of false detections. Table 1 summarizes the main characteristics of the two sensors integrated for concealed weapons detection. The extended range of the frequency-agile radar will provide early warning of concealed weapons and command the high-resolution ultrasound aperture to slew to the indicated individual(s). The best ultrasound image resolutions (1 to 2 cm) will be realized for fixed-site applications, where 60-cm-diameter aperture receiving antennas can be accommodated. As can be seen from Table 1, the integrated ultrasound/radar approach can address applications of both long-range (10 to 15 m), early-warning threat detection, as well as close-range imaging and identification for low false-detection rates.

An important feature in fusing the sensors will be the interface link between the frequency-agile radar and the ultrasound source/receiver subsystems. This link will provide for radar handover of data to the ultrasound subsystem and also provide for health and status checks on each subsystem to the operator. Figure 2 is a sketch of where the various interface links could be implemented in an integrated sensor.

Table 1. Advantages/trade-offs of ultrasound/radar system.

Property	Radar	Ultrasound
Range	10-15 m	3-5 m
Resolution	N/A	1 to 2 cm
Frequency	0.5-4 GHz	200 kHz
Aperture	60 cm	60 cm
Potential configurations	Fixed site, mobile	Fixed site, mobile, handheld
FOV	Crowd	Body
Penetration	Excellent	Excellent
Nonmetallic CWD	Good	Excellent
Safety	Excellent	Excellent
Social acceptance	Satisfactory	Excellent

3. ULTRASOUND SENSOR

The heart of the ultrasound sensor is the proprietary ultrasound generator. It produces high-power coherent ultrasound radiation, tunable from about 10 kHz (high audible) to at least

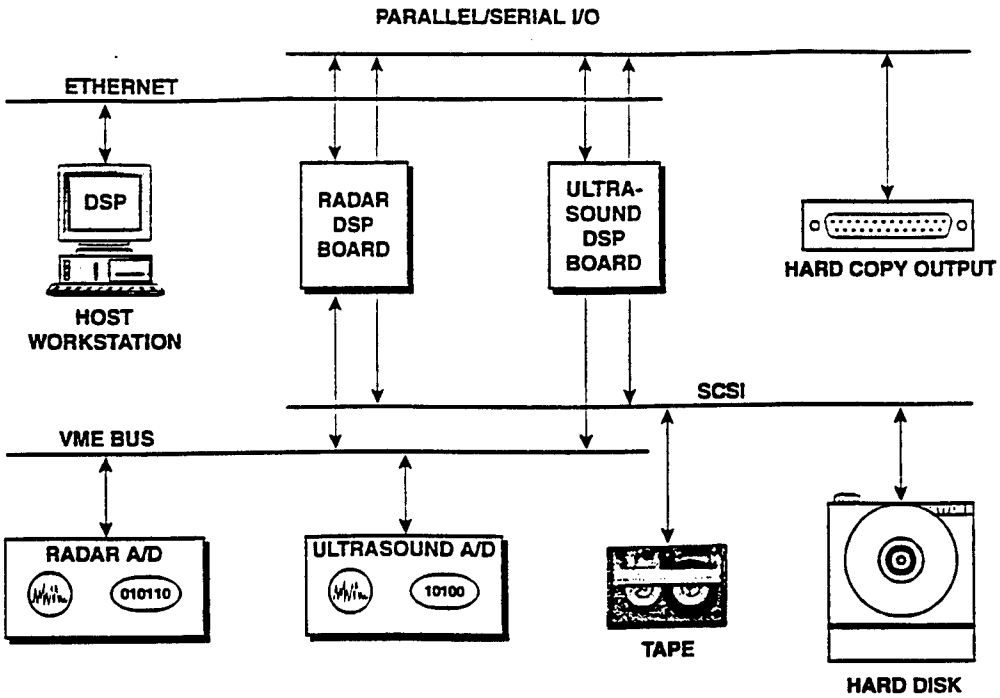

Figure 2. Block diagram showing system components and potential sensor and signal processing interface linkages.

660 kHz. The electrical-to-ultrasound efficiency of up to 5 to 10 percent is much better than that of commercial piezoelectric-crystal air-ranging transducers. The ultrasound power is up to ten times higher than the rated powers of commercial piezoelectric transducers. And unlike transducers, at peak power, this ultrasound source can operate continuously, and not just at some low duty cycle. The ultrasound frequency, burst repetition frequency, and burst duration are all tunable. By contrast, commercial transducers have a narrow-band (generally less than 1 percent) resonance in the power spectrum at some fixed frequency.

With the active ultrasound imaging sensor, we have achieved both diffraction-limited resolution and the theoretical limit of resolution determined by geometrical optics. In resolution tests, the ultrasound signal was reflected from a 1.6-cm-diameter cylindrical post over a range $r = 1.3$ m onto a mirror with a diameter $d = 13$ cm and a focal length $f = 8$ cm. The mirror focused the 200-kHz ultrasound at the face of a 200-kHz transducer. The transducer had an aperture of diameter $a = 1$ mm immediately in front of it. With this setup, the detector was in the far (radiation) zone of the source. The effective source of ultrasound is equivalent to a narrow slit at the surface of the cylindrical post and at the angle that produces specular reflection from the true source into the transducer.

According to geometrical optics, the resolution R_g of the detector/aperture should be the same as the footprint of the 1-mm-diameter aperture projected onto the post. Under the conditions of our test, the pixel footprint, or geometrical-optics resolution, is

$$R_g = \frac{a}{f} r = \frac{1\ mm}{8\ cm} 1.3\ m = 1.6\ cm. \tag{1}$$

According to Fraunhofer scalar diffraction theory, the resolution R_d given by the full-width-at-half-maximum (FWHM) of the central diffraction bright spot is

$$R_d = 1.03 \frac{\lambda}{d} r = 1.03 \frac{1.7\ mm}{13\ cm} 1.3\ m = 1.75\ cm. \tag{2}$$

The actual FWHM source width was measured with the ultrasound to be 1.6 cm, which was the same as the resolution limit of geometrical optics in our test. Our measured source width was slightly smaller than the diffraction limit, though within experimental error. We performed another ultrasound resolution test at 40 kHz (λ = 8.5 mm) and a range of 4.5 m using a nearly three-foot receiver dish, and measured a diffraction-limited resolution of 5 cm. In any experiment, the larger of the two resolution limits, R_g and R_d, should pertain.

4. ULTRASOUND IMAGE PROCESSING

We have produced reasonably good remote ultrasound images of metallic and nonmetallic weapons concealed under clothing on a human body. And we have demonstrated that when the imaging process is repeated under identical conditions, but with no weapon, the weapon image is gone, leaving a blank or nearly blank picture.

Because we use only a single ultrasound detector, instead of an imaging array, the imaging process requires a painstaking pixel-by-pixel scan of the body. Although the ultrasound exposure time per pixel is only about 1 ms, the process of imaging a concealed weapon and then imaging the control without the weapon lasts 1 to 2 hours. An imaging array of ultrasound detectors is in an early development stage. When the array of detectors becomes available to produce real-time video images of ultrasound "scenes", the image processing will differ substantially from the processing we used for producing images pixel-by-pixel. In this section, we describe the image processing we actually used for the pixel-by-pixel imaging.

The receiver dish and detector are scanned over a rectangular grid on the body using a semi-automatic x-y positioning stage. At 200 kHz, the pixel footprint on the body is about 2 cm at a range of 1.3 m, where we have done most of our imaging. A typical scan might involve a rectangular grid of 10 to 15 pixels on an edge, with center-to-center spacings at the body of about 1 to 3 cm.

At the end of the scanning process, our data is one ultrasound waveform per pixel. Each ultrasound waveform has 512 data points, typically at 1-µs or 2-µs intervals. With about 100 to 200 waveforms, all the data for a single image typically fits on one 1.44-MB floppy disk. A typical ultrasound waveform for a single pixel is shown in Fig. 3(a). In the following, we will show the steps we used to process data into an image of a concealed weapon. The image is of a nonmetallic lexan knife concealed under a wool sweater on an author's body at a distance of 1.3 m from the ultrasound sensor. The proprietary ultrasound source was used at a frequency of 203.5 kHz.

We developed an image processing program, IMAGE, using the commercial Mathcad® Plus 6.0 program as a platform. If the image has *nxm* pixels, the IMAGE program reads all the data into a 512 by *nxm* array. Then it filters for noise, frequency, brightness, and contrast.

The noise filtering exploits the fact that our 100-µs ultrasound waveforms are much shorter than our 1-ms exposure times. IMAGE calculates the standard deviation σ_{nm} of each waveform. Then it sets equal to zero each data point in a waveform having an amplitude less than some multiple of the standard deviation of that waveform. Of course, the same multiple is used for all pixels, or else we could produce any picture we like. A filter set at $1.5\sigma_{nm}$ seems to work best for our images. If the waveform contains a signal, then the signal is evident as a "localized" pulse, as in Fig. 3(a). The $1.5\sigma_{nm}$ noise filter acts on this waveform to produce the filtered waveform shown in Figure 3(b). On the other hand, if the waveform is just noise with no signal from a weapon, then the noise pattern is fairly "uniform", as in Fig. 3(c), and is mostly eliminated by the $1.5\sigma_{nm}$ noise filter, as shown in Fig. 3(d).

A frequency filter in IMAGE works synergistically with this noise filter. IMAGE calculates the fast Fourier transform of each noise-filtered waveform. The absolute square of the Fourier transform of the filtered waveform of Fig. 3(b) is shown in Fig. 4(a). Since low-amplitude noise at 200 kHz was mostly filtered out by the noise filter, those filtered waveforms not carrying a signal have a broad frequency spectrum. A 4-percent-bandwidth filter around the transmitter frequency, as shown in Fig. 4(b), is adequate to enhance the signal-to-noise. The final image is insensitive to filter bandwidth between about a few percent and 20 percent. The frequency filter is prudent to eliminate spurious noise sources, such as the 60 kHz noise that afflicts our laboratory, and acoustic noise sources.

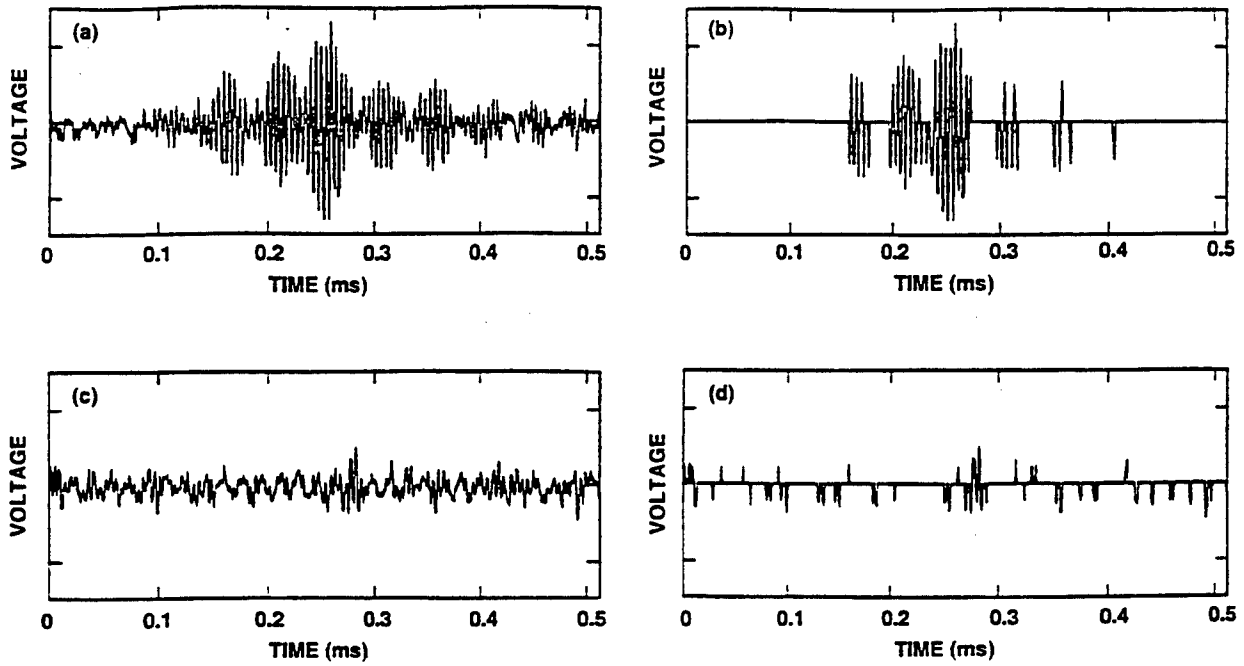

Figure 3. **(a) Typical ultrasound signal waveform from a single-pixel 0.5-ms exposure. (b) Same waveform after $1.5\sigma_{nm}$ noise filtering. (c) Typical waveform from a pixel with no concealed weapon. (d) Waveform of (c) after $1.5\sigma_{nm}$ noise filtering.**

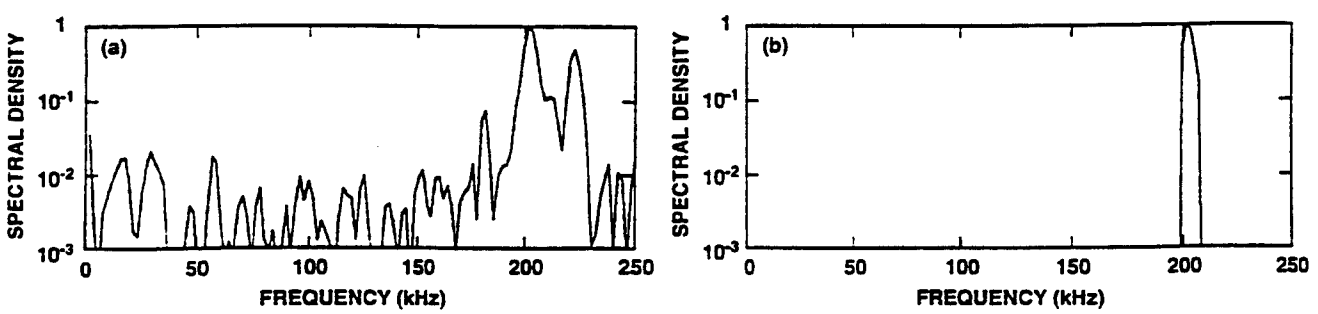

Figure 4. **(a) Absolute square of fast Fourier transform of waveform in Fig. 3(b) versus frequency. (b) Same as (a) after 4-percent-bandwidth frequency filtering.**

After the noise and frequency filtering, IMAGE extracts from the filtered spectral density of each pixel waveform, like the one in Fig. 4(b), only a single number, the maximum within the frequency window. These $n \times m$ numbers for the image of the knife are arrayed linearly in Fig. 5(a). IMAGE assembles these numbers into a matrix, following the pixel roadmap from the image scan. A two-dimensional plot of the matrix is shown in Fig. 5(b) and a contour plot in Fig. 5(c).

A brightness filter sets equal to zero all points in the image matrix that are less than a threshold. The contour plot of Fig. 5(c), with low-intensity points filtered out, is shown in Fig. 5(d). In this sense, the brightness filter is really a spectral-density amplitude filter.

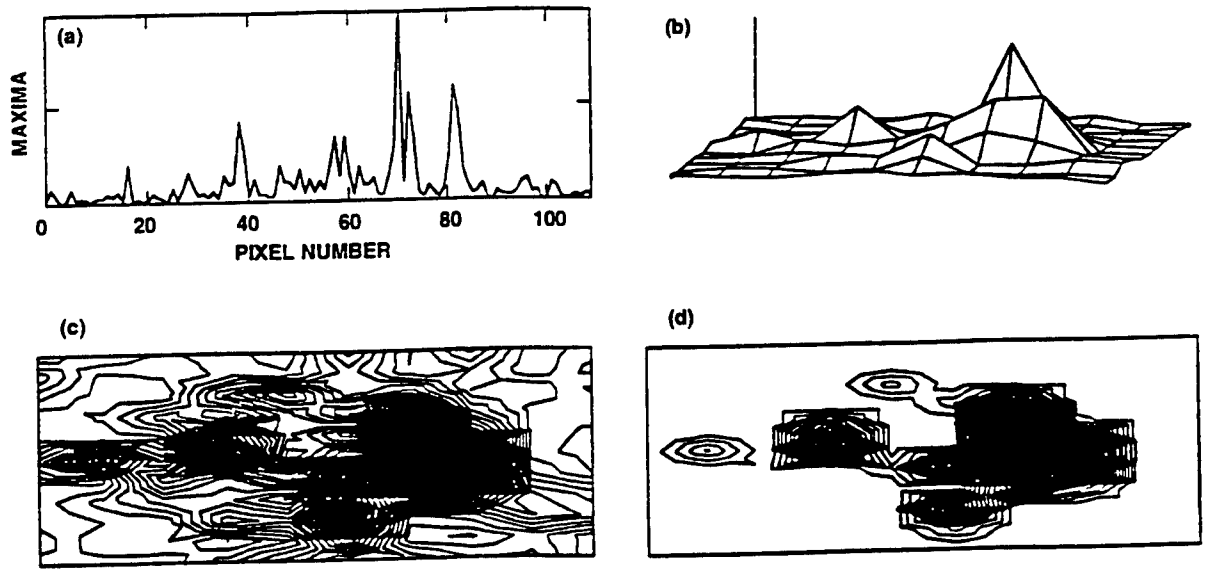

Figure 5. (a) Maximum filtered spectral densities of waveforms versus pixel number. (b) Surface plot of (a) arranged in image matrix. (c) Contour plot of (b). (d) Same as (c) after brightness filtering.

Finally, a contrast filter in IMAGE sets equal to a threshold all points in the image matrix that exceed the threshold. The contrast filter eliminates ultrasound glints, or highly specular reflections, from individual pixels, since they only distract from the perception of an ultrasound image. The contrast filter threshold is set 1 percent above the brightness filter threshold to give the best appearance of an image in a contour plot.

The concealed lexan knife that was imaged is shown in Fig. 6(a). The final ultrasound image, after processing for noise, frequency, brightness, and contrast, is shown in Fig. 6(b). The knife and the ultrasound image are depicted in Fig. 6 with the same length scale. The box around the image represents a rectangular area at the sweater of 8.89 cm by 24.0 cm. The image comprises 11 pixels vertically, separated by 0.89 cm, and 10 pixels horizontally, separated by 2.67 cm. (Each corner of the box is the center of a pixel.)

When the knife was removed from under the sweater, the image taken under identical conditions of the same body in the same motionless position, and processed by IMAGE with exactly the same filter settings, showed a complete blank. No pixel signals from the unarmed human survived the filtering. Of the four images of humans with and without concealed weapons that have been processed by IMAGE, the rate of false-positive pixels (signals from areas of clothing not concealing weapons) has been less than 2 percent.

The remote ultrasound image of a handgun concealed on an author under a heavy sweatshirt is shown in Fig. 7. The image and the photograph of the handgun are depicted with the same scale length. This 10x12 pixel image, processed by IMAGE, had two false-positive pixels. When the handgun was removed from under the sweatshirt, the resulting image showed just one false-positive pixel, determined to have been caused by a seam in the sweatshirt that was crimped towards the sensor.

5. RADAR SENSOR

JAYCOR has developed a forward-looking, frequency-agile ground penetrating radar system (GPR) that can detect and locate both buried and surface-deployed land mines at a stand-off distance. The GPR is currently mounted on a jeep, although it could easily be installed at a fixed site. It is capable of detecting land mines at ranges between 3 and 30 meters in front of the vehicle. It is currently capable of scanning a path 4 meters wide directly in front of the vehicle traveling

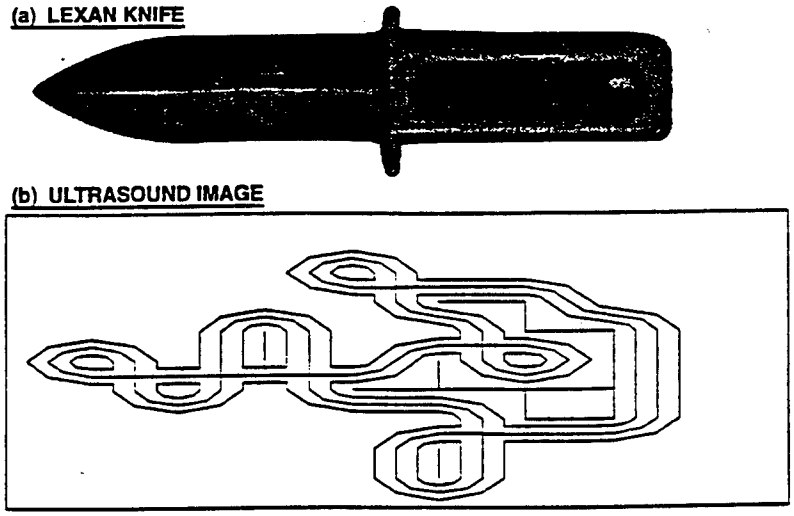

Figure 6. **(a) Lexan knife. (b) Remote (1.3 m) ultrasound image of same knife concealed on human body under wool sweater.**

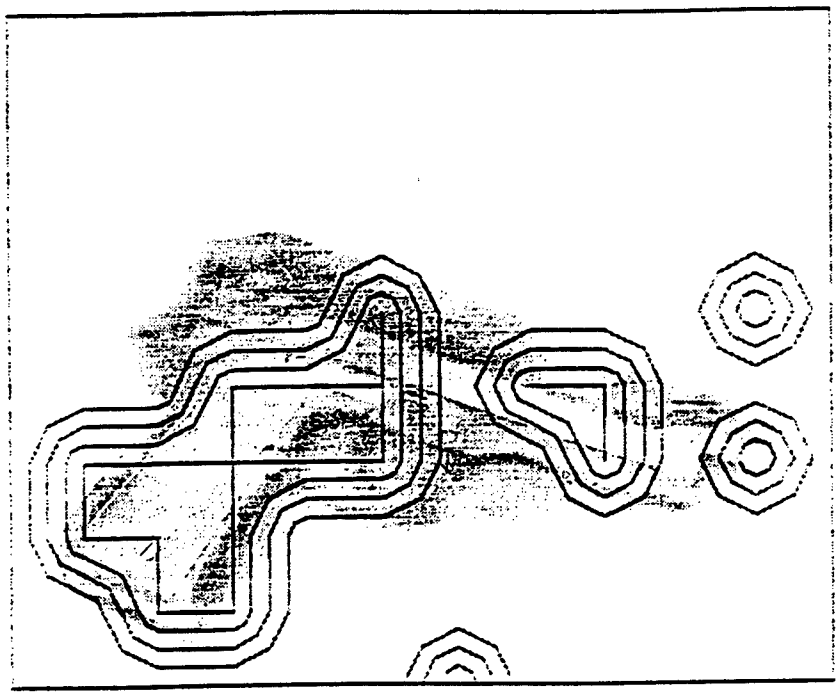

Figure 7. **Remote (1.3 m) ultrasound image of handgun concealed on human body under heavy sweatshirt overlaid on the handgun to same scale.**

at speeds of up to 5 kph, but this can easily be modified for a path of up to 10 meters wide (requiring faster processors). The current system uses approximately 1 kW of electrical power, weighs approximately 91 kg (200 lbs), and takes up a volume of approximately 1.4 m^3 (50 ft^3) exclusive of power generation equipment

Frequency-agile radars have an advantage over conventional radars because they use multiple carrier frequencies to characterize a target. Most targets, including land mines, reflect different amounts of energy at different frequencies. At a single frequency, many targets may look alike or be totally indistinguishable from the background, also other targets return

no signal at some frequencies due to nulls in the RF response. Consequently, by using many frequencies, the probability of detecting and identifying a target is dramatically increased.

The JAYCOR frequency-agile radar uses three antennas. The transmit antenna is in the center and the two receive antennas are mounted one meter to either side of the transmit antenna. The radar transmits narrow pulses at 36 different carrier frequencies. Objects in front of the radar reflect a portion of the energy in the pulses back to the radar receivers. The receivers coherently detect the amplitude, phase, and time delay of the reflected pulses and store this radar return to be processed by our signal processing software algorithms.

The software algorithms begin by mathematically increasing the signal-to-noise ratio in the radar return signals. The magnitude of the radar return is initially used to detect an object. The approximate location of the object is determined by comparing the time delay of the reflected pulse between the two receivers. Once the approximate location of the object is known, the phase of the radar return at each receiver is used to accurately locate the object. The spectral density, or magnitude versus carrier frequency, of the return is used to uniquely identify the object.

The JAYCOR frequency-agile ground penetrating radar system (GPR) consists of three major parts: the radar, the signal and data processing, and the display system. The radar consists of one transmitter, two receivers, three antennas, one timing control unit, two digitizers, and one radar controller. The signal and data processing consists of a digital signal processor (DSP), a master controller, and software. The display system consists of software and a display screen.

The signal and data processing section consists of a master controller computer with a graphics accelerator and digital I/O board, a DSP card containing four i860 digital processing units, and the accompanying software. The software is responsible for controlling the data acquisition and processing the data, all of which happens concurrently. The data processing software can be divided into four basic steps as shown in Figure 8. The first step performs the initial signal conditioning and enhances the signal-to-noise ratio (S/N) of the radar returns through pulse return averaging. This step also provides a rough estimate of the target range, but no azimuth information. The second step computes the correlation between the right and left channels to get azimuth information. The third step computes the correlation between the outgoing pulse and the return signal to accurately determine the target range. The final step is the reduction of false alarms through the classification and identification of the targets.

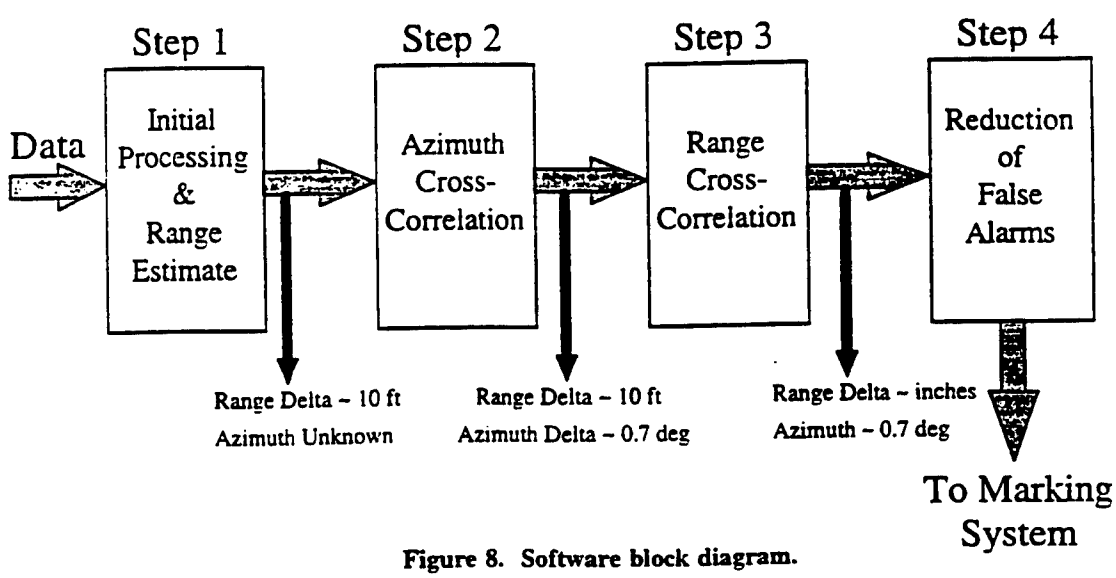

Figure 8. Software block diagram.

6. ACKNOWLEDGMENTS

This work was sponsored by the Air Force Materiel Command and the Defense Advanced Research Projects Agency under Contract No. F30602-95-C-0274. The authors gratefully acknowledge helpful discussions with Irv Smietan, David Ferris, Robert McMillan, Nicholas Curry, and Michael Wicks.

APPENDIX B

Ultrasound Sensor for Remote Imaging of Concealed Weapons

F. S. Felber, C. Mallon, N. C. Wild, and C. M. Parry*
JAYCOR
P. O. Box 85154, San Diego, CA 92186
*GenCorp Aerojet
P. O. Box 296, Azusa, CA 91702

ABSTRACT

A breadboard ultrasound sensor was developed for remotely detecting and imaging concealed weapons. The breadboard sensor can detect metallic and non-metallic weapons concealed on a human body under heavy clothing at ranges up to 8 m and image the concealed weapons at ranges up to 5 m.

This breadboard sensor has produced the only remote ultrasound images of concealed weapons ever published,[1] including lexan (plastic) knives and a handgun concealed under a heavy sweatshirt at 15 feet. The remote imaging by ultrasound was made possible by several new technological developments. The sensor includes a novel, highly efficient source of high-power, tunable ultrasound radiation suitable for remote imaging in air. Together with millimeter-sized, highly sensitive ultrasound detectors and high-gain transceivers, these advances make possible the centimeter-resolution imaging of concealed weapons at ranges between 1 m and 5 m.

The ultrasound images are processed by our IMAGE binary-thresholding program, which filters for noise, frequency, brightness, and contrast. To be developed is a brassboard sensor with an imaging array of ultrasound detectors, capable of real-time, video-frame-rate imaging of weapons concealed on moving humans.

KEYWORDS: ultrasound, sensor, concealed weapons, imaging, concealed weapons detection, non-metallic weapons, ultrasound detectors, image processing

1. INTRODUCTION

The feasibility of an ultrasound sensor that can remotely detect and image concealed weapons has been demonstrated. A breadboard ultrasound sensor has imaged metallic and non-metallic weapons concealed on human bodies under heavy clothing at ranges up to 5 m.

The ultrasound sensor was designed to be integrated with an active radar sensor that would detect concealed weapons at long ranges. The integrated ultrasound and radar sensors were intended for fixed-site use in law enforcement and military applications. A scenario for the use of such an integrated sensor in law enforcement is illustrated in Figure 1. From an unobtrusive site more than 10 m away, an active radar sensor can specify with a high probability of detection which individuals in a moving crowd may be concealing metallic or non-metallic weapons. The radar would then hand over the location of the potential concealed weapon to the ultrasound sensor. At ranges up to a few meters, the ultrasound sensor could image, and enable a guard to identify, the concealed weapon on a moving person.

The objective of this effort was to develop and demonstrate a breadboard concealed weapons detection (CWD) sensor that can detect and identify metallic and non-metallic weapons at distances of 1 to 10 m. Figures of merit for the breadboard CWD sensor include reliability, safety, public acceptability, low cost, and unobtrusiveness. An additional important consideration is scalability of the CWD sensor to lightweight, handheld devices.

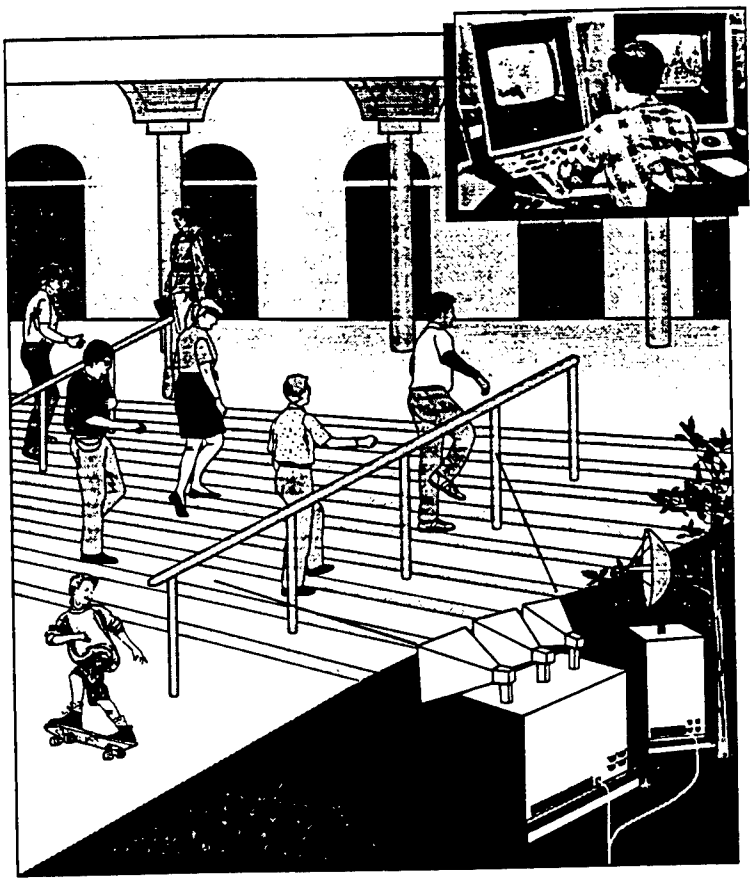

REM-33393

Figure 1. Artist's concept of CWD system at building entrance.

The breadboard ultrasound sensor succeeded in meeting the objective and in ranking high on figures of merit. The sensor has produced the only remote ultrasound images of concealed weapons ever published.[1] Remote ultrasound images have been produced of metallic and non-metallic weapons concealed on human bodies under heavy clothing. The attenuation of ultrasound by a variety of types of clothing from thin shirts to heavy winter coats has been characterized. The penetration of clothing by ultrasound at 40 kHz is excellent, and at 200 kHz is lower generally by less than 10 dB. Section 4 will show that metallic or non-metallic, hard concealed weapons return much louder ultrasound echoes than clothed human bodies. Both the low return from the body and the resolution of the images eliminate concerns about privacy issues that beset certain other high-resolution CWD imaging systems. The public acceptability of an ultrasound CWD system should be high.

The safety of the ultrasound CWD imaging system adds to the public acceptance. Ultrasound is generally considered by the public, the medical community, and regulatory agencies to be benign. The American National Standards Institute (ANSI) imposes no safety standards for ultrasound, either for effects on hearing, for tissue penetration, or for thermal effects.[2,3] The Food and Drug Administration (FDA) imposes the normal regulatory guidelines for the manufacture and use of medical diagnostic ultrasound equipment that it imposes on any medical equipment. Of course, the guidelines allow unlimited real-time ultrasound imaging of a fetus in utero.

The ultrasound images of concealed weapons were achieved through development of: novel, high-power ultrasound sources; novel, mm-sized, sensitive ultrasound detectors in arrays; and image processing adapted to the hardware. Section 2 summarizes the conceptual design of the breadboard ultrasound CWD sensor. The breadboard sensor and its operation are described more fully in Section 3. Image processing for the breadboard ultrasound sensor is described in Section 4.

2. CONCEPTUAL DESIGN

The breadboard ultrasound sensor is an active imaging system like an active imaging radar. It comprises an ultrasound source and an imaging receiver. The receiver has focusing optics and detectors on a focal plane. The ideal illumination source for an active ultrasound sensor is the acoustic equivalent of daylight. That is, we would like to have ultrasound illumination of concealed weapons from a wide range of angles. In practice, however, the range of illumination angles for the ultrasound is limited. The limited range of angles of illumination causes glints, or specular returns from flat facets, from the concealed weapons. If the sensor has a video frame rate of 30 Hz, then the glints will appear to pass over the moving concealed weapons, and will not unduly affect the visual perception of the ultrasound image. Glints can even be favorable in the sense that the intensity of the specular return from a glint falls with range only as r^{-2}, rather than the r^{-4} typical of active radar returns.

We have tried two approaches, and gotten good results from both, to increasing the uniformity of the reflected intensity. The first approach was to use a roughened transmitter dish with a novel, coherent, high-power point source of ultrasound. The transmitter dish was roughened on a length scale of about 0.1 to 0.2 of the ultrasound wavelength in order to spoil the coherence of the point source. The roughening turned the transmitter dish into a diffuse source of ultrasound, instead of a plane wave. The effective range of angles of incidence of the ultrasound on the concealed weapons, therefore, was increased to the order of the transmitter dish diameter divided by the range to target. The second approach was to use an array of small, inexpensive ultrasound transducers. The array subtended an area larger than that of the roughened transmitter dish. The transducers were pulsed in unison. Generally, though, the signal into each detector element was dominated by the specular glint of only a single transducer at the transmitting array. Therefore, the effective power of the array was the power of a single transducer for each detector element.

We intended an active radar to perform long-range detection at 10 m or greater ranges, and an ultrasound sensor at 200 kHz to image the detected concealed weapons at closer ranges up to about 3 m. Our tests of an ultrasound sensor at 40 kHz, however, have shown that such a sensor might be able to handle much of the long-range detection mission of an active radar. Table 1 shows the range and resolution tradeoffs of ultrasound sensors at 40 and 200 kHz. The range of 200-kHz ultrasound is limited by attenuation in air to about 3 m for CWD. Because of its short wavelengths, however, 200-kHz ultrasound offers excellent resolution for imaging and identifying concealed weapons. At 40 kHz, the range of an ultrasound sensor is not limited by air attenuation. Rather, it is limited by the need to project a wide range of illumination angles at the concealed weapon. Since the resolution is proportional to wavelength, 40 kHz is more appropriate for detection and for locating a general area in which the higher-frequency ultrasound should be directed for imaging. To exploit the respective strengths of ultrasound sensors at 40 and 200 kHz, we were led to the concept of a dual-frequency sensor.

In a dual-frequency sensor, the field of view (FOV) of the 40-kHz sensor is about the length of a human body at ranges up to 8 m. The lower-frequency sensor can scan a crowd and find those bodies that appear likely to be carrying concealed weapons. It can then hand off the directional information to the higher-frequency sensor for close-range imaging and positive identification of concealed weapons. The higher-frequency sensor has a smaller FOV, about the width of a human torso. The resolution of the lower-frequency sensor, however, should be good enough to point the higher-frequency sensor to the area of interest. Various configurations allow the transmitters and receivers for both frequencies to be combined within the same system. For example, low-frequency and high-frequency transducers can be intermingled in a transmitting array. We even have some designs for detector arrays that allow the same array and same receiving dish to be used at 40 and 200 kHz.

Table 1. Comparison of ultrasound CWD sensor characteristics at 40 and 200 kHz.

Property	Ultrasound @ 40 kHz	Ultrasound @ 200 kHz
Range	From 2 to 8 m	From 1 to 3 m
Resolution	2 to 10 cm	1 to 2 cm
Aperture	90 cm	90 cm
FOV	Body	Torso
Penetration	Excellent	Very Good
Non-metallic CWD	Excellent	Excellent
Safety	Excellent	Excellent
Public Acceptance	Excellent	Excellent
Potential configurations	Fixed site, mobile, handheld	Fixed site, mobile, handheld

Table 2 shows that the penetration of clothing by 40-kHz ultrasound is excellent. At 200 kHz, the penetration is not quite as great, but certainly adequate for all but the heaviest winter coats. Both frequencies are able to image non-metallic weapons and have excellent discrimination between the weapons and clothing or bodies. Also, the ultrasound frequency has no bearing at all on the perception by the public that ultrasound radiation is both safe and acceptable.

Table 2 shows the percentage of voltage signal transmitted through various clothing materials relative to a baseline of no intervening clothing. Transmitting and receiving transducers were placed on both sides of these clothing materials, separated by 2 m. The ratios of the peak-to-peak voltage, with and without the clothing between, are shown in the table at the two frequencies, 40 and 200 kHz. A transmitted voltage signal of 0.11 percent for the down-filled winter coat with nylon shell at 200 kHz implies that the total attenuation of intensity at that high frequency, from a round-trip through the coat, is of the order of 120 dB. The attenuation of intensity for a round-trip at 40 kHz is only about 74 dB for the same winter coat. That is another reason why the lower frequency is being considered for long-range detection, and the higher frequency only for close-range imaging. At close ranges, air attenuation would not affect the higher frequency so much. We measured the attenuation of 200-kHz ultrasound in air to be about 9 dB/m. In comparison, the worst-case attenuation of 40-kHz ultrasound in air (at relative humidity of 50%) is only 1.3 dB/m.

Table 2. Amplitude of ultrasound signal (in volts) transmitted through various articles of clothing at 40 and 200 kHz as a percentage of baseline signals measured at the same 2-m distance with no intervening clothing.

Material	Transmitted Voltage Signal (%) @ 40 kHz	Transmitted Voltage Signal (%) @ 200 kHz
Baseline	100	100
Heavy Polyester Sweatshirt	69	44
Nylon/Polyester Shop Coat	67	55
Cotton Flannel Shirt	57	33
Acrylic Sweatshirt (folded double)	52	16
Wool Sweater	47	11
Wool Navy Pea Coat	34	11
Cotton Sweatshirt (folded double)	23	0.82
Wool Suit Coat #1	18	7.7
Wool Suit Coat #2	15	5.5
Wool Suit Coat #3	12	2.2
Down-Filled Winter Coat, Nylon Shell	1.4	0.11

As is the case with several other breadboard CWD technologies, the breadboard ultrasound sensor produced images by exposing one pixel at a time. A brassboard will contain an array, probably of 50 x 50 ultrasound detectors, that can produce moving images at real-time video frame rates. Since the breadboard sensor is only equipped with single detectors, the images must be produced pixel-by-pixel of stationary scenes over periods of many minutes. The exposure process with the single detector in the breadboard sensor was speeded up by equipping the receiver dish with a motorized drive unit on an x-y translation stage. We have also written a drive-control and data-acquisition computer program, CWD, that coordinates the motion of the receiver dish with the pulsing of the ultrasound source and the collection of data from the detector. Of course, this will become unnecessary once an imaging detector array is developed for a brassboard sensor.

Table 3 shows the characteristics of the existing breadboard ultrasound sensor in the first column and the upgraded characteristics of a brassboard ultrasound sensor in the second column. The breadboard sensor requires about 30 minutes to produce a 12 x 12 image one pixel at a time. The brassboard ultrasound sensor will produce 50 x 50 images at video frame rates of about 30 Hz. The breadboard sensor can operate at any single frequency. High-frequency ultrasound is appropriate for close-range imaging. Low-frequency ultrasound is appropriate for distant detection of concealed weapons. A brassboard sensor will have dual-frequency capabilities that will allow it to detect distant concealed weapons and then hand over that information to the higher-frequency sensor that will perform close-range imaging. The breadboard sensor generates data that is post-processed with tuning and filtering algorithms. The brassboard will be equipped with knobs that can tune and filter a real-time image on a video monitor. The breadboard images are produced by binary thresholding of pixels for brightness and contrast. The real-time brassboard images will have gray-scale shading or perhaps colors corresponding to the intensity of the ultrasound signal in each pixel. The brightness and contrast will be controllable by knobs, just as in many computer monitors. Before scanning a scene with the breadboard sensor, the scene must be pre-framed using a laser pointer. The brassboard ultrasound sensor will have automatic centroiding that centers the receiver on the area producing the brightest return. The breadboard uses two inexpensive parabolic solar concentrators for receiving and transmitting dishes. It has also used a small array of 9 transmitting transducers. The brassboard ultrasound transmitter will probably be a much larger array, perhaps 3' by 5', of about 30 transducers at each of the two frequencies. Each transducer is only about 1 cu. in. and can be mounted on a very lightweight frame for fixed-site applications. The larger effective transmitter area will produce a greater range of incident angles of ultrasound at the concealed weapons. The breadboard has been using an 18-in. parabolic reflector for a receiver at 40 kHz and a 4-in. spherical mirror at 200 kHz. The brassboard receiver dish will probably be a good quality parabolic dish with about a 30-in. diameter and a focal plane that automatically translates axially for focusing. The rangefinder for the autofocus will probably be similar to the ultrasound rangefinders in cameras. The larger receiver dish will improve the resolution at both frequencies and will improve the gain at least at the lower frequency.

3. BREADBOARD ULTRASOUND SENSOR

Figure 2 shows the main components of the breadboard ultrasound sensor. The three main subsystems are the transmitter, receiver, and image processor. All operate from the same 110-V wall socket.

The transmitter power supply conditions the electrical power and produces pulses of the desired repetition frequency, typically about 1 Hz, and duration, typically about 100 μs at 200 kHz and 500 μs at 40 kHz. The ultrasound source was either our novel high-power coherent point source, which requires a transmitter dish, or an array of small, inexpensive transducers at 40 kHz. The array does not require a transmitter dish. If the point source is used, then the transmitter is roughened to spoil the coherency and spread the range of angles in the beam incident on the target. The tunable point source has a higher efficiency (about 5 to 10%) of conversion of electrical to ultrasound power and a broader spectrum, which helps avoid speckle. But the point source has less shot-to-shot repeatability than the transducer array. Also, the transducer array can be made to have a wide spread of angles of radiation in the beam more easily than the point source. Even with a wide spread of angles in the incident beam, however, any facet on a weapon typically reflects ultrasound specularly to a detector from just one transducer in the array.

Table 3. **Characteristics of existing breadboard CWD ultrasound sensor (first column) compared to brassboard (second column).**

Breadboard CWD Sensor	Brassboard CWD Sensor
30 minutes/image	30 milliseconds/image
12 x 12 pixel images	50 x 50 pixel images
Close imaging <u>or</u> distant detection	Close imaging <u>and</u> distant detection
Single frequency	Dual frequencies
Post-processed tuning/filtering	Real-time tuning/filtering knobs
Binary thresholding of pixels	Variable amplitudes of pixels
Laborious preframing of images	Automatic centroiding
Resolution limited (18" rcvr)	Improved resolution (30" rcvr)
Range limited (18" x-mtr)	Improved range (36" x 60" array)

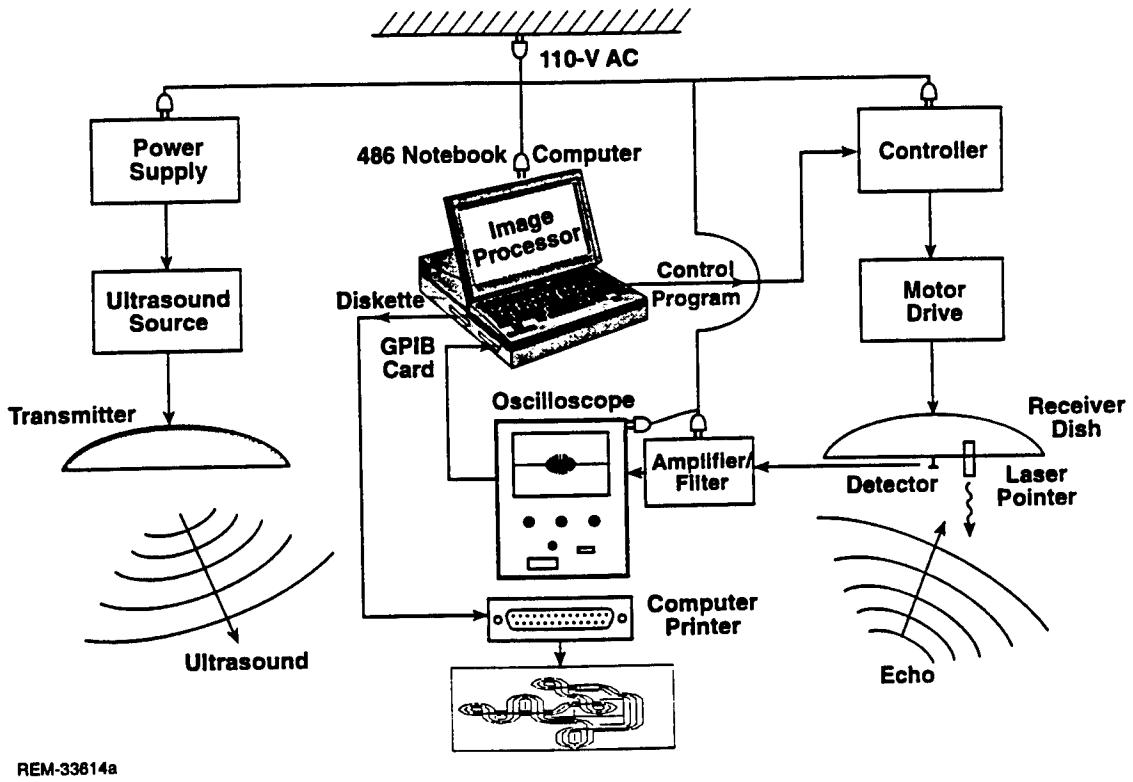

Figure 2. Schematic of breadboard ultrasound sensor.

The breadboard receiver has just a single ultrasound detector at the focal plane. The receiver dish is rotated incrementally to scan a rectangular grid at the target. The x-y translation stage that controls the rotation of the receiver dish has been motorized in the vertical, but not azimuthal, scan direction. The vertical scans are controlled, and the azimuthal scans are prompted, by the computer program, CWD. After the receiver dish is moved to each new location, the ultrasound source is pulsed, and the reflected signal is registered on an oscilloscope and recorded by the CWD program. The grid spacing at the target is generally chosen to be about half of the diffraction-limited and geometrical-optics-limited resolutions. Generally, the detector size and optics are such that the diffraction limit is a little bigger than the geometrical-optics limit.

Although the breadboard sensor could only acquire data from one detector at a time, the detectors were developed in arrays to demonstrate fabricability. We have tried several different detector types, and settled on the design that offers the greatest sensitivity and fabricability in small arrays. The detectors are piezoelectric-film benders. They vibrate as edge-clamped thin plates. The 40-kHz detectors are about 2 mm square. The frequency of these detectors are proportional to the ratio of thickness to area. Thus, 160-kHz detectors can be made by quadrupling the thickness or halving the diameter of the 40-kHz detectors. An array of 50 x 50 40-kHz detectors is about 4 inches across. An array of 50 x 50 160-kHz detectors might be only 2 inches across. Alternatively, a higher frequency mode of the 40-kHz detectors could be amplified for detection at a higher frequency.

A tuned amplifier/filter was custom built for the 2-mm sized 40-kHz detectors. The amplifier needed to be designed specifically to handle the few picofarad capacitance of these small detectors. The quality factor Q of the transmitting transducers was of the order of 20 to 40. The amplifier/filter was tuned to the relatively narrow waveband of these transducers. The signal from the tuned amplifier was fed into an oscilloscope. An oscilloscope display is not needed for a brassboard ultrasound sensor, but was useful for research and development of the breadboard sensor. The oscilloscope data was fed through a GPIB card into a notebook computer, where it was collected and stored by the CWD program. Each voltage waveform comprised 512 data points at a sampling rate of 2.5 data points per ultrasound period. For example, at 40 kHz, one voltage sample was collected every 10 μs. The low sampling rate relative to the period, just above the Nyquist criterion, gave the highest frequency resolution in the Fourier transforms, and also the greatest depth of field. With a total record length of about 5 ms, echoes from the target were recorded over a depth greater than 5 feet.

After voltage signals were recorded for each pixel of the image, the data was uploaded from the CWD program to the image processing program, IMAGE. The IMAGE program is described in the next section. It processed the image, which was then printed out. As mentioned in Section 2, and specifically in Table 3, all parts of the breadboard sensor, including the image processing, will be vastly different in a brassboard ultrasound sensor. The breadboard sensor has performed its mission of demonstrating feasibility of the important aspects of ultrasound imaging of concealed weapons.

4. ULTRASOUND IMAGE PROCESSING

For the ultrasound breadboard sensor, we developed an image processing program, IMAGE, using the commercial Mathcad® Plus 6.0 program as a platform. If the image has n x m pixels, the IMAGE program reads all the data into a 512 by n x m array. Then it filters for noise, frequency, brightness, and contrast.

IMAGE calculates the standard deviation σ_{nm} of each waveform. Then it sets equal to zero each data point in a waveform having an amplitude less than some multiple of the standard deviation of that waveform. A filter set at $1.5\sigma_{nm}$ seems to work best for our images. If the waveform contains a signal, then the signal is evident as a "localized" pulse, as in Figure 3(a). The $1.5\sigma_{nm}$ noise filter acts on this waveform to produce the filtered waveform shown in Figure 3(b). On the other hand, if the waveform is just noise with no signal from a weapon, then the noise pattern is fairly "uniform," and is mostly eliminated by the $1.5\sigma_{nm}$ noise filter.

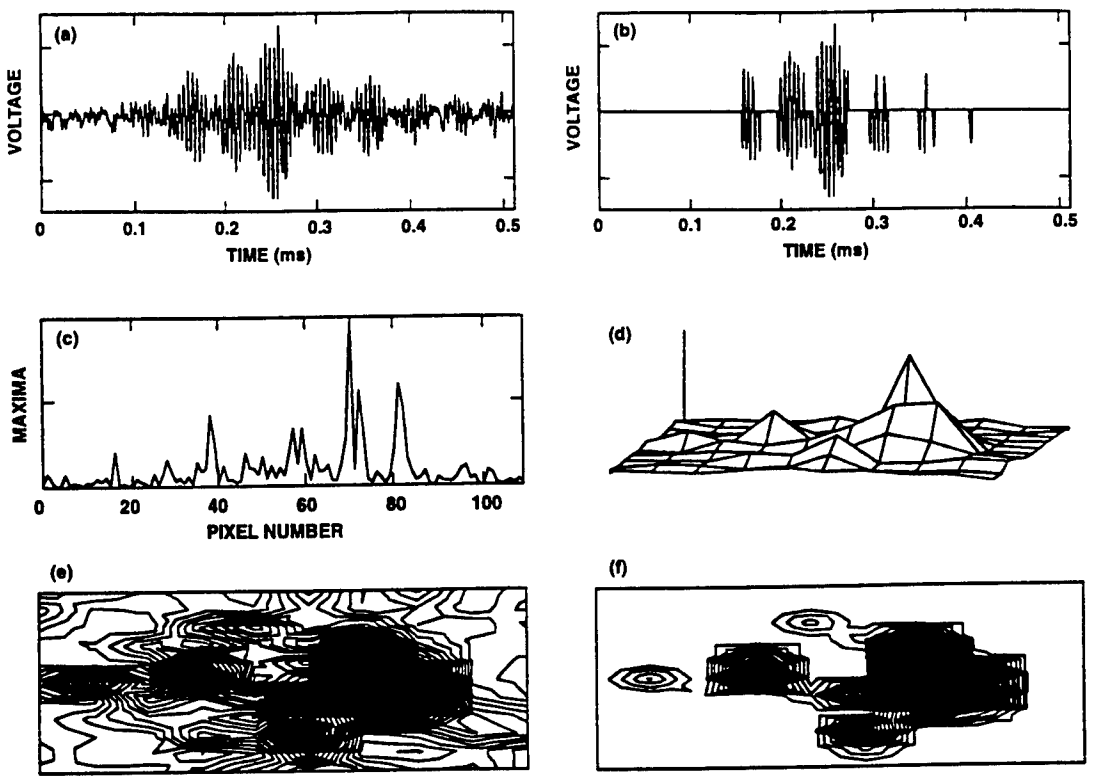

REM-334878

Figure 3. (a) Typical ultrasound signal waveform from a single-pixel 0.5-ms exposure. (b) Same waveform after $1.5\sigma_{nm}$ noise filtering. (c) Maximum filtered spectral densities of waveforms versus pixel number. (d) Surface plot of (c) arranged in image matrix. (e) Contour plot of (d). (f) Same as (e) after brightness filtering.

A frequency filter in IMAGE works synergistically with this noise filter. IMAGE calculates the fast Fourier transform of each noise-filtered waveform. Since low-amplitude noise at the transmitted frequency was mostly filtered out by the noise filter, those filtered waveforms not carrying a signal have a broad frequency spectrum. A 4-percent-bandwidth filter around the transmitter frequency is adequate to enhance the signal-to-noise. The final image is insensitive to filter bandwidth between about a few percent and 20 percent. The frequency filter is prudent to eliminate spurious noise sources and audible noise sources.

After the noise and frequency filtering, IMAGE extracts from the filtered spectral density of each pixel waveform only a single number, the maximum within the frequency window. These n x m numbers for the image of a concealed lexan knife are arrayed linearly in Figure 3(c). IMAGE assembles these numbers into a matrix, following the pixel roadmap from the image scan. A surface plot of the matrix is shown in Figure 3(d) and a contour plot in Figure 3(e).

A brightness filter sets equal to zero all points in the image matrix that are less than a threshold. The contour plot of Figure 3(e), with low-intensity points filtered out, is shown in Figure 3(f). In this sense, the brightness filter is really a spectral-density amplitude filter.

Finally, a contrast filter in IMAGE sets equal to a threshold all points in the image matrix that exceed the threshold. The contrast filter eliminates ultrasound glints from individual pixels, since they distract from the perception of a motionless ultrasound image. The contrast filter threshold is set 1 percent above the brightness filter threshold to give the best appearance of an image in a contour plot.

The concealed lexan knife that was imaged is shown in Figure 4(a). The final ultrasound image, after processing for noise, frequency, brightness, and contrast, is shown in Figure 4(b). The knife and the ultrasound image are depicted in Figure 4 with the same length scale. The box around the image represents a rectangular area at the concealing sweater of 8.89 cm by 24.0 cm. The image comprises 11 pixels vertically, separated by 0.89 cm, and 10 pixels horizontally, separated by 2.67 cm. (Each corner of the box is the center of a pixel.)

When the lexan knife was removed from under the sweater, the image taken under identical conditions of the same body in the same motionless position, and processed by IMAGE with exactly the same filter settings, showed a complete blank. No pixel signals from the unarmed human survived the filtering. Of the images of humans with and without concealed weapons that have been processed by IMAGE, the rate of false-positive pixels (signals from areas of clothing not concealing weapons) has generally been less than or about 2 percent.

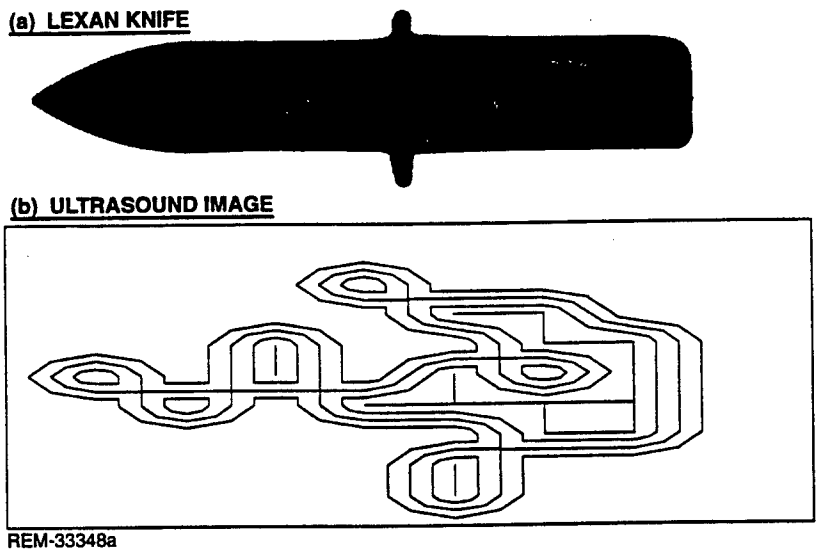

REM-33348a

Figure 4. (a) Lexan knife. (b) Remote (1.3 m) ultrasound image of same knife concealed on human body under wool sweater.

The reason for the low rate of false-positive pixels is seen in Figure 5. Figure 5(a) shows a surface-plot image of a handgun concealed behind a heavy sweatshirt and suspended motionless within inches in front of a standing human subject, who was wearing a shirt and tie. Figure 5(b) shows the identical image after the handgun was removed from the scene. Therefore, Figure 5(b) is an image of the torso area of an unarmed, clothed individual behind a heavy sweatshirt. The vertical voltage scale was the same in Figure 5(b) as in 5(a). Only the normal $1.5\sigma_{nm}$ noise filter was applied in both images. No frequency, brightness, or contrast filters, which would have altered heights in the surface plots, were applied.

The diffraction-limited resolution for these images produced by a transducer array at 40 kHz was 1.2 in. The measured resolution was 1.6 in. vertically and 2.1 in. azimuthally. The vertical and azimuthal center-to-center pixel spacing (grid cell size in Figure 5) was 1.5 in.

• IMAGE OF HANDGUN ON HUMAN BEHIND HEAVY SWEATSHIRT

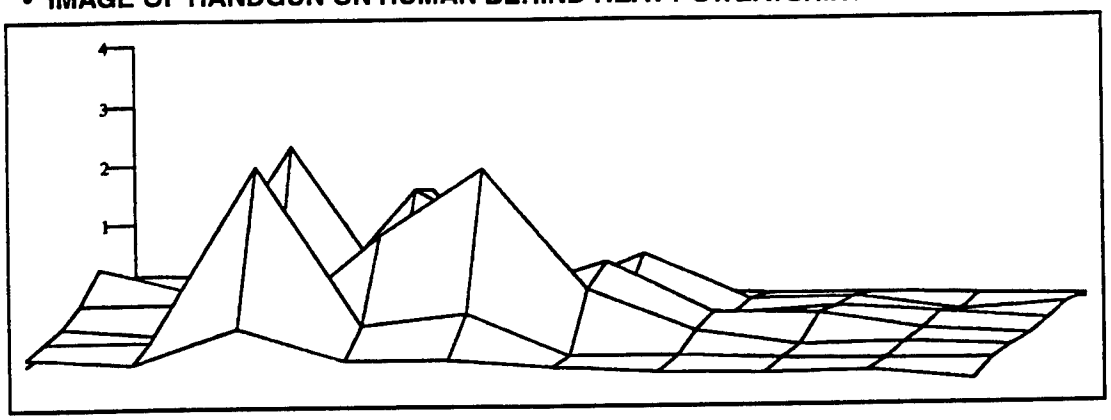

• IDENTICAL CONDITIONS, EXCEPT NO HANDGUN

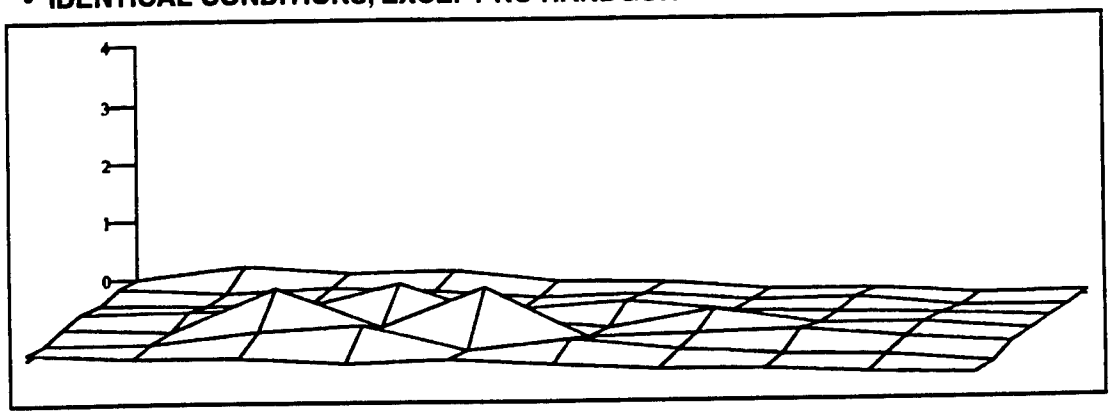

REM-33728a

Figure 5. (a) Remote (1.5 m) 40-kHz ultrasound surface-plot image of handgun concealed by heavy sweatshirt on clothed human body background. (b) Identical to (a), except no handgun. Both images are same scale and without filtering for brightness or contrast.

5. ACKNOWLEDGMENTS

This work was sponsored by the Air Force Materiel Command and the Defense Advanced Research Projects Agency under Contract No. F30602-95-C-0274. The authors gratefully acknowledge helpful discussions with Irv Smietan, David Ferris, Robert McMillan, Nicholas Curry, Kathleen Zyga, and Michael Wicks.

6. REFERENCES

1. F.S. Felber, H. T. Davis III, C. Mallon, and N. C. Wild, "Fusion of Radar and Ultrasound Sensors for Concealed Weapons Detection," in *Signal Processing, Sensor Fusion, and Target Recognition V*, Ivan Kadar, Vibeke Libby, Editors, Proc. SPIE 2755, 514 - 521 (1996).

2. *Biological Effects of Ultrasound: Mechanisms and Clinical Implications*, National Council on Radiation Protection and Measurements, NCRP Report No. 74, Bethesda, MD, 1983.

3. *Exposure Criteria for Medical Diagnostic Ultrasound*, National Council on Radiation Protection and Measurements, NCRP Report No. 113, Bethesda, MD, 1992.

©U.S. GOVERNMENT PRINTING OFFICE: 1999-610-130-81073

AIR FORCE RESEARCH LABORATORY
IFEA
ATTN: DAVID FERRIS
32 BROOKS ROAD
ROME, NEW YORK 13441-4114

JAYCOR
9775 TOWNE CENTRE DRIVE
SAN DIEGO, CA 92121

AFRL/IFOIL
TECHNICAL LIBRARY
26 ELECTRONIC PKY
ROME NY 13441-4514

ATTENTION: DTIC-OCC
DEFENSE TECHNICAL INFO CENTER
8725 JOHN J. KINGMAN ROAD, STE 0944
FT. BELVOIR, VA 22060-6218

DEFENSE ADVANCED RESEARCH PROJECT AGENCY
3701 NORTH AIRFAX DRIVE
ARLINGTON VA 22203-1714

MISSION OF AFRL/INFORMATION DIRECTORATE (IF)

The advancement and application of information systems science and technology for aerospace command and control and its transition to air, space, and ground systems to meet customer needs in the areas of Global Awareness, Dynamic Planning and Execution, and Global Information Exchange is the focus of this AFRL organization. The directorate's areas of investigation include a broad spectrum of information and fusion, communication, collaborative environment and modeling and simulation, defensive information warfare, and intelligent information systems technologies.